INVESTIGATION OF RUNOFF GENERATION RESPONSES IN STEEP, SEMI-ARID HEADWATER CATCHMENTS, SOUTH PARE MOUNTAINS, TANZANIA

SUBMITTED BY

Timo Kessler

October 2008





Diploma thesis

INVESTIGATION OF RUNOFF GENERATION RESPONSES IN STEEP, SEMI-ARID HEADWATER CATCHMENTS, SOUTH PARE MOUNTAINS, TANZANIA

SUBMITTED BY

Timo Kessler

matriculation number 2079181

October 27th, 2008

SUPERVISION

PhD Marloes Mul Prof. PhD Stefan Uhlenbrook

UNESCO-IHE
Institute of Water Education
Department of Water Management



EXAMINATION

Prof. Dr. rer.nat. Dr.-Ing. habil. András Bárdossy

University of Stuttgart
Institute of Hydraulic Engineering
Department of Hydrology und Geohydrology



Author's Statement			
I hereby certify that I have sources, aids and advisors			
Date	Sig	gnature	

Abstract

In semi-arid Southern Africa access to fresh water resources poses one of the biggest risks for the local people. The surface water resources are scarce and low precipitation and high water losses lead to a humble annual recharge. On the way forward towards a sustainable water resources management it is crucial to gain an improved understanding of the flow dynamics and the catchment hydrology. The Makanya catchment is a poorly gauged basin located in the South Pare Mountains in Northern Tanzania. The research presented in the following thesis was carried out in two steep headwater catchments nested in the Makanya catchment. It was aimed to investigate runoff generation responses and to further develop an understanding of the dominant hydrological processes. A detailed process understanding enables more secure predictions and can contribute an improved water resources management.

A multi-method approach was applied to gain insight into hydrological processes from different perspectives. The numerous data were carefully interpreted, processed and merged into a conceptual model to demonstrate the flows. As different flow regimes give rise to different processes, the runoff generation was studied during both, baseflow and storm-flow conditions. The base-flow investigation focused on the quantification of diurnal stream flow fluctuations that have been discovered in previous studies. The inspection of storm-flow aimed the understanding of runoff generation responses. In particular, the discharge contribution from subsurface storages and the role of event water were of primary interest. During several rain events the discharge was recorded and stream water was sampled for hydro chemical and isotope analysis. The time variation of natural tracers during the hydrographs provided profound information on source areas, flow paths and residence times. Hydrograph separation showed pre-event water to contribute the bulk of discharge during storm-flow whereas event water has a minor effect of approximately 15 %, depending on the rainfall characteristics. Against the background of different stream contributions the installation of two stream gauges at different stream-points was quite useful to quantify lateral inflows from adjacent hillslopes. The subsurface fluxes show different hydro chemical and physical characteristics, depending on their origin within the catchment. Longitudinal transects of the electrical

conductivity (EC) supported the identification of sources and revealed inverse trends of EC for two different streams. The lateral inflows occur either as diffusive sources or as small springs. In both cases the sources show distinct hydro chemical signatures of $> 220~\mu \rm Siemens~cm^{-1}$ compared to the stream EC of 100-120 $\mu \rm Siemens~cm^{-1}$. In addition to the stream measurements, the soil moisture contents and the groundwater levels have been monitored in the riparian zone to also learn about infiltration rates of rain water. This report describes the applied methods and presents the key results of the investigation. The outcome of the research is a thorough understanding of flow dynamics and dominant hydrological processes — a prerequisite for process-based modeling of runoff generation.

I will skip acknowledgements, nevertheless I want to mention the names of all those people living in the Makanya catchment whose assistance and support contributed greatly to this research.

Abraham Petro, Ally Husseini, Anna Mbonea, Eliatosha Rafaeli, Eliawangu Eliamini, Ghuheni Johane, Godfrey Joeli, Joeli Ghureni, Juma Ally, Loveness Senkoro, Luka Mzawa, Maliki Abdallah, Mama Mzawa, Mary A. Mndeme, Mataini Joeli, Mbonea Mchome, Moses Elitwanga, Mzee Heri Amani, Rajabu Ally, Ramadhani Shabani, and Salehe Athumani.

Contents

1	Intr	oduction	1
	1.1	Motivation	1
	1.2	Research background	3
	1.3	Problem statement	4
	1.4	Objective of research	6
2	Stud	y area	8
	2.1	Makanya catchment	9
		2.1.1 Topography	9
		2.1.2 Land use	10
		2.1.3 Climate	11
	2.2	Study headwater catchments	14
	2.3	Local rainfall patterns	17
3	Met	nodology	19
	3.1	Outline	19
	3.2	Components of field campaign	20
		3.2.1 Stream flow gauging	20
		3.2.2 Soil moisture monitoring	22
		3.2.3 Longitudinal transects of hydro chemistry	26
	3.3	Stream sampling during rain events	27
		3.3.1 Sampling procedure	27
			28
		·	30

4	Base	e-flow investigations	34
	4.1	Runoff analysis	34
		4.1.1 Seasonal trends	35
		4.1.2 Diurnal fluctuations	36
	4.2	Groundwater levels and soil moisture contents	40
		4.2.1 Kiwene spring site	40
		4.2.2 Kiwene forest site	41
		4.2.3 Chamasae cultivated site	47
	4.3	Stream chemistry and sources	48
5	Stor	m-flow investigation	55
	5.1	Rainfall-runoff analysis	55
	5.2	Hydro chemical stream responses	59
	5.3	End-members of runoff	63
	5.4	Quantification of contributions	65
6	Synt	thesis	69
	6.1	Conceptualisation of runoff generation	69
		6.1.1 Base-flow conditions	69
		6.1.2 Storm-flow conditions	72
	6.2	Diurnal fluctuations in the saturated and unsaturated zone	76
	6.3	Estimation of water balance	80
		6.3.1 Simplification of flows in a box model	80
		6.3.2 Quantification of flow ratios	83
7	Con	clusions	85
Bi	bliogi	caphy	88
Αŗ	pend	ices	93
A	-		02
A	Λ 1	Data for notah rating aurus	93
	A.1	Data for notch rating curve	93
	A.2	Rating curve notch formula	96 96
	$A \cdot 1$	NOICH HEIG CAHDFAHOH	90

В			97
	B.1	Watermark calibration	97
C			98
	C.1	Results of the calibration of the isotope analyser	98
D			99
	D.1	Hydrograph with Oxygen isotopes	99
	D.2	End-member mixing analysis with Oxygen isotopes	100
	D.3	Hydrograph separation with Oxygen isotopes	100
	D.4	Hydrograph separation with rain water and dissolved silica	101
	D.5	Hydrograph separation with overland flow and EC	102
	D.6	Hydrograph separation with rain water and EC	102

List of Figures

2.1	Catchment area of the Pangani Basin	8
2.2	Location of the Vudee catchment	10
2.3	Climate diagrams for Bangalala	12
2.4	Map of the two study catchments	15
2.5	Comparison of daily rainfall during Masika 2008	17
3.1	Map of measuring equipment within the study catchments	21
3.2	Lateral cross section of forest study site with installations	22
3.3	Images of field setup at forest site	24
3.4	Measuring principle of Profile Probe	25
3.5	Images of EC and pH meter and sensors	27
3.6	Images of devices for the chemical analysis	29
4.1	Time variation curve of discharge recorded at the Kiwene forest notch .	36
4.2	Comparison of Kiwene and Chamasae discharge	37
4.3	Correlation of potential transpiration and stream discharge	38
4.4	Comparison of discharge at both Kiwene stream gauges	39
4.5	Groundwater level in surrounding of Kiwene spring	41
4.6	Soil moisture contents from watermarks at forest study site	42
4.7	Soil moisture contents in root zone beneath tree	43
4.8	Diurnal fluctuations of soil moisture contents at forest study site	44
4.9	Soil saturation profiles measured with the profile probe at forest site	47
4.10	Soil saturation profiles measured with the profile probe at cultivated site	48
4.11	Longitudinal transects of electrical conductivity in Kiwene and Chamasae	
	stream	49

LIST OF FIGURES

4.12	Images of Kiwene stream	50
4.13	Images of soil exposures along Chamasae stream	51
5.1	Time variation curve of discharge recorded at the Kiwene forest notch .	56
5.2	Images of forest notch during storm-flow	58
5.3	Hydrographs of rain event on 27^{th} March with different tracers	60
5.4	Image of storm-flow samples	62
5.5	Mixing analysis of the runoff end-members at the forest stream gauge .	64
5.6	Time-source hydrograph separation using Deuterium isotopes	66
5.7	Geographic source hydrograph separation using dissolved silica	67
6.1	Conceptual model of flow mechanisms in the Kiwene spring basin	70
6.2	Conceptual model of flow mechanisms on the forested slopes	74
6.3	Simplified model of water flows	81

List of Tables

2.1	Annual precipitation and evaporation at Bangalala weather station	13
2.2	Surface area and stream lengths of the two study catchments Kiwene	
	and Chamasae	14
2.3	Elevation dependency of rainfall in the Vudee catchment	18
2.4	Correlation of daily rainfall data	18
4.1	Comparison of transpiration and soil moisture during rain events	46
4.2	Hydro chemical analysis of two small springs along the Kiwene stream	53
5.1	Rain amount, duration and intensities of selected events during Masika	
	2008	57

Chapter 1

Introduction

1.1 Motivation

In Southern Africa sustainable water resources management is temporary one of the most urgent and important challenges for the development of the region. Various problems arise in questions of sustainable water supply, equitable water allocation, and a good water quality. Some of the problems affect a large number of people and transboundary solutions need to be found to ensure sustainable development. Besides the increasing pollution of open water and groundwater resources, the permanent water scarcity is the biggest threat to the people in the region. Southern Africa shows a fast population growth and as a result more and more people need to make a livelihood with a limited amount of water resources. To prevent irreversible exploitation of the remaining resources, new ways of efficient water use and water recycling need to be found and implemented. In addition, climate change impacts the abundance and the recharge of water resources and may alter the water cycle and the rainfall distribution. Recent studies let expect that besides the known effect of global warming, the spatial and temporal variability of rainfall will change. It is hypothesised that climate change could lead to further desertification especially in regions that are already threatened by long and frequent dry spells.

In the South Pare Mountains in northern Tanzania the above mentioned categories particularly apply. The people are living predominantly of subsistence farming [Mwamfupe, 1999] and a great portion of the available water resources is used to irrigate agricultural

plots. Cultivation is done only during the rainy seasons but supplementary irrigation is regularly needed to secure the yields. The water availability is the limiting factor for food production and a steadily increasing demand for agricultural products adds pressure on the limited resources. In the past, crop production has been increased through the expansion of cultivated areas and the exploitation of available water resources. As water resources become scarce it is now crucial to find and to implement solutions for sustainable water management. The quantification of resources, the minimisation of water losses, an equal water allocation, and finally an efficient water use constitute the central tasks in future water management. To address the challenges of increasing food production and improving rural livelihoods, while safeguarding other critical ecological functions, a research program 'Smallholder System Innovations in Integrated Watershed Management' (SSI) was launched in 2003. The project follows an integrated and applied research program on how to balance water for food and nature. Particular focus in this program is given to research on opportunities to upgrade smallholder rainfed agriculture through water system innovations, while securing water to sustain critical ecological functions, in vulnerable semi-arid tropical and sub-tropical river basins [Bhatt et al., 2006].

The SSI project is divided into several work packages including different aspects of research. One research theme deals with the catchment hydrology and the quantitative aspects of the water resources in the South Pare Mountains. The theme aims to investigate available water resources and to make predictions for runoff generation and recharge of water storages. The research has been started in 2003 and meanwhile a widespread network of measuring equipment has been installed throughout the catchment, including a first order weather station, five automatic rain gauges, several stream gauges and a big weir at the outlet of the catchment. The hydrological research has been continued for several years and a number of papers have been published in international journals. The research was followed up in the first half of 2008 under the supervision of UNESCO-IHE Institute of Water Education, located in the Netherlands. The most recent results are presented in the following thesis that was submitted in October 2008 to receive a diploma in environmental engineering at the University of Stuttgart, Germany.

1.2 Research background

In the South Pare Mountains hydrological research has been started in 2003 when the SSI project was initiated. Since that time research has emphasised on spatial rainfall distribution analysis, hydro-geological characterisation and runoff generation responses [Mul et al., 2007d], [Mul et al., 2007a], and [Mul et al., 2007c]. The study presented here builds mainly on the runoff generation theme.

A number of studies has been done on runoff generation and the estimation of stormflow contributions in headwater catchments. In most of them pre-event water is considered to be the most important contribution during storm-flow [Sklash and Farvolden, 1979], [Bazemore et al., 1994], [Laudon and Slaymaker, 1997], and [Mul et al., 2007d]. However, only little is known about the source area and the storage of pre-event water and how this water is mobilised. Bazemore et al. [1994] suggests that mobilised soil water is the most important storm-flow source, although few estimates exist on soil water contributions. Other researchers found that shallow groundwater removed from subsurface storages dominates the storm-flow runoff generation [Brown et al., 1999] and [Uhlenbrook and Hoeg, 2003]. This scenario implies a large and rapid increase of the hydraulic head in near-stream groundwater bodies. Sklash and Farvolden [1979] discovered that groundwater particularly from areas proximate to the stream contributes to runoff and that upland areas have only little influence on early runoff. He argues that rainfall converts the capillary fringe of the soil into a pressure saturated zone. This would develop a groundwater ridge close to the stream that rapidly discharges pre-event water into the stream. McGlynn et al. [2004] supported this theory and stated that stormflow runoff is generated primarily in the riparian zone of the headwater catchments.

Most researchers consider event water as minor contribution to storm-flow runoff. The ratio depends on the topography, the infiltration capacity and the rainfall pattern. In some studies event water was recognised in the stream after passing subsurface flow paths. Brown et al. [1999] found that water can be rapidly delivered through the surface and forwarded to the stream with maximum inflows during recession. Also Uhlenbrook and Hoeg [2003] stated that in mountainous catchments event water occurs on the falling limb of the hydrograph. In these studies event water likely did not occur as overland flow. In dry basins however, intensive rainfall can generate fast overland flow

transporting event water into the stream during peak flow [Sklash and Farvolden, 1979].

Besides the global theme of runoff generation responses, local phenomena are always of particular interest to hydrologists. One of these phenomena are diurnal stream flow fluctuations that were first discovered in humid headwater catchments [Burt, 1979] and [Kobayashi et al., 1990]. In the semi-arid South Pare Mountains Mul et al. [2007b] recognised similar fluctuations in a small sub-catchment during base-flow conditions. Tree transpiration was hypothesised to cause these fluctuations. Bond et al. [2002] showed that diel sap flow is directly coupled to diurnal variations in stream flow for small headwater basins. Sap flow is fed by root water uptake extracting water from the saturated zone. Anderson and Burt [1977] stated that the size of the saturated wedge controls stream discharge at all flow stages. That implies that the saturated wedge must be fluctuating in parallel with the regular rise and fall of the stream.

Apart from the diurnal fluctuations that have been investigated in a couple of catchments, the processes controlling the soil moisture contents and the subsurface water levels in mountainous catchments are yet not well known or understood. Burt et al. [2002] states that a number of different factors control the development of soil moisture contents. A lot more experimental research has to be done to completely understand the dominant processes as they vary with different boundary conditions. In order to achieve this ambitious goal, extensive knowledge of the physio-graphic characteristics is essential for a valid interpretation of field data [Uhlenbrook et al., 2002].

1.3 Problem statement

Similar to other catchments in developing countries, the South Pare Mountains are considered as an ungauged catchment, essentially because of the lack of adequate resources [Mazvimavi, 2003]. Recently, the SSI project installed a small number of gauging stations to initiate data collection in this catchment. Nevertheless, there is yet no database available that could provide long-term information on rainfall or stream discharge. The missing data adds complexity to runoff predictions that are crucial for the local people, considering their dependency on the scarce water resources.

In order to improve the predictions it is necessary to gain insight into the catchment hydrology and to improve the understanding of the hydrological processes [Sivapalan, 2003]. In particular, subsurface processes are of great relevance as they determine runoff paths, residence times and water quality issues [Uhlenbrook et al., 2005]. Identifying and explaining the dominant processes is a fundamental task on the way forward to a conceptual understanding of the catchment hydrology.

The water resources in the South Pare Mountains are limited to a number of small springs in the upper parts of the mountain range and to some narrow streams winding through the forested slopes down into the floodplains. The delivery of the springs is generally small but varies over the year depending on the groundwater levels in the surrounding of the springs. The stream discharge is short-term controlled by rainfall that is attributed with a high spatial and temporal variability. The variable rainfall pattern adds complexity to predictions concerning runoff generation and recharge of water resources. Some streams additionally show diurnal fluctuations lowering the discharge during the day when water is most needed. Unfortunately, only little research has been done on diurnal stream flow fluctuations in mountainous catchments and processes causing the fluctuations are not yet completely understood.

The abundance and the locations of subsurface water resources are highly unknown in the catchment. There are a few wells installed but no network of piezometers to monitor the developing of groundwater levels. Without information on water tables it is impossible to quantify storage capacities and potential recharge of subsurface storages. Uncertainty is added by the fact that aquifer recharge does not directly correlate with the amount of rainfall. Intensity and duration of rain events highly differ and impact the infiltration rate of the soil.

In summary, there is only little knowledge about the catchment hydrology and the dominant processes at the different scales. Hydrological processes and their interactions are neither well described nor completely understood yet. Also the links between different water bodies are more or less unknown. The rudimentary information on rainfall and discharge is not sufficient for reliable predictions in terms of runoff generation and recharge of water resources. The lack of data and monitoring equipment complicated the learning process in the past and still poses a big challenge for future research.

1.4 Objective of research

The main objective of this research is to develop an overall understanding of the catchment hydrology in the South Pare Mountains. With respect to the fact that the whole catchment is poorly gauged and time and resources are limited, a small-scale subcatchment within the South Pare Mountains is chosen for investigations. Experiences from former studies have shown that it can be wise to start from a small scale in order to truly understand the complicate interactions of hydrological processes. A small-scale catchment furthermore allows to install a dense network of measuring equipment and gauging stations to overcome problems with spot data collection. The study aims to execute multiple measurements in small distances and to monitor hydrological parameters in short intervals as this provides fundamental structure for understanding runoff production [McGlynn et al., 2004].

It is intended to develop a basic idea of how to quantify hydrological processes in the catchment applying a multi-method approach [Blume et al., 2008]. The underlying idea of this approach is the combination of data from separate measurements to better understand and to explain unexpected or unknown responses. Multi-method approaches have been applied in several studies executed in ungauged basins as they allow more reliable conclusions without having long-term data series. Further advantages are the possibility to link different processes and to create a conceptual model of the catchment hydrology.

Besides the understanding of hydrological processes some specific goals have been defined for the research. Since the time frame of the study covers the whole rainy season, a focus is set on the comparison of runoff generation during base-flow and during stormflow. The most important objectives during base-flow conditions are outlined in the following list:

- investigation of diurnal stream flow fluctuations,
- identification of flow paths, water storages, and source areas, and
- a conceptualisation of dominant hydrological processes.

During rain events when storm-flow is expected to alter the hydrological regime, additional objectives can be defined, including

- understanding of runoff generation responses and
- quantification of runoff contributions during storm-flow.

The research is designed as a descriptive study that focuses on explanations of hydrological phenomena and process understanding. In the first instance the aim is to gain insight into both, surface and subsurface flow processes. For instance, soil saturation will be explored to make statements about infiltration paths and residence times. In the second instance an improved understanding of catchment responses shall be developed, analysing hydro chemical data collected in the stream during rain events. Two separate sub-catchments will be investigated for comparative analyses. In the third instance a simplified water balance will be set up to roughly quantify flows and subsurface fluxes within the catchment.

In summary, the expected information can extend the knowledge about the abundance, the recharge and the quantities of the available water resources. Besides the scientific outcome, the results are of great value for the people living in the region because it can help to avoid problems arising with potential shortcuts in water supply.

Chapter 2

Study area

The study has been carried out in the South Pare Mountains in northern Tanzania. The mountain range is part of the Eastern Arc Mountains and is located in the Pangani river basin (Fig. 2.1). The Pangani river collects water from the Kilimanjaro massif and the Pare and Usambara mountains flowing in south-eastern direction and discharging into the Indian ocean. The Pare Mountains are a fertile and densely populated area because it receives more rainfall than the vast, dry savanna to the west. The people living in the Pare mountains are mainly subsistence farmers, keeping livestock and growing crops. The population concentrates in the lowlands of the mountains. However, population pressure forces people to move and to cultivate the steep slopes in the uplands. The hilltop areas of the mountains are declared as forest reserve, where land use is restricted.

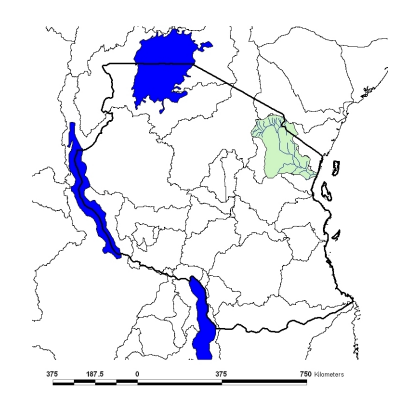


Figure 2.1: Catchment area of the Pangani Basin

2.1 Makanya catchment

2.1.1 Topography

The Makanya catchment is a 300 km² large catchment nested in the Pangani Basin draining the South Pare mountains in western direction. It is mainly mountainous area with a river valley stretching from north to south (Fig. 2.2). The elevation ranges from 800 m a.s.l. in the lowlands to above 2000 m a.s.l. in the upper areas closer to the ridge. The Shengena Peak marks with 2460 m a.s.l. the highest point in the South Pare Mountains. The mountain range is composed predominantly of weathered igneous rocks and superficial deposits [Bagnall, 1963]. Metamorphic transformations in the region led to strong foliation of the underlying meta-igneous rocks and created geological faults. These faults are orientated towards the eastern edge of the range and influence the subsurface flow systems in the catchment [Mul et al., 2007a]. The superficial deposits are different depending on their spatial occurrence. The soils in the forested hilltop areas and on the connected slopes are of reddish-brown and dark-reddish colour and are composed of loamy silts with clay fractions. On the steep slopes below the rim of the mountain range coarse material of yellow colour resulting from weathering processes dominate the superficial soils. These deposits are often interrupted by limestone outcrops, where deposits have been eroded. The lowlands at the foot of the range consist of red alluvial soils sedimented by floods [Mul et al., 2007a]. These soils resulting from erosion and deposition are fertile and allow wide agricultural land use in this area.

The rainfall in the catchment is drained to the eastern and the western side of the Pare Mountains joining the main Pangani river system some 50 km downstream. However, surface water rarely reaches the outlet of the catchment as infiltration and periodic flooding of non-draining swamp areas capture the runoff generated in the highlands [PBWO, 2006]. The soils in the floodplains of the river valley are made of highly permeable sands and deposits that facilitate fast infiltration and recharge of alluvial aquifers. Four perennial rivers flow towards the Makanya valley draining the western slopes of the mountains. One of these rivers is the Vudee river with an associated meso-scale catchment covering an area of approximately 22.5 km². The Vudee is split into two smaller catchments, the Ndolwa catchment and the upper-Vudee catchment (Fig. 2.2).

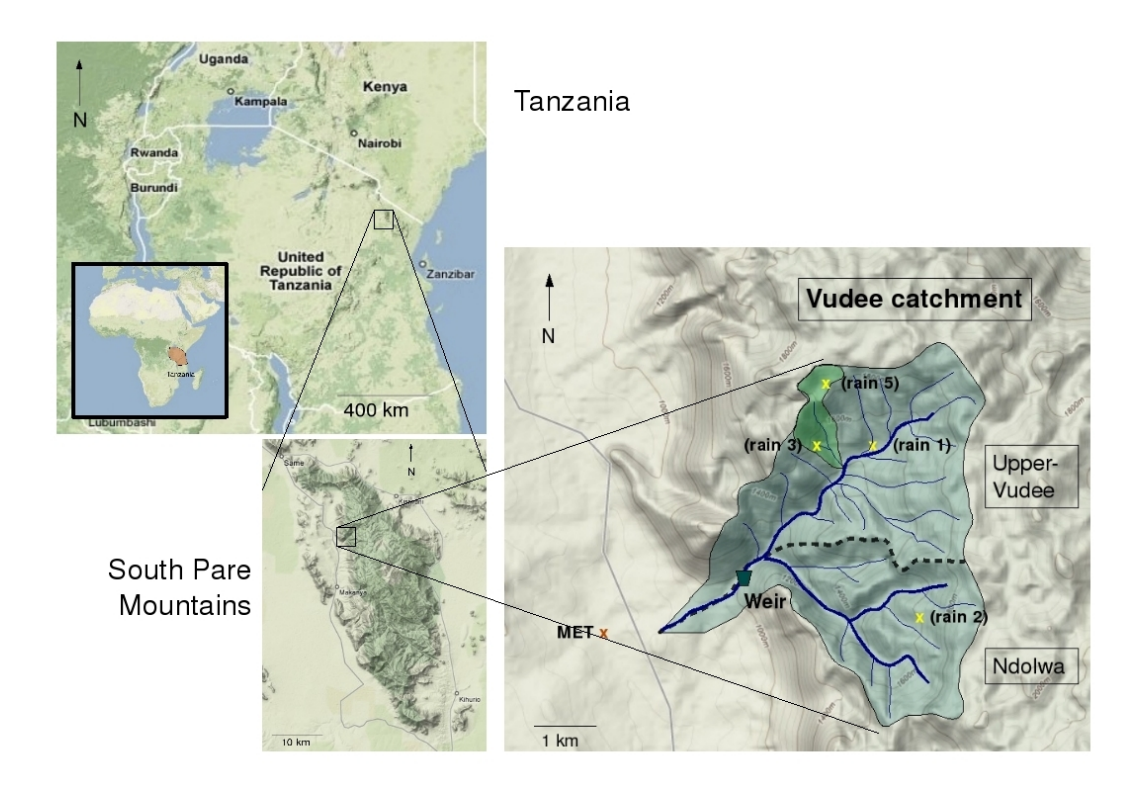


Figure 2.2: Location of the Vudee catchment

* A yellow x in the map indicates an automatic rain gauge and the MET sign is the location of the first order weather station in Bangalala

2.1.2 Land use

The upper areas of the mountains are mainly forested with deciduous woodland and dense fern vegetation. The hilltops are closely covered with forest, whereas in moderate elevations the forest concentrates along the streams where most water is available. The areas around the forest are despite the steep slopes increasingly used for cultivation of vegetables and crops. The local people are living predominantly of subsistence farming facing challenging transformations in the near future. In particular, fast population growth and decreased yields have put pressure on the existing agricultural plots. As a result more and more forested areas have been cleared for conversion into agricultural land. The previously forested areas are temporary fertile, due to organic top soils that

allow good yields on a mid term. However, deforestation leads to irreversible loss of fertile soils because missing tree root systems can not prevent soil erosion anymore. At this stage the depletion of the natural resources has already approached a critical stage.

The dominating crops are maize and beans that are widely cultivated in the whole catchment. Besides, the humid forested slopes are used to grow vegetables, root vegetables and bananas. In the lowlands of the catchment agriculture is applied on a larger scale. There is a necessity for supplementary irrigation as the rainfall in the lowlands is significantly lower and direct solar radiation evaporates a great portion of the soil moisture. The cultivation cycle is aligned with the rainy seasons as irrigation alone is not sufficient to grow water intensive crops such as maize. In the river valley the ubiquitous water scarcity is the limiting factor of crop yields as soils in the fluvial topography are generally fertile. The widespread farming impacts the natural environment and consumes great parts of the available land. In addition to the crop farming, livestock farming with goats and cattle is widespread in the Makanya catchment that contributes the depletion of natural resources.

2.1.3 Climate

The Makanya catchment is classified as a semi-arid region with high spatial and temporal rainfall variability. In Fig. 2.3 two climate diagrams from the first order weather station in Bangalala (Fig. 2.2) are shown. The diagrams are based on annually data from the extreme years 2005 and 2006, illustrating the time variations of temperature and precipitation. In both cases the temperature variation curve is fairly stable with maximum values in January and February. This indicates a rather diurnal than annual temperature cycle. In contrast, the rainfall varies both in occurrence and amount. In 2005 the total amount of rainfall was 300 mm and 846 mm in the following year. The standard deviation of the monthly rainfall in the period from 2004 to 2008 ranges between 1.7 mm in July and 84.7 mm in December. The available rainfall data starting form 2004 clearly can not represent average rainfall patterns since the data series is too short. An approximate value for the mean annual rainfall is 570 mm in the lowlands and 660 mm in the highlands of the mountains [Mul et al., 2006]. Despite the great variations, two rainy seasons per year can be identified in the diagrams. The short rainy season called 'Vuli' occurs between October and December and the long rainy season 'Masika' between

March and May. The rainfall is often erratic and interrupted by long and frequent dry spells [Enfors and Gordon, 2007]. These dry periods are distinguished into a dry, hot period in January and February and a dry, cool period after 'Masika'. The diagrams also display the challenges for the farmers in the Pare Mountains. During the wet season in the year 2006, five months indicated humid conditions according to Walter and Leith [1960–1967]. In contrast, in the previous year humid conditions were only achieved in March and the rest of the year was burdened with arid weather conditions.

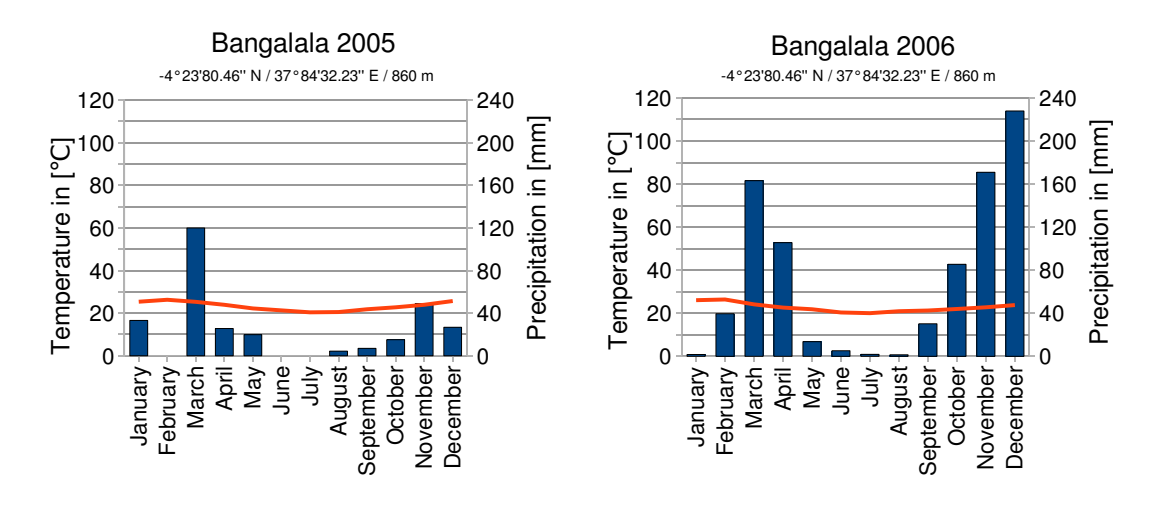


Figure 2.3: Climate diagrams for Bangalala

Besides the precipitation, the evaporation has a large influence on the climatic conditions as it controls the loss of moisture. In the three year period between 2005 and 2007 the potential evaporation reached an annual average of 2331 mm (Tab. 2.1). This value exceeds the mean annual precipitation by factor 4.4 and is another indication for the arid conditions outside the rainy seasons. Interestingly, the highest evaporation goes together with the lowest precipitation in the year 2005 and the inverse dependency is observed in the following year. This leads to an exceptional ratio of 1:8.1 between precipitation and evaporation in 2005 and demonstrates the exacerbation of the farming conditions during this year.

	2005	2006	2007	mean	std dev	Masika 08
Precipitation [mm]	300	847	447	531	282.7	271
pot Evaporation [mm]	2431	2180	2381	2331	133.1	1027
pot Transpiration [mm]	2051	1826	1998	1958	117.7	861
ratio P : E	1:8.1	1:2.6	1:5.3	1:4.4		1:3.8

Table 2.1: Annual precipitation and evaporation at Bangalala weather station

The potential evaporation and potential transpiration has been computed with the Penman and Penman-Monteith equation respectively. These sets of equations are the standard method of the United Nations Food and Agricultural Organisation (FAO) to model evapotranspiration [Allen et al., 1998]. The Penman equation is used for the calculation of the potential open water evaporation. In practice, the potential evaporation is never reached as water availability in the soil is restricted. Furthermore, soils and vegetation reflect a greater part of the incoming radiation and have a lower atmospheric conductance depending on the type of vegetation. The Penman-Monteith equation takes some additional factors into account leading to the potential evaporation from vegetation canopy, also denoted as potential transpiration. Both equations require daily mean temperatures, wind speed, relative humidity, and solar radiation. The Penman equation for the open water evaporation is presented in Equ. 2.1 [Allen et al., 1998],

$$E_{pot} = \frac{\Delta(R_{net,water} - G) + \rho_{air} * c_p * \frac{(e_{sat} - e_{actual})}{r_{aero}}}{\rho_{water} * \lambda (\Delta + \gamma)}$$
(2.1)

where E_{pot} is the potential evaporation in mmd⁻¹. $R_{net,water}$ is the difference of the incoming short-wave radiation and the outgoing long-wave radiation and G represents the soil heat flux. The density of air at a constant pressure is expressed with ρ_{air} and the specific heat capacity of air with c_p . The next term (e_{sat} - e_{actual}) considers the vapour pressure deficit and r_{aero} is the aerodynamic resistance. The terms in the denominator are the latent heat of vaporization λ , the slope of the saturation vapour pressure curve Δ and finally the psychrometric constant γ .

The following Penman-Monteith equation (Equ. 2.2) is used to calculate the potential transpiration of forests or cultivated areas. Each land use has specific coefficients and consequently the results are only representative for a reference vegetation, for instance grass land. The equation takes a higher plant-specific albedo coefficient into account and also includes a term respecting the higher surface resistance compared to open water.

$$E_{t,pot} = \lambda * T = \frac{\Delta (R_{net,soil} - G) + \rho_{air} * c_p * \frac{(e_{sat} - e_{actual})}{r_{aero}}}{\Delta + \gamma (1 + \frac{r_{surface}}{r_{aero}})}$$
(2.2)

T is the transpiration in mmd^{-1} with a specific net radiation of $R_{net,soil}$. The surface resistance is represented by the term $r_{surface}$ in the denominator. For a complete explanation of all terms and sub-equations please refer to Mul [2008].

2.2 Study headwater catchments

The study was carried out in two sub-catchments in the upper-Vudee catchment, locally called Kiwene and Chamasae (Fig. 2.4). These headwater catchments are both less than 1 km² large. The exact surface area and stream lengths are presented in Tab. 2.2. They are both orientated in southern or southeastern direction receiving sunshine only from late morning till early evening depending on the season. The hillslopes range from 1400 to 1950 m a.s.l. with generally steep slopes. The two adjoined catchments have similar geological features whereas the land use differs.

	Surface Area	Stream length	Flowing stream length
	[ha]	[m]	[m]
Kiwene complete	68.0	1320	1320
Kiwene forest	29.3	950	950
Chamasae	28.8	900	330

Table 2.2: Surface area and stream lengths of the two study catchments Kiwene and Chamasae

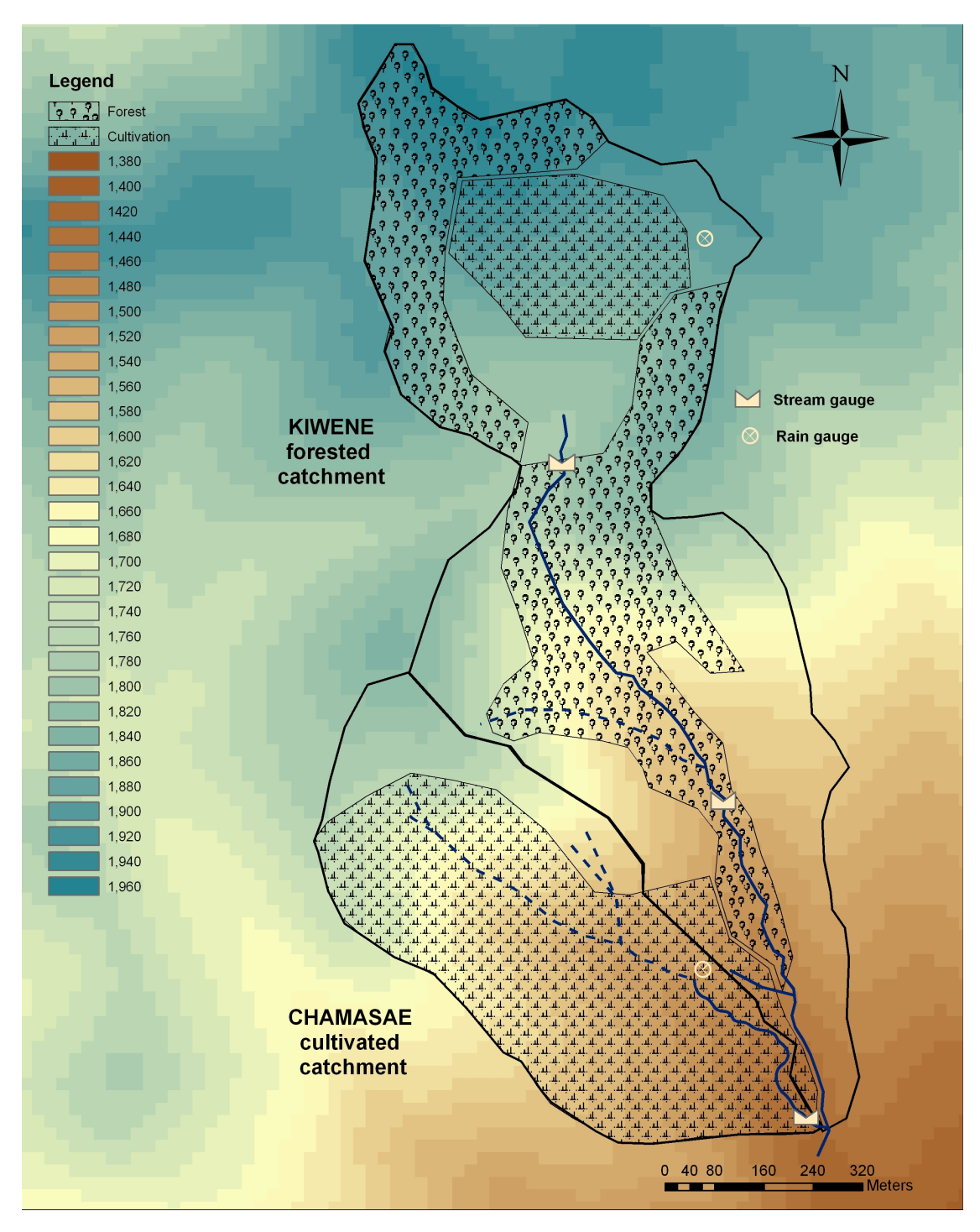


Figure 2.4: Map of the two study catchments

The smaller Chamasae catchment is cultivated land on steepest slopes with an average gradient of 40 %. The loamy soils with clay portions in places are fertile and enable good crop yields. The dominant crops are beans, bananas, and partially maize. Despite the steep slopes and the lack of big trees, soil erosion does not occur, thanks to artificial prevention measures. Terraces and all-season scrub lines hamper runoff and simplify infiltration of rain water at the same time. There is no spring visible in the catchment resulting in a dry stream-bed except for the rare rain events. Only the last section of the streambed flows perennially. The water originating from subsurface flow networks appears at a small rock outcrop (end of dashed line in Fig. 2.4).

The Kiwene catchment is divided by a steep mountain ridge. In Fig. 2.4 a 3Delevation model was applied where the graduated colours uncover the steep gradients in the area. Uphill the rim the land is less steep and predominantly used for crop farming. The plots are surrounded by tropical rain forest and swamplands. The vegetation is generally wetter, due to conspicuously higher rainfall and a rather flat topography that allows water to accumulate in the soil. In a small basin close to the ridge two small springs were found surrounded by swampland and exfiltration ponds. These springs feed the Kiwene stream year-round and provide water supply for the populated areas downstream. The slopes downhill the ridge are densely forested along the stream alternating with small agricultural zones in between. These cultivated islands are planted with bananas, beans and often sugar cane. The partition of forest and cultivated land is also illustrated in Fig. 2.4, where the different hatchures denote the land use as it is indicated in the legend. The soils in the forested catchments are composed of coarser material compared to the cultivated catchment. Particularly in the upper layers of the soil, loose material with sandy loam fractions were found. However, the material close to the stream is rather silty with clay lenses incorporated, where debris flow was frequently observed. This diffusive exfiltration occurs along the entire stream continuously increasing the discharge of the stream. In addition, two small springs were identified in the downstream section of the catchment. The Chamasae and Kiwene stream coalesce at the outlet of the sub-catchments with Kiwene stream contributing the bulk of discharge.

2.3 Local rainfall patterns

The micro-climate of the study catchments is stamped with a high spatial variability of rainfall. The relevance of rainfall to runoff generation gives reason for a closer look on the rainfall pattern within the catchment. One automatic rain gauge is located on the border between the two study catchments Kiwene and Chamasae (Fig. 2.4). This rain gauge called 'Chamasae' represents the rainfall for the lower parts of the study catchments but may be vague for the region above the ridge. On this account a second gauge called 'Kiwene' has been installed close to the uphill boundary of the Kiwene catchment (Fig. 2.4). The locations of other gauging stations are revealed in Fig. 2.2.

The daily rainfall recorded at Chamasae and Kiwene gauge is demonstrated in the following graph Fig. 2.5. Despite the small distance of 1000 meters between the two gauges the difference is remarkable. The rain gauge in Chamasae received during some days in Masika 2008 only 60–70 % of the rain recorded in Kiwene. Moreover, the rainfall on April 19th with 14 mm at Kiwene seems to not even reach the rain gauge downhill. Less than 1 mm rainfall were recorded here during this event. The great variation evidences highly localised rainfall in the area.

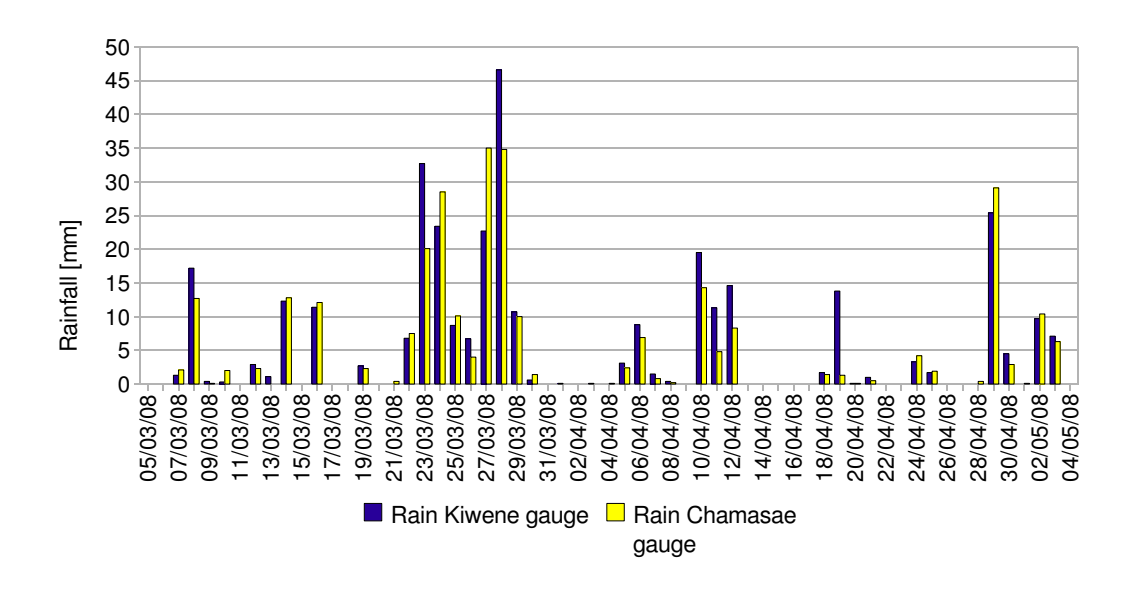


Figure 2.5: Comparison of daily rainfall during Masika 2008

The spatial rainfall variability has some more distinctive features. For instance, the total monthly rainfall shown in Tab. 2.3 gives evidence for a relation between altitude and rainfall. In every month during Masika 2008 the highest located rain gauge in Kiwene received most rainfall. The order of declining rainfall in March corresponds to the lower elevations of the rain gauges with Vudee station as the lowest. However, the difference in altitude of the Vudee and Chamasae gauge is rather small and consequently the stations appear to have similar rainfall amounts.

	Vudee	Chamasae	Kiwene
	(1390 m)	(1540 m)	(1920 m)
March 2008 [mm]	178.7	200.8	212.6
April 2008 [mm]	84.5	79.6	110.9
May 2008 [mm]	28.5	24.2	33.9
Masika 2008	291.7	304.6	357.4

Table 2.3: Elevation dependency of rainfall in the Vudee catchment

A good description for the spatial variability are the correlations of the daily rainfall series. In Fig. 2.4 the correlations between the four rain gauges in the Vudee catchment including the rain gauge in Ndolwa are displayed. The correlations have been computed for days with more than 5 mm of rainfall. The highest correlation was found between the gauges Vudee and Chamasae which are closest to each other. The lowest correlation was obtained comparing Kiwene and Ndolwa, the rain gauges in the greatest distance (Fig. 2.2). In general, the correlations indicate a high rainfall variation considering the small distance of a couple of hundred meters up to a few kilometers in between the rain gauges.

	Vudee	Chamasae	Kiwene	Ndolwa
Vudee		0.945	0.736	0.782
Chamasae			0.852	0.754
Kiwene				0.682
Ndolwa				

Table 2.4: Correlation of daily rainfall data

Chapter 3

Methodology

3.1 Outline

The study was designed to investigate runoff generation and hydrological processes in steep headwater catchments. The above described Kiwene and Chamasae catchments have been selected for this purpose. The data collection in the field has been done from February to May 2008 covering the complete 'Masika' rainy season. The hereby applied methodology is split into two separate parts. The first part deals with the investigation of hydrological processes during base-flow conditions. It includes discharge measurements, monitoring of soil moisture contents and groundwater levels, as well as hydro chemical water quality analysis. Some of the measurements were executed continuously over whole Masika season in order to detect seasonal changes and to identify short-term influences, for example rain events. An emphasis of the study was laid on the verification and explanation of diurnal discharge fluctuations. The second part of the field work deals with the storm-flow investigation. The runoff generation during rain events is the concurrence of complex surface and subsurface flow processes that requires diligent and frequent data collection. The investigation is based on stream sampling and analysis of hydro chemical and hydro physical parameters. Furthermore, the samples have been examined on environmental isotopes to obtain information on the origin of the runoff water. Hydrograph separation was applied to identify runoff components and to quantify the contributions of potential end-members.

3.2 Components of field campaign

3.2.1 Stream flow gauging

The runoff is an elementary variable investigating catchment hydrology. In previous studies the discharge was recorded at the outlet of each catchment to examine stream flow fluctuations. For Masika 2008 these two stream gauges ('Kiwene forest gauge' and 'Chamasae gauge') were reactivated and a third stream gauge was constructed at Kiwene headwaters. This additional gauge ('Kiwene spring gauge') is located upstream the mountain ridge just before the streams enters the steep forested slopes (Fig. 3.1). The expanded discharge measurements at different stream points will follow up the previous studies on the diurnal discharge fluctuations and will provide supplementary information on the inflows from adjacent hillslopes. The stream discharge data is also the most important input quantity for the subsequent event investigation.

The gauging stations were constructed as compound weirs consisting of 90° V-notches. The water level is recorded with pressure transducers, measuring the hydraulic head in 15 minute intervals in a defined depth next to the notch. The principle is a twin-sensor measuring the hydraulic pressure with a submerged sensor as well as the atmospheric pressure above the stream. The difference in pressure gives the exact water head. In order to ensure exact measurements the sensor has to be cleaned and re-adjusted regularly. Therefore, the level is also read manually with a calliper rule and the values are used for the correction of the digital logger data. The corrected hydraulic heads are then transformed into discharge with the following notch formula,

$$Q = 1.341 * h^{2.48} \tag{3.1}$$

where Q is the discharge in m^3s^{-1} and h is the hydraulic height above the notch in meter. The function has been found with empirical values from Bos [1989] listed in App. A.1. The discharge for notch levels $h < 0.05 \, m$ had to be extrapolated, due to data unavailability. The results of the formula have been verified on-site using different field methods such as bucket measurements and salt dilution tests. The results of the verification are attached in App. A.3.

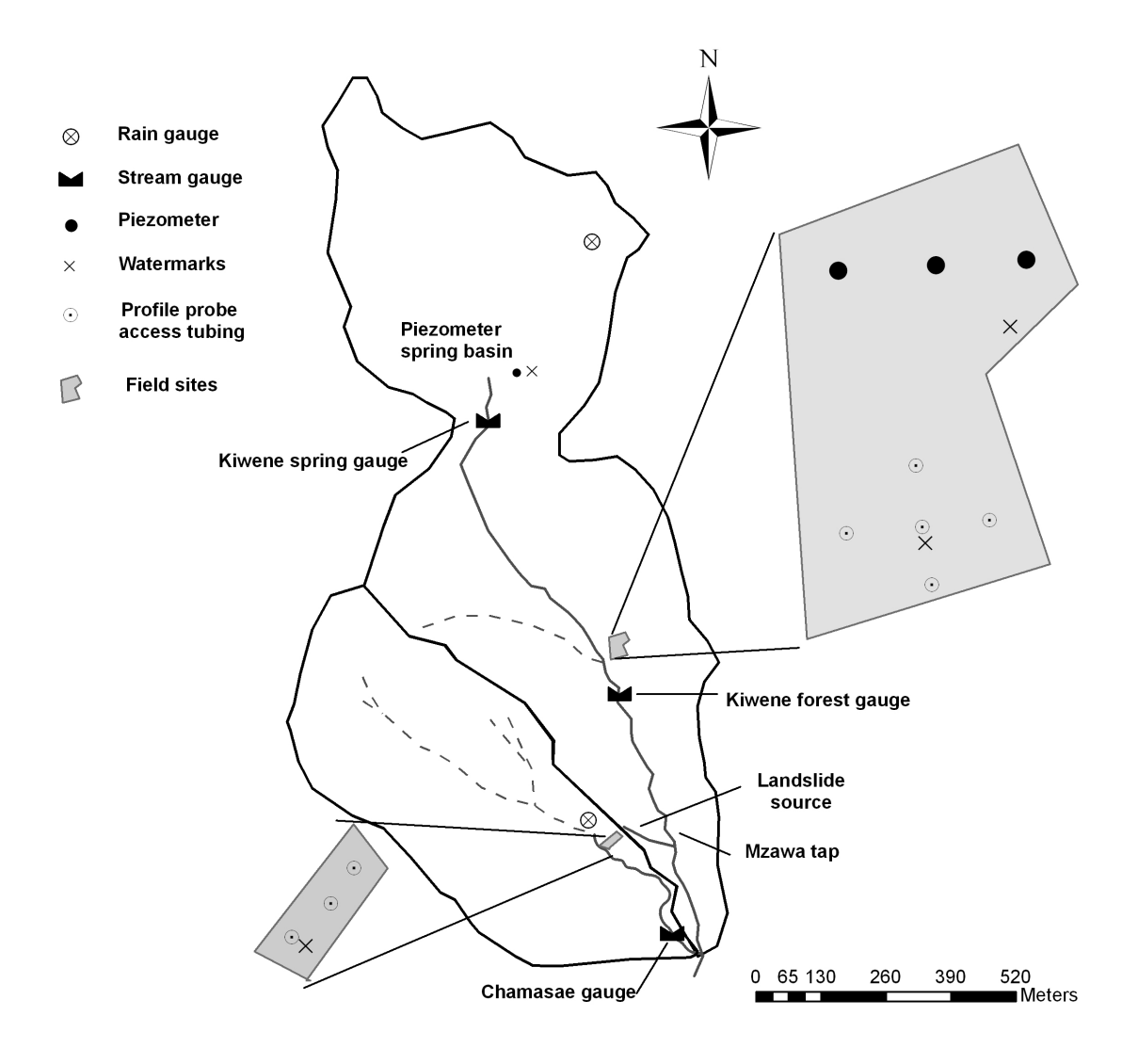


Figure 3.1: Map showing the locations of the measuring equipment at the two study catchments

3.2.2 Soil moisture monitoring

In order to investigate the subsurface processes in adjacent hillslopes to the stream, numerous soil moisture measurements have been conducted. The time variation of soil moisture contents provides valuable information on the infiltration rate and the percolation depth of rain water. Therefore, an accessible study site of 1130 m² has been selected 100 m upstream the forest stream gauge in the forested catchment. In Fig. 3.1 all gauging stations and the field sites including the complete setup are mapped. The forest site in the Kiwene catchment has some unique characteristics in terms of vegetation, soil properties and location to the stream, that particularly qualifies it for measurements. Regardless of the steep slopes in the forest, the site is planted with scattered bananas and yam plants in between tall trees. These crops have a high leaf area index (LAI) indicating a high water consumption. This circumstance let expect to find fairly high soil water contents. Furthermore, loamy-silty soils give reason to a high field capacity. At the foot of the site, diffusive inflows were observed resulting from lateral fluxes towards the stream. The soil moisture dynamics have been monitored with a combination of two sets of watermarks and a profile probe. One watermark was installed proximate to a large tree to provide an insight into potential root system influences. The other watermarks and access tubing for the profile probe were placed as it is outlined in Fig. 3.2.

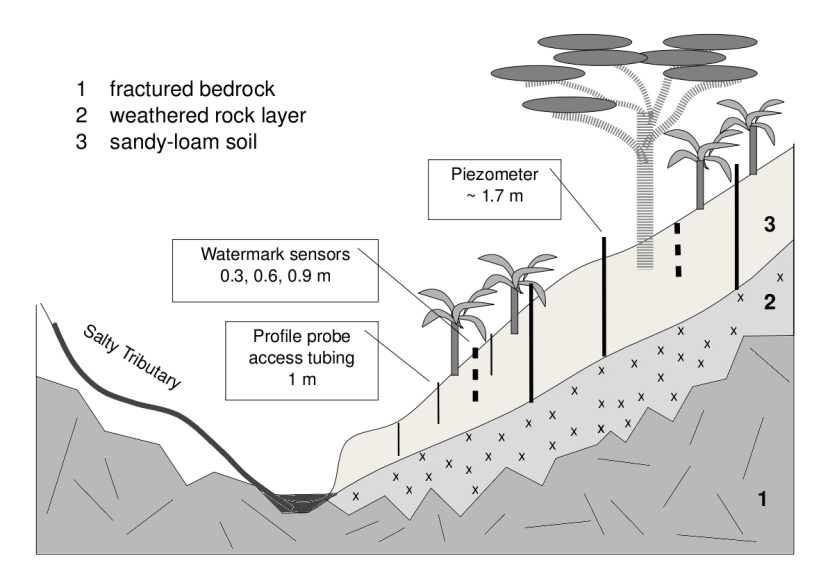


Figure 3.2: Lateral cross section of forest study site with installations

An appropriate site has been selected in the Chamasae catchment. Similarly, watermarks and profile probe access tubing have been installed in a lateral transect close to the stream (Fig. 3.1). Unlike the forested site, here the probes are placed within a plot cultivated with sprouting beans, where the soil is exposed to solar radiation and rainfall without canopy. More watermarks in conjunction with a piezometer have been installed in the spring area of Kiwene upstream the ridge. All the soil measurements were executed on the plot-scale in order to get a spatially high-resoluted insight into the subsurface processes.

Watermarks

The watermarks are used to continuously monitor soil saturations in the ground. Three sensors are wired in soil openings measuring in 0.3, 0.6 and 0.9 meter depth (Fig. 3.3a). Each sensor consists of two concentric electrodes embedded in a reference matrix material [Chard, 2005]. If soil water diffuses inwards or outwards the matrix, the electrical resistance between the electrodes changes and is detected by the sensor. The electrical resistance can then be converted to soil water potential. The conversion is complex as the relation is non-linear and soil-specific. In theory, for each soil type a calibration with an accurate water potential gauge such as a tensiometer should be done in the run-up of the measuring campaign. However, there was neither the equipment nor the resources to complete the full calibration. On this account the calibration was done with data from the profile probe, but the results should be interpreted only qualitatively due to technical uncertainties. The results of the calibration can be found in App. B.1. In this application the watermark sensors are connected to data loggers and record the soil water potential in 30 minutes time steps. The short intervals produce a high resoluted time variation of the soil water during events and over the whole Masika season.

Profile probe

The soil moisture contents have also been measured with a profile probe (Fig. 3.3c). This additional method is based on discontinuous measurements but delivers saturation profiles of the soil. It measures in defined depths between 100 and 1000 mm. The probe itself is portable but it needs suitable access tubing where the probe can be inserted.







Figure 3.3: Images of (a) watermark sensors, (b) tree at forest site, (c) profile probe with access tubing

Several 1 m profile probe access tubes have been installed in either catchment. The output data of the probe is optional but can be set to Vol % saturation after defining the soil type. Some of the access tubes have been installed in direct vicinity to the watermark sensors in order to calibrate the watermark readouts. The profile probe is appropriate for calibration purposes because they produce reliable results with a high accuracy of \pm 3 % according to DeltaT-Devices [2001].

The measuring principle of the profile probe is illustrated in Fig. 3.4. Once the probe is inserted into the access tube it creates a high-frequency signal that is applied to the pairs of steel rings affixed in different depths of the probe. This signal creates a horizontal electromagnetic field that extends 100 mm into the soil matrix. The surrounding soil operates as a dielectric whose immobile charge carriers are polarised by the electromagnetic field. The response to the polarisation is soil specific and dependent on the properties of the dielectric. The water content of the soil determines these properties as water has an exceptionally high dielectric constant ε compared to soil or air. Depending on the dielectric properties the signal is reflected to the probe where it forms together with the outgoing signal a standing wave [DeltaT-Devices, 2001]. The voltage of this wave is measured by the probe and can be converted directly into the soil moisture content.

The conversion is of course different for each soil type. For this application a predefined calibration for an organic soil type has been used that is shown in Equ. 3.2.

$$\theta_{org} = -0.084 + 1.77 * V - 3.88 * V^2 + 9.42 * V^3$$
(3.2)

$$\theta_{org} = \frac{V_W}{V_S} \tag{3.3}$$

 θ_{org} is the volumetric soil moisture content in Vol % which is defined as the ratio of the volume of water contained in the soil sample V_W and the total volume of the soil sample V_S . V represents the voltage measured by the probe.

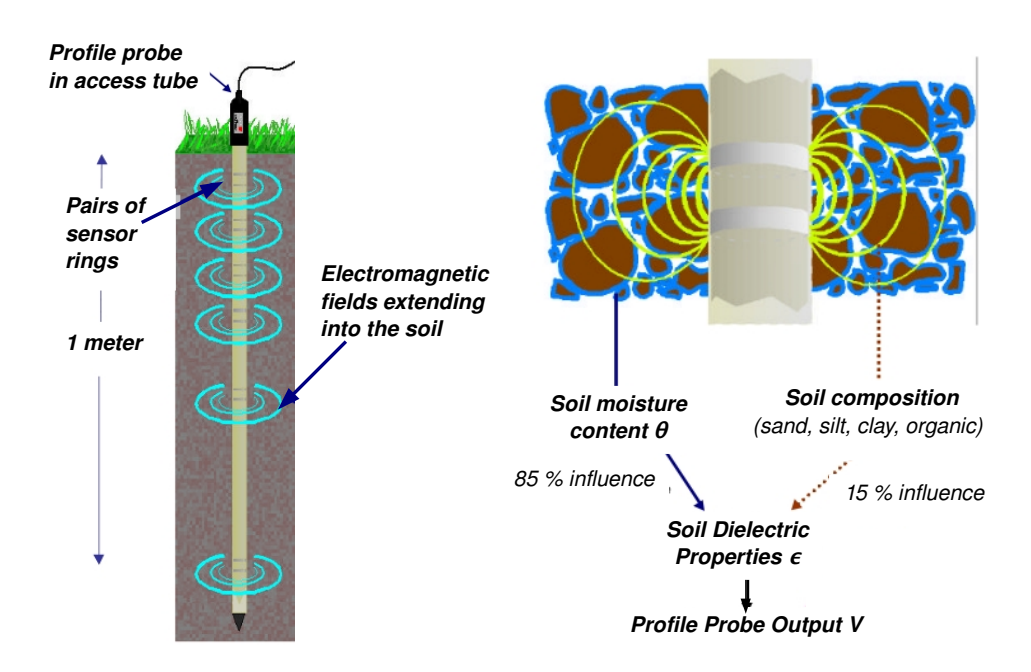


Figure 3.4: Measuring principle of Profile Probe [DeltaT-Devices, 2001]

Piezometers

Three aligned piezometers have been drilled at the forest study site in the Kiwene catchment (Fig. 3.1). The filtered PVC tubes have been built-in at 1.7 meter depth prior to the rainy season. At 1.7 meter depth a solid layer of weathered rock was hit and further drilling became unfeasible. The piezometers were intended to observe the groundwater level during Masika. However, at beginning of the season the boreholes were dry. Another piezometer tube was installed in the swampy vicinity of the Kiwene spring upstream the mountain ridge. The tube is built-in at 2.2 meter depth finding the preseasonal groundwater table at 0.8 m below the surface. The water level is measured with a pressure transducer in combination with manual readings.

3.2.3 Longitudinal transects of hydro chemistry

The hydro chemistry of the Kiwene and Chamasae stream has been examined prior to, during and after Masika season. The parameters electrical conductivity (EC), pH and temperature have been measured in-situ with portable EC and pH-meter (Fig. 3.5). Longitudinal transects from the source to the confluence of the two streams show the developing of these parameters along the stream including significant changes. Leaps in EC are an indication of potential subsurface sources with different hydro chemical signatures. Wherever sources along the stream were identified, a more detailed chemical analysis of the source water has been undertaken. The water samples were examined in the laboratory on major ions, dissolved silica and isotopes. For an exact description of the chemical analysis please refer to Section 3.3.2. In addition, the contributions from the sources were attempted to be quantified. Water samples were collected from the source itself and from upstream and downstream the inflow. The respective concentrations allow an exact quantification of the source contribution. The calculation is based on mass-balance equations (Equ. 3.4 and Equ. 3.5),

$$Q_{dstr} * c_{dstr} = Q_{upstr} * c_{upstr} + Q_{source} * c_{source}$$
(3.4)

$$Q_{dstr} = Q_{upstr} + Q_{source} \tag{3.5}$$

where Q is the discharge in ls^{-1} and c is the electrical conductivity in μScm^{-1} .





Figure 3.5: Images of EC and pH meter and sensors

3.3 Stream sampling during rain events

3.3.1 Sampling procedure

The forest notch in the Kiwene stream was selected for event sampling. The notch is easy accessible and has a clear geometry for precise discharge calculations. The sampling is made up of three parts. In a first step daily morning samples are taken in combination with manual water head measurements to obtain a reference sample prior to the event. Immediately after the beginning of a rain event, runoff samples are taken in 1–2 hour intervals as rainfall often has short-term varying intensities. The samples are later analysed on major ion concentrations, dissolved silica and isotope composition (see Section 3.3.2). Concurrent with the sampling the electrical conductivity and the pH value is measured in-situ with a portable EC meter and the hydraulic head is pinpointed with a calliper rule. In-situ measurements are needed as reference data for the analysis in the lab. In a third step the recession is sampled in larger time steps, in the ideal case until the hydraulic head has reached the initial height.

The sampling series have been executed with all major events during Masika 2008. As the number of rain events are limited and often unpredictable even smaller events around 20 mm of rainfall were investigated. The series total in most cases ten samples excluding the morning sample of the previous day.

3.3.2 Chemical analysis

The water samples have been analysed in a field laboratory in Makanya. The quantification of the ion contents has been realised with alkalinity titrations. Due to difficulties with the equipment on location, only hydrogen carbonate (HCO_3^-), Magnesium (Mg^{2+}) and Calcium (Ca^{2+}) have been examined. The amount of HCO_3^- ions was determined utilising sulfuric titration. In a first step a few drips of Bromocresolgreen-methylred indicator were added to the water sample. Then the water sample was titrated drip by drip with sulfuric acid (H_2SO_4). The sulfuric acid dissociates in water creating hydronium ions that in turn react with the hydrogen carbonate ions to carbonic acid (Equ. 3.6 and Equ. 3.7). As soon as no hydrogen carbonate ions are available anymore, the free hydronium ions let the pH value instantaneously drop. This point can be observed because the indicator reacts with a colour change to pH decline. The number of added drips of sulfuric acid can ultimately be calculated back into HCO_3^- concentration in [mgl^{-1}]. The parameter HCO_3^- is not stable and an immediate analysis after collecting the sample is crucial in order to avoid an adulteration of the chemical constitution.

$$H_2SO_4 + H_2O \rightleftharpoons HSO_4^- + H_3O^+$$
 (3.6)

$$HCO_3^- + H_3O^+ \rightleftharpoons H_2CO_3 + H_2O$$
 (3.7)

The cations Mg^{2+} and Ca^{2+} are analysed with analogous titrations, but using Na_2EDTA as titration solution and different indicators. The procedure of calculating the initial ion concentrations in [mg Mg^{2+} l⁻¹] and [mg Ca^{2+} l⁻¹] respectively, follows the same way as HCO_3^- but using different coefficients. The EC is measured with an electrical conductivity meter in [μ Scm⁻¹].

The concentration of dissolved silica has been determined with a portable photometer (Fig. 3.6 a) measuring the specific colour of silica compounds after adding some reagents. First, two small cells are filled with the water sample of which one is put aside as a reference sample. To the other cell two powder pillows containing an acid reagent and molybdate ions are added. The silica and phosphate molecules in the sample conjoin under acidic conditions with the molybdate to yellow silicomolybdic and

phosphomolybdic acid complexes. In the next step a citric acid is added that destroys the phosphate complexes. The remaining silicomolybdic complexes produces a yellow colouring of the sample. Both cells are then measured with the photometer and the difference gives the amount of silica molecules (SiO_2) in [mgl⁻¹]. An important point to consider is a short holding time especially in case of high loads of suspended solids in the sample. The adherent silica molecules go slowly into solution altering the real concentration of dissolved SiO_2 molecules at the sampling time. In order to get reliable results a prompt analysis in the laboratory is most advisable.







Figure 3.6: Images of (a) photometer (upper left), (b) isotope sampler (upper right), and (c) isotope analyser (lower)

The isotope analysis is more sophisticated and requires high-tech devices. This part of the chemical analysis was done a couple of weeks after the field work in a well equipped laboratory in the Netherlands. The water samples have been analysed on Deuterium (²H) and ¹⁸Oxygen (¹⁸O) isotopes using an H₂O Isotope Analyser (Fig. 3.6 b, c). The principle is an off-axis integrated-cavity output spectroscopy. The procedure of the analysis is largely automated. The sample cells are assembled in the device in a pre-

assigned order and the scheme of testing has to be programmed. The field samples are analysed alternating with standard samples. The standard samples have different isotope compositions and are used to control the precision and reliability of the analysis. For both isotopes (²H and ¹⁸O) the standard samples have specific fault tolerances. The literature proposes an error margin of 0.6 % for ²H and 0.2 % for ¹⁸O. Applying the error margins on the mean of several repetitive measurements of the standard samples the ²H isotopes seem to be more stable compared to the ¹⁸O. The range of the standard samples and the error margins are illustrated in App. C.1. In Chapter 5 mostly the ²H isotopes are presented and used for the hydrograph separation. In the automated process of analysing, the samples are injected six times whereof the first three results are deleted and the second three are averaged. The outcome of the device is the deviation of the isotopic composition compared to the Vienna Standard Mean Ocean Water (VSMOW). The deviation is calculated with Equ. 3.8 and Equ. 3.9,

$$\delta^{2}H_{sample} = \left(\frac{R_{sample} - R_{VSMOW}}{R_{VSMOW}}\right) * 1000$$
(3.8)

$$R = \frac{^2H}{^1H} \tag{3.9}$$

where $\delta^{2}H_{sample}$ is in parts per mille of the VSMOW reference. The ¹⁸O isotopes are computed in a uniform manner.

3.3.3 Hydrograph separation

Natural tracers are useful tools for the identification of flow components and subsurface flow paths. They are abundant in most hydrological systems and can provide information on flow networks of even inaccessible water bodies. In general, natural tracers are distinguished into hydro chemical tracers and environmental isotopes. The first group includes major anions (Chloride, Sulfate, hydrogen carbonate, Nitrate) and major cations (Sodium, Potassium, Calcium, Magnesium). The electrical conductivity as a sum parameter for ion concentrations is also classified as a hydro chemical tracer. The listed tracers are fast reacting and most abundant in soils. An inconvenience poses the non-conservative behaviour and the high spatial variability [Kendall and McDonnell,

1998]. One special member of chemical tracers is dissolved silica that originates from weathering of minerals. Percolating water slowly dissolves crystallised silica molecules from weathered or fractured rocks and carries the load downslope ending up in the stream channel. The silica contents are consequently dependent on the contact time and the contact surface between water and mineral as well as on the weathering resistance and the pH. This tracer is particularly suitable for the determination of flow paths and source areas [Uhlenbrook and Hoeg, 2003]. The second group comprises isotopes of different chemical elements. In hydrology the most relevant isotopes are Deuterium (²H) and heavy Oxygen (¹⁸O) [Kendall and McDonnell, 1998]. In comparison to chemical tracers, isotopes are more stable, conservative and facilitate the determination of the age of water. Isotopes are not subject to decay or similar corruption. A disadvantage of these tracers, however, is the risk of fractionation if the sample is exposed to evaporation in the moments of sampling and analysing. A very accurate operation is required to receive true results.

The total stream discharge during a rain event is composed of different contributions, for instance from groundwater inflows, surface runoff or direct rainfall into the stream. These inflows have different hydro chemical signatures and isotopic constitutions. The hydrograph separation utilises natural tracers to divide the total stream discharge into separate contributions from spatially disjoint sources. For instance, the tracer dissolved silica can help to distinguish between surface and subsurface inflows [Wels et al., 1991]. Moreover, it is possible to quantify the contributions assuming that all involved end-members were identified and taken into account. The calculation of the inflows is based on mass-balance equations giving the ratios of the flow components to the total discharge. The hydrograph separation arose by reason of the precise quantification to an elementary component of runoff generation investigations.

The hydrograph separation is distinguished into time-based separation (black-box) and geographic-source separation (white box). The first kind is a two-component separation to divide the discharge into slow and fast runoff components. In the literature this terminology is also known as event and pre-event water [Kendall and McDonnell, 1998]. This method allows first of all the temporal distinction of inflows. It utilises environmental isotopes that are able to provide information on the age, and therefore the temporal derivation of the water.

With the following set of mass-balance equations (Equ. 3.10 and Equ. 3.11) the ratios of event and pre-event water can be calculated.

$$Q_t * c_t = Q_p * c_p + Q_e * c_e \tag{3.10}$$

$$Q_t = Q_p + Q_e \tag{3.11}$$

The parameter Q represents the discharge and c is the specific tracer concentration. In the time-based separation it is usually the isotope composition of either Hydrogen or Oxygen. The subscription t, p, e indicates total stream discharge, pre-event and event water respectively.

On the other hand the geographic-source separation sheds light on the source of water contributions using mostly hydro chemical tracers. These tracers are fast-responding and vary unlike the isotopes notably in different subsurface storages. Depending on the number of end-members this separation method can be extended to a three- or multi-component separation usually differentiating between surface water, soil water or shallow groundwater and deep groundwater. The mass-balance has then three or more unknowns which requires additional equations. As a result more than one chemical parameters or isotopes have to be taken into account in a system of equations.

End-member mixing analysis

In many poorly gauged basins the hydrological processes and geological composition are only little known and as a result the number of end-members is often not guaranteed. A simple method to ensure whether the present catchment is a two- or three-component system is the end-member mixing analysis (EMMA) [Kendall and McDonnell, 1998]. If both, isotopic and hydro chemical tracer data is available, the results can be logged against each other in a scatter plot. A linear array indicates a two-component system whereas a spread array often has a third component contributing to the total discharge. However, the identification and observance of all relevant end-members is the biggest obstacle for the application of hydrograph separation. Even if all end-members were found it is often not feasible to collect pre-event samples for example of deep ground-water. In this case the contributions have to be accounted by some other means. A

second weakness are the non-conservativeness of hydro chemical tracers and the spatial variation of tracer compositions. Only if the end-members have distinct and unique tracer signatures without gradients the separation will produce reliable results.

Chapter 4

Base-flow investigations

In this chapter the results of the field measurements during low flow are presented. A broad knowledge about the base-flow generation is the basis on the way forward to a good understanding of runoff generation during events. The applied methods provide information specially on water storages, water sources and runoff paths during preevent conditions. Most of the measurements also cover some high-flow periods as they have been done continuously over the whole season. These incisions provide additional information on catchment responses and seasonal changes.

4.1 Runoff analysis

The very low base-flow discharge in both catchments pose a risk for precise measurements. As a consistency the applied methods require a fine calibration to obtain reliable results. Different techniques have been applied to verify the relationship between the notch head and the associated discharge. The notch formula is the most reliable method for discharges above $2.5 \, \mathrm{ls^{-1}}$, corresponding to a water head of $h = 0.08 \, \mathrm{m}$. Below that number the notch formula becomes inaccurate and the extrapolation for heads $h < 0.05 \, \mathrm{m}$ adds uncertainty. Salt dilution experiments and bucket tests have also been executed during base-flow conditions at the Kiwene forest stream gauge. The salt dilution experiments yield a 40 % higher discharge during low-flow compared to the calculation with the notch formula. The experiments have been repeated several times on different days without a significant change. Yet ten repetitions of the bucket test

at the notch overflow confirmed the suspicion on the uncertainty of the notch formula. The averaged discharge was found in a 95% range of the salt dilution tests (App. A.3). The field experiments are considered as the more reliable data source and demonstrate the weakness of the notch formula specifically at water heads below 0.08 meter. Most accurate results were obtained using the original notch formula for high-flows but an corrected formula for low-flows calibrated with the field experiments.

4.1.1 Seasonal trends

The time variation curve of the discharge at the Kiwene forest notch is illustrated in Fig. 4.1. The chart covers the whole Masika season from March to June 2008. The mean pre-seasonal base-flow was found at approximately $0.6 \, \mathrm{ls^{-1}}$, not altering after the rain events on 15^{th} and 22^{nd} March. These first events of the season show a sharp peak flow but did not impact the base-flow after recession. The extensive rain events between 26^{th} and 29^{th} March mark the biggest rain period in the season. The recession lasted for several days and the base-flow remained on a higher level at averaged $1.1 \, \mathrm{ls^{-1}}$. This increased base-flow lasted for almost two months and declined only towards the very end of the season. The following rain events did not impact the seasonal base-flow anymore. Single rain events caused slightly longer recessions of up to three days, but most rainfall occurred in short and intense events without long-term influence on base-flow runoff. The last month of data collection did not have significant rainfall but the discharge remained on a 40 % higher level compared to the pre-seasonal conditions.

The missing response to the first events could be due to the capture of rain water in the upper soil layers. The water infiltrates into desiccated, often under-saturated ground and triggers a wetting process of the upper soil layers. The consequence is a raise in soil moisture and a reconnection of hydraulically disconnected soil regions. Subsequent rainfall can initiate local flow processes and replenish underlying aquifers. Higher phreatic levels consequently result in higher inflows into the stream and sustain the higher base-flow discharge of 1.1 ls⁻¹. This process of recharging riparian aquifers by infiltrating rain water can also explain the slight seasonal recession curve as subsurface flow velocities are slow and responses are delayed.

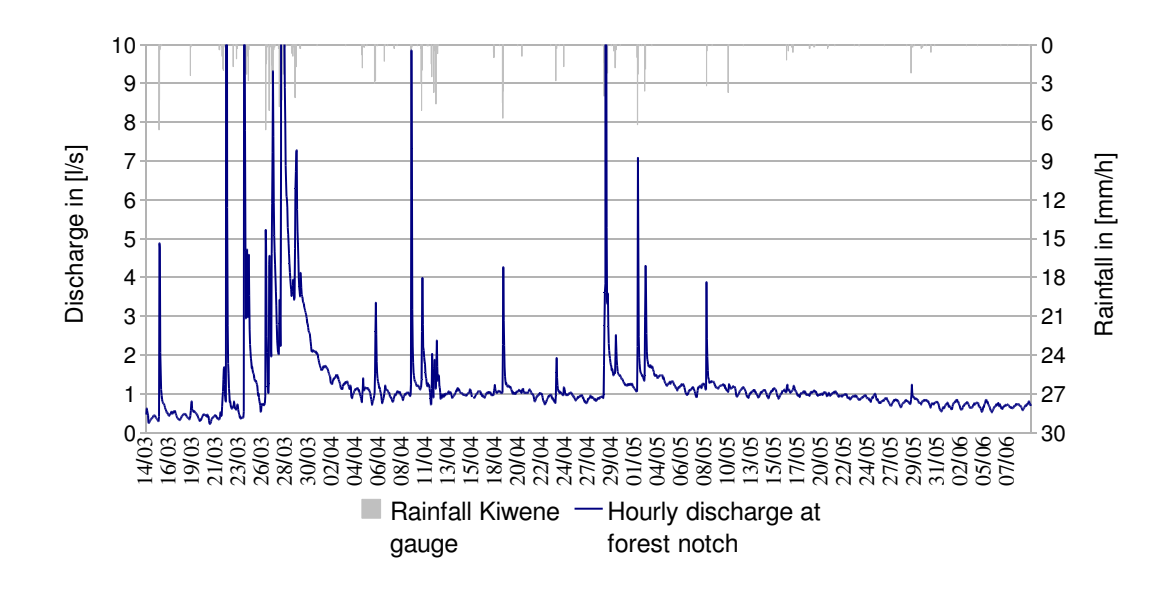


Figure 4.1: Time variation curve of discharge recorded at the Kiwene forest notch

4.1.2 Diurnal fluctuations

The discharge of the Kiwene stream does not only have a seasonal variation but shows diurnal fluctuations. These fluctuations were found particularly in the forested areas of the catchment, but were not observed in the cultivated catchment. Fig. 4.2 compares the discharge of the Kiwene and Chamasae stream. The stream gauge at the outlet of the cultivated catchment recorded no diurnal fluctuations but evidences short recession after rain events and a constant seasonal discharge. The mean discharge was found at 0.15 ls⁻¹ and ranges between 10 and 20 % of the Kiwene discharge. The Chamasae catchment is only half the size of the Kiwene catchment and the watersheds in the catchment are partially uncertain. In addition, the subsurface flow systems can not be identified easily because only the last section of the streambed is flowing perennially. The Kiwene stream shows remarkable diurnal fluctuations of different amplitude. The fluctuations account for 20-25 % of the total discharge and differ between 0.1 and 0.25 ls⁻¹. The discharge variations are greatest during low-flow and show a regularity in terms of the time of the observed extrema. The highest discharge was recorded early in the morning whereas the minimum discharge occurs in the afternoon. The fluctuation phenomena can be explained with transpiration of riparian trees or tree water uptake.

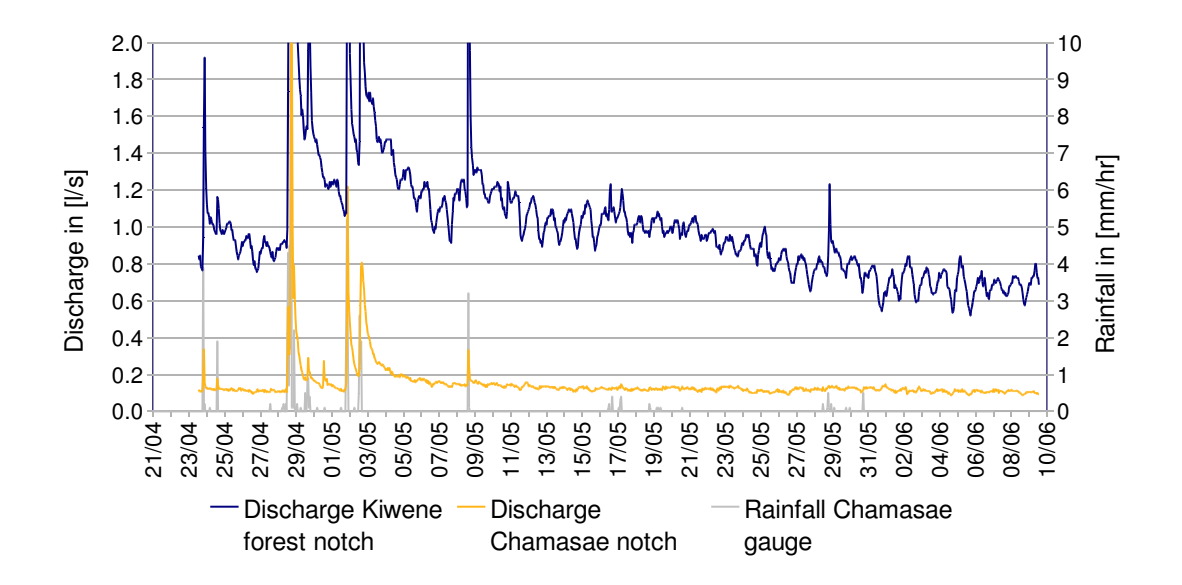


Figure 4.2: Comparison of Kiwene and Chamasae discharge

The transpiration rate of trees has similar to the observed stream discharge a diurnal cycle, but with inverse extrema. The transpiration is a function of the potential evaporation and is dependent on several factors such as solar radiation, cloud cover, temperature, relative humidity and wind speed. During the day, solar radiation as well as highest temperatures and low relative humidity promote the transpiration of trees evaporating the cell water from leafs and stems. This leads to an increased suction pressure and a high water uptake from deep tree root systems reaching the saturated zone. Water extractions from the saturated zone eventually impact the phreatic level and result in lower inflows into the stream. The reversed process occurs during the night when tree transpiration drops to zero and the phreatic level recovers from the high suction pressures. Especially during base-flow when groundwater contributions form the bulk of the discharge, varying groundwater inflows result in significant discharge fluctuations in the stream.

The diurnal cycles of transpiration and discharge do not correlate perfectly. There has been stated a time delay of a couple of hours. On days without cloud cover the maximum transpiration was measured between 12 p.m. and 2 p.m. averaged over an annual period. The lowest discharge, however, was usually recorded between 3 p.m. and 5 p.m. (Fig. 4.3). In the morning highest discharges have been observed just before

trees start transpiring. The time delay is here to a greater or lesser extent negligible. In general, the delay is attributed to the subsurface processes involved. Especially the recovery of the hydraulic head in the afternoon is enabled by water slowly flowing from uphill towards the stream. This process of recharging the groundwater level takes time and leads to a delayed impact on the lateral inflows. On the other hand, the decline of the pressure head in the morning is caused by riparian trees standing proximate to the stream taking up water directly from the near-stream saturated zone. The groundwater level responses are fast and the signals reach the stream almost real-time as lateral travel paths are short.

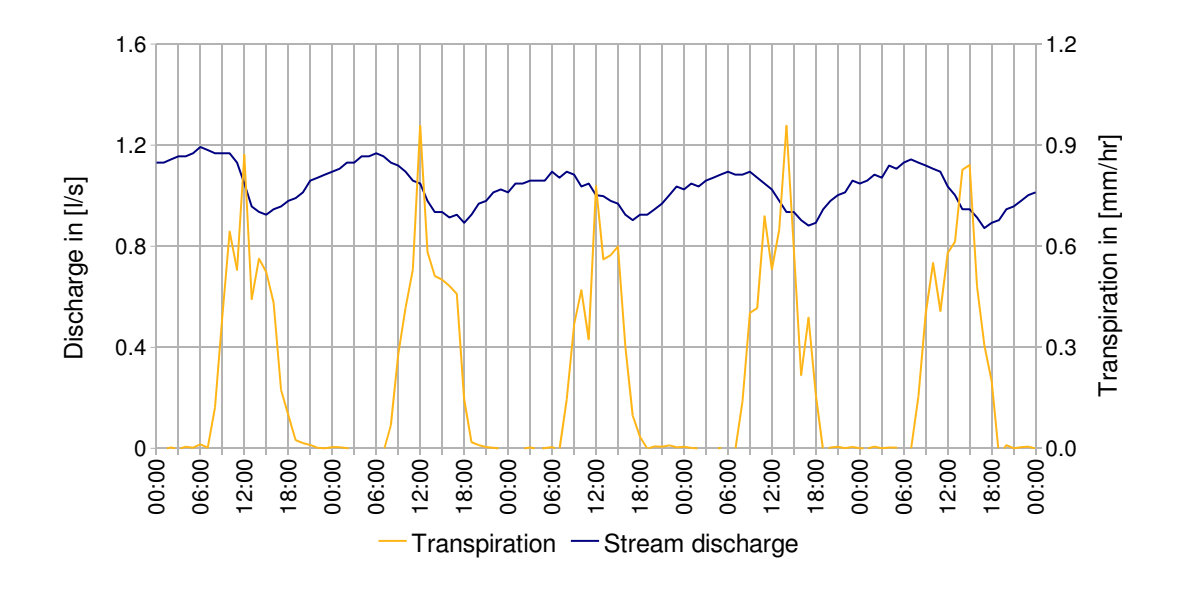


Figure 4.3: Correlation of potential transpiration and stream discharge

The time variation curves of the discharge at both Kiwene stream gauges are presented in Fig. 4.4. The diurnal fluctuations are remarkably greater at the forest notch. The difference in amplitude must therefore be caused by processes occuring on the forested hillslopes in between the two stream gauges. Transpiration of riparian trees as the main cause for discharge fluctuations seems to be proved here, considering the dense vegetation along the stream channel. Towards the end of the season a couple of high fluctuations for instance on 4^{th} and 5^{th} June are in line with small fluctuations recorded at the spring notch. Enhanced water uplift in the groundwater body of the swamplands

was stimulated by high transpiration rates. The uplift created a very strong signal that was possibly transported to the distant stream upstream the notch (Fig. 2.4).

To better understand the occurrence of the fluctuations it is necessary to have a look at the distribution of riparian vegetation. On the forested slopes of Kiwene the trees are standing proximate to the stream. The deep root systems possibly reach the saturated zone at the foot of the slopes and can directly influence the lateral inflows. High flow velocities and a short distance to the stream gauge support a clear detection of the variations. In contrast, on the banks upstream the ridge notch the trees are distant from the stream. In the vicinity of the stream the grass and uliginous vegetation do not extract enough water to cause serious fluctuations. The trees probably reach the saturated zone as the area is flat and swampy but the level variations are likely absorbed on the long travel path to the stream.

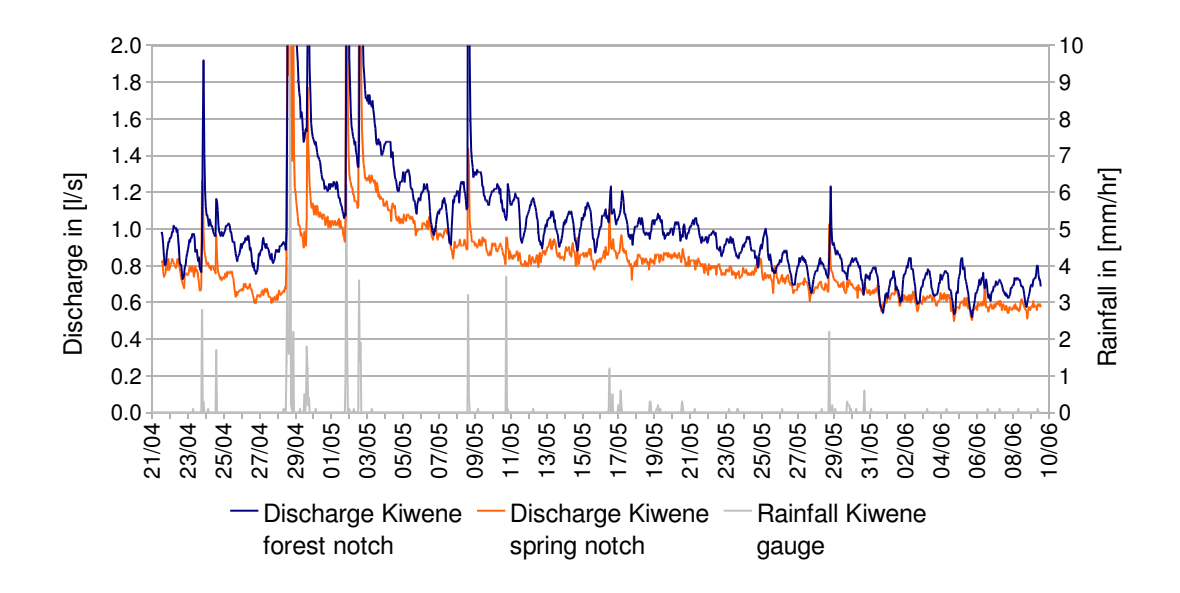


Figure 4.4: Comparison of discharge at both Kiwene stream gauges

The base-flow discharge at the forest notch is slightly higher than at the spring notch. During base-flow 80–90 % of the total Kiwene runoff is generated in the spring basin. Despite the great fluctuations, the discharge at the spring notch exceeds at no point the discharge measured at the forest notch. The stream discharge is apparently not

diminished along the stream, but has small contributions instead. During peak-flow and early recession of rain events the runoff generation is altered. The peak discharge at the forest notch is twice as high compared to the spring notch (*not visible in the chart*). Even during early recession after events the discharge remains on a higher level but approaches the spring discharge after 3–5 days.

4.2 Groundwater levels and soil moisture contents

Besides the runoff analysis, investigations of subsurface flows are an elementary part of an integrative approach. The easiest method to gain insight into the subsurface systems is to monitor groundwater levels with a piezometer. Unfortunately, this method only delivers information on the saturated zone. The results from the watermarks and profile probe measurements complete the soil investigation including the upper soil regions and the unsaturated zone.

4.2.1 Kiwene spring site

The piezometer in the swamplands of the Kiwene spring substantiates a groundwater table at a depth of about 1.4 m below surface. The soil above the phreatic level consists of dense material of smallest grain size arguing for high capillary forces. In addition, a thick layer of compacted organic material was identified. The high phreatic level keeps the soil at a high moisture content evidenced by wetland vegetation in the surroundings. The developing of the phreatic level is demonstrated in Fig. 4.5, where the yellow graph represents semi-daily manual measurements and the blue graph represents the logged measurements with the pressure transducer. In this figure it is evidenced that the infiltration depth of rain water is not only dependent on the rainfall amount, but on the temporal distribution of the rain. The first big rain event on 9^{th} April fell with an amount of 19.2 mm within three hours. However, the groundwater level did not show any reaction. In contrast, only 14.6 mm fell during the following rain event on 11^{th} April. The rain was distributed over 17 hours and the groundwater level rose by 10 centimeter during this period. On 28^{th} April 23.1 mm of rain fell in a period of ten hours. A similar amount of rainfall combined with a lower rain intensity led to a rise of the phreatic level by 15 centimeter with a delay of 24 hours.

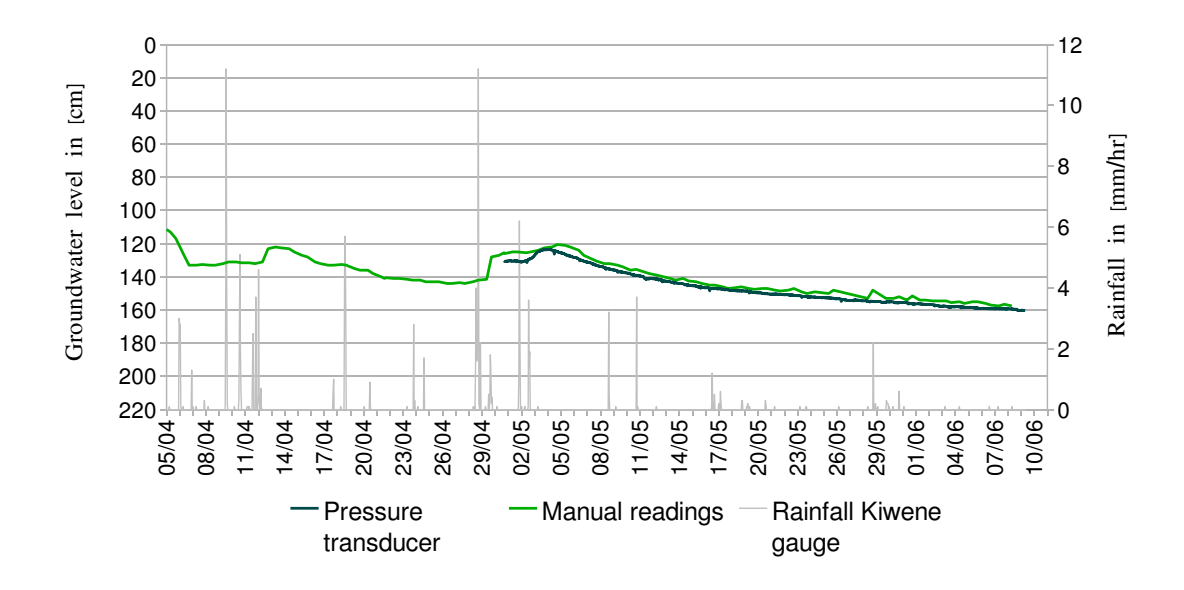


Figure 4.5: Groundwater level in surrounding of Kiwene spring

The soil moisture contents during these rain events measured in 0.3, 0.6 and 0.9 m depth directly next to the piezometer show little response to the rainfall (graph is not shown). During the event on 28^{th} April only the upper sensor recorded a leap in saturation by 10 %. The other sensors responded imperceptibly. It is conspicuous that the lower sensor measured fairly constant soil moisture contents despite the proximity to the saturated zone. The high density of the soil column argues for slow infiltration and possibly the sensor was not perfectly connected to the surrounding soil matrix.

4.2.2 Kiwene forest site

The three piezometers installed in a transect at the forest site did not monitor any water during whole Masika season. Even after the long rain period end of March the filtered tubes stayed dry. The piezometers are installed in a distance of 25 m to the stream and are grounded on a layer of compacted weathered rock that is covered by sandy-loamy material (Fig. 3.2). A good infiltration rate can be assumed, but rain water did never develop a perched aquifer. The weathered layer possibly has a high porosity and directs water into deeper zones of the ground. In fact, the dry piezometers indicate that between the surface level and the weathered layer the soil was not or only temporary saturated.

Watermarks

The watermarks measured the soil moisture in the upper meter of the ground and provide, due to continuous data logging, information on the infiltration rate of rain water. Technical problems hampered the measurements and some of the installed sensors did not record valuable data. In addition, the uncertain calibration of the watermarks with profile probe data made quantitative interpretations impossible. The linear calibration with a regression coefficient of 0.72 is presented in App. B.1. The watermarks show unlike the profile probe saturation data only within a small range of soil moisture. Extreme values are therefore not reliable and should be carefully interpreted.

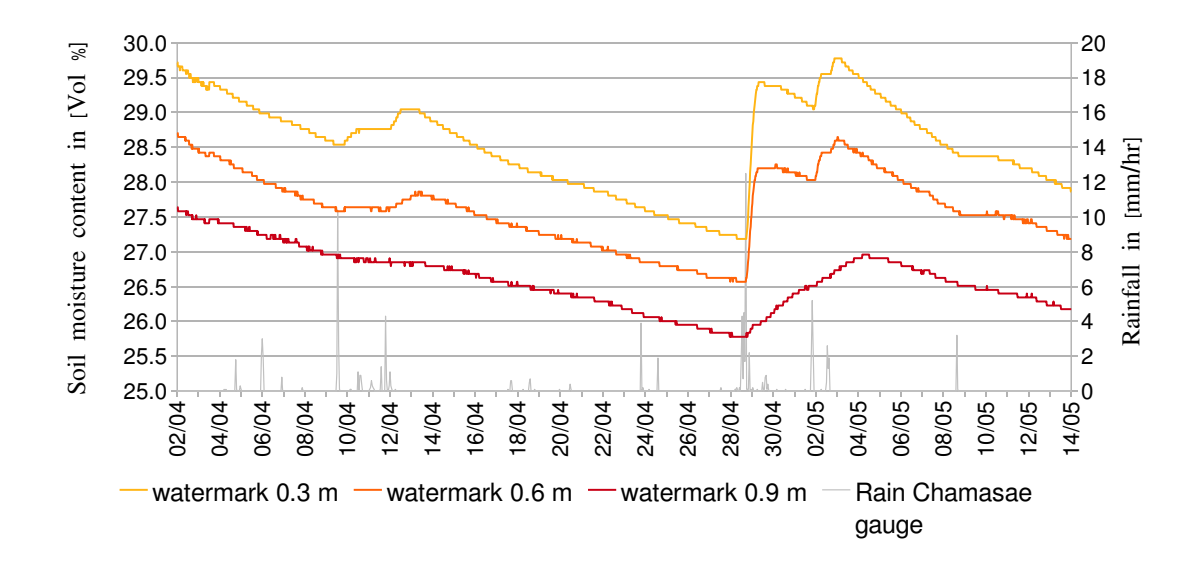


Figure 4.6: Soil moisture contents in different depths at the forest study site

The most near-stream set of watermarks at the forest site (Fig. 3.1) delivered valuable data that is illustrated in Fig. 4.6. The graphs show a drying trend of the soil over the course of the season. Nevertheless, the trend is interrupted by the major rain event on 28th April, that rapidly wetted the soil to different extent. More precisely, the responses of the three sensors to the rainfall are almost in phase, with the upper sensor detecting the largest changes. This sensor shows a leap in soil moisture whereas in 0.9 m depth only a slight change of the gradient appears. Interestingly, the soil moisture contents generally seem to only respond if rain events have certain characteristics. For instance,

the short and intense rain on 9^{th} April with 10 mm has none or only little impact. On the other hand, the rather small event two days later on 11^{th} April produces a larger response. The largest event on 28^{th} April let the saturation ultimately rise in all monitored depths. After reaching higher saturations, even smaller events of moderate intensity and short duration for instance on 5^{th} May can lead to further wetting. It seems that not only the rain intensity but also the temporal distribution and the pre-conditions of the soil play a role in the vertical infiltration processes.

Interesting cognition delivered two watermark sensors installed proximate to a large tree in the centre of the forest study site (Fig. 3.3 b). These sensors were intended to investigate the influence of root induced suction pressure on the soil conditions. In fact, the watermarks detected diurnal fluctuations in moisture content (Fig. 4.7). These variations were only observed at this specific location and are considered to be caused by the tree root systems.

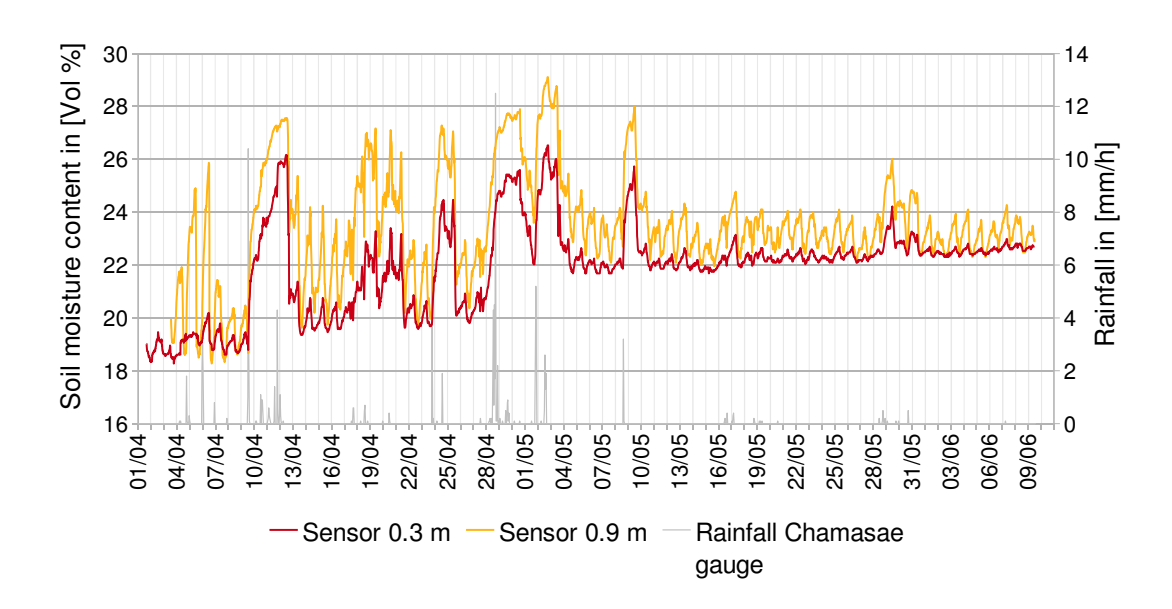


Figure 4.7: Soil moisture contents in the surrounding of the large tree at the centre of the forest study site

In order to better understand the diurnal moisture fluctuations, the recession period between 21^{th} and 27^{th} May has been analysed in detail in Fig. 4.8. The fluctuations detected by the two sensors in different depths correlate well in terms of the appearance

of extreme values. The lower sensor recorded greater fluctuations because it is situated in the denser root zone of the tree. Except for one day, the maximum in soil moisture was always measured between 6 and 9 *a.m.* and the minimum between 3 and 6 *p.m.*. These hours correspond exactly the time spans when the fluctuations in the stream showed their extrema. This means that high groundwater levels go in line with higher soil moisture contents in the unsaturated zone and the other way round.

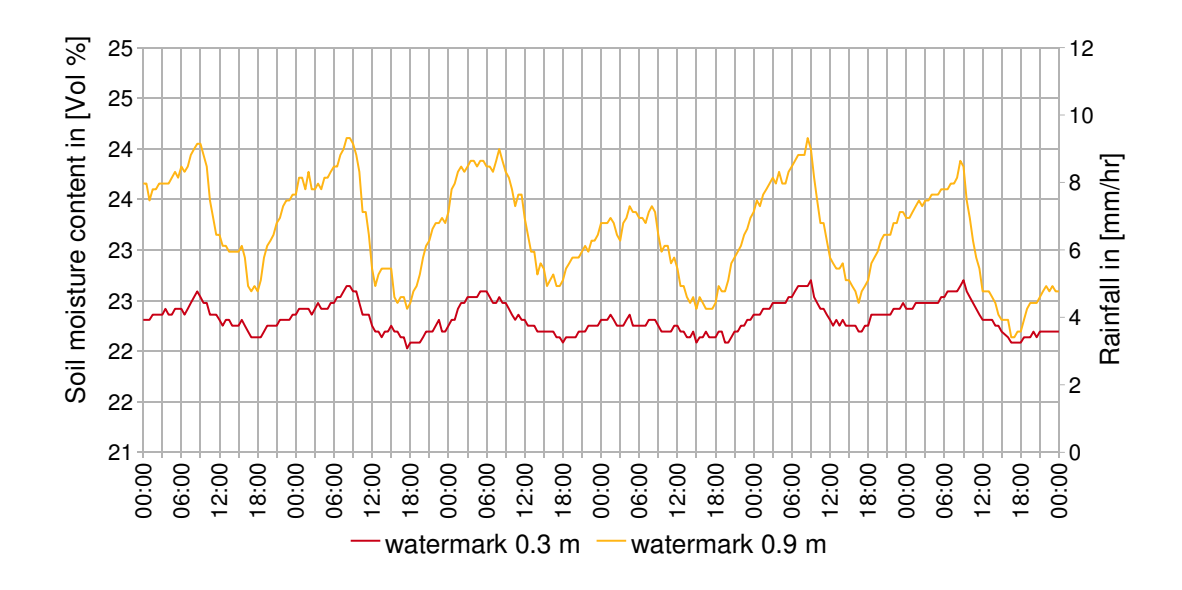


Figure 4.8: Diurnal fluctuations of soil moisture contents at forest study site

Unlike the watermarks near the stream, the soil region around the tree experiences a general wetting trend throughout the season. Naturally, after major rain events the soil moisture is leaping upwards, but even during the last month of data collection a slight increase in soil moisture is visible. During this period no further rainfall was detected and the climbing trend must be caused by subsurface processes. The trend is steady but varying only in a small range, not considering the direct impact of rainfall. It is hypothesised that hydraulic processes in the unsaturated zone around the tree and fairly constant in- and outflows from the tree root zone establish an equilibrium in soil moisture. This equilibrium is slowly shifted when processes are changing in the course of the year. For instance, the potential transpiration declines towards the cold season (July/August), possibly lowering the outflow and leading to higher soil moisture contents.

A third important observation in Fig. 4.7 are the soil moisture responses during and after rainfall. The incisions caused by the rain events self-evidently violate the regular diurnal variations and the seasonal trend. The graph shows that the soils generally respond quickly and almost parallel at both sensors. Similar to other watermarks discussed previously, the infiltration velocity seems to be negligible. One important difference is the steep decrease of soil moisture some few days after the gain of soil water. As would seem natural that the tree transpiration is responsible for this rapid decline. However, the question remains why the tree consumes the surplus of soil water up to three days after the rise. This phenomena becomes more clear looking at the time when these rapid soil moisture declines occurred. Interestingly, they all started in the time span between 11:30 a.m. and 3:00 p.m. on days with least rainfall or cloud cover. This behaviour indicates a dependency on the peak transpiration as a function of the solar radiation. In fact, the weather station in Bangalala (Fig. 2.2) recorded the highest daily maximum of solar radiation on those days showing the rapid decreases. The sharpness of the declines suggest that the maximum transpiration is decisive for the trend reversal of soil moisture. After exceeding a certain transpiration threshold the process of building up suction pressure and taking up water is stimulated.

The coherency of these processes shall be clarified with two distinct examples of temporally shifted soil moisture recession, one from the event on 9^{th} April and another from the event on 28^{th} April (Fig. 4.7). Tab. 4.1 shows the transpiration and soil moisture contents during these events. The numbers show an immediate rise in soil moisture by 20 % after the rain event on 9^{th} April. An instantaneous decrease of soil moisture after the event was initially averted by further rainfall on the following days. Three days later the decline started at 1 p.m. with the highest radiation of 5.24 mm in the period since the leap of soil moisture. A very similar behaviour was demonstrated on the event on 28^{th} April. The following day had little rainfall but a dense cloud cover during the day, as it is indicated by the low transpiration rate. On the 30^{th} April a rapid decline in soil moisture was initiated by a transpiration maximum of 4.61 mm, twice as high as on the previous days (Tab. 4.1). These examples demonstrate the strong relationship between transpiration and soil moisture. A comparison with the recession of other events showed that the decline in soil moisture is caused by averaged transpiration extrema above 4.5 mmd^{-1} .

Date	Rainfall	total T	max T	Time max T	Soil moisture
	[mm]	$[\text{mm d}^{-1}]$	$[\mathrm{mm}\ \mathrm{hr}^{-1}]$	[hrs]	[% of prev. day]
09 th April	4.2	2.61	0.50	13:00	+ 20
10 th April	2.2	3.46	0.58	14:00	+ 09
11 th April	3.2	4.58	0.77	13:00	+ 06
12 th April	2.2	5.24	0.96	14:00	- 19
28 th April	13.8	1.47	0.23	11:00	+ 21
29 th April	2.1	2.12	0.37	13:00	+ 02
30 th April	1.2	4.61	0.83	14:00	- 12

Table 4.1: Transpiration rates and soil moisture developing for two distinct rain events in April 2008

Profile probe

The profile probe was used to verify the measurements of the watermarks and to obtain a higher resoluted profile in vertical direction. The sets of graphs in Fig. 4.9 illustrate the water saturations of the soil horizon at two adjoined locations. The different graphs represent single measurements taken in regular intervals of three days during the recession of the 28th April event. The highest saturation (*light blue graph*) indicates the first measurement shortly after the event and the coloured graphs are subsequent measurements during recession.

The discontinuous profile probe measurements support the results obtained from the watermarks. The similar moisture behaviour at the two access tubes that are installed laterally in two meters distance prove the reliability of the measurements. The highest fluctuations occur in the uppermost layer of the ground, decreasing towards greater depths. This phenomena is in line with the greatest leaps after rain events recorded by the 0.3 m watermark sensor at the same site. In depths greater than 0.4 m the soil water contents at the forested site are almost constant at 25 to 35 % saturation. The constancy denotes that there is no real moisture front moving into the ground. The water is rather consumed by transpiration or captured by evaporation or preferentially transferred into underlying soil regions on unknown paths.

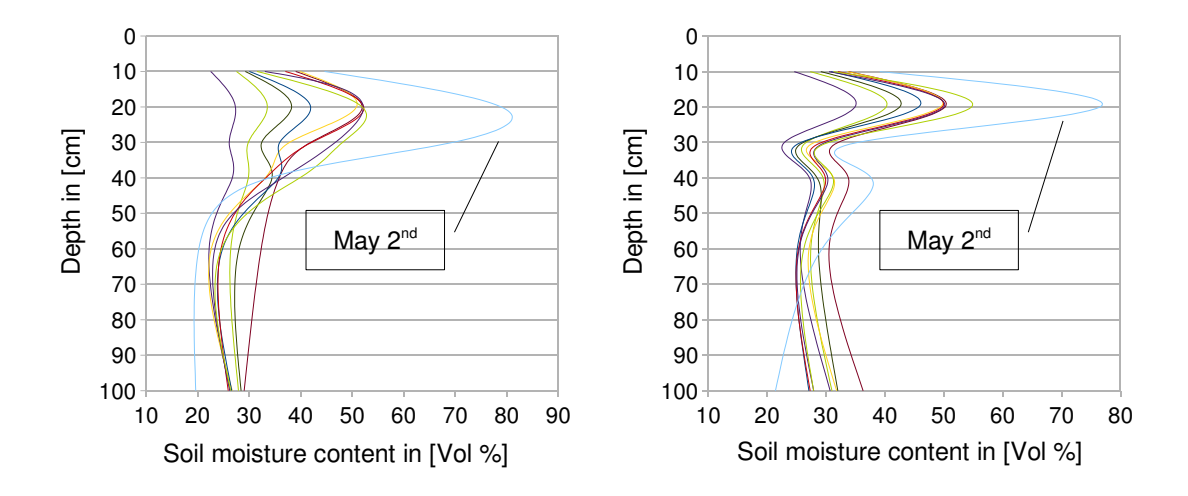


Figure 4.9: Saturations around two adjoined profile probe access tubes at the forest study site

4.2.3 Chamasae cultivated site

At the Chamasae site in the cultivated catchment only the profile probe delivered valuable soil moisture data. The two profile probe access tubes were installed laterally in 2 and 5 m distance to the stream and therewith closer to the stream compared to the forest site. The results from the two access tubes are illustrated in Fig. 4.10, where the first chart represents the tube closer to the Chamasae stream. At first sight the great fluctuations up to 70 % in the top layer resemble the results from the forest site. Also the fairly constant soil moisture contents in moderate depths between 0.3 and 0.5 meter seem to represent a congruent moisture pattern. An important difference are the variable saturations at the lower end of the access tubes. Around the near-stream tube the rain event on 2^{8th} April evoked a remarkable rise of soil moisture in 1 m depth to even full saturation on 2^{nd} May. It stands to reason that the vicinity to the stream and the close phreatic level have an influence on the rise. Especially the last factor is of great importance as the infiltrating rain water is not or only momentary wetting the soil matrix above. The measurements in the second tube a couple of meters uphill show a similar developing after the event, but saturated conditions lasted far longer.

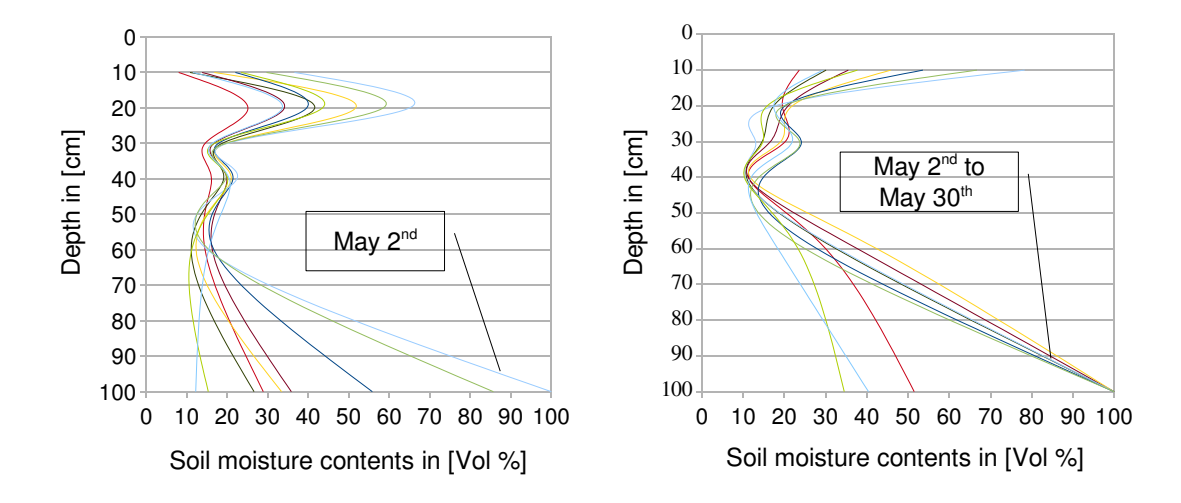


Figure 4.10: Saturations around two adjoined profile probe access tubes at the cultivated study site

4.3 Stream chemistry and sources

In-situ monitoring of the electrical conductivity along the streams have been undertaken in order to record global changes of ion concentrations over the season and to identify potential sources. The electrical conductivity (EC) is a sum parameter for ion concentrations respectively the salt contents in the water. Determining ion concentrations is also important for the quantification of discharge contributions, for instance from adjacent hillslopes, and for the understanding of whole catchment responses.

Longitudinal transects from the spring to the confluence of Chamasae and Kiwene stream are presented in Fig. 4.11. The four different graphs represent transects measured previous, during and after Masika season. The transects have been done in dry interim periods of rain events to exclude direct rain water impacts. They reveal a seasonal decline in EC of 20–30 % for the Kiwene stream and 10–15 % for the Chamasae stream. In the Kiwene stream the highest EC was measured in mid February strictly diminishing with each series of measurements. Rainfall diluting the connected aquifers and the stream itself are likely to be causing the reduced stream concentrations. The Chamasae transects show the same trend except for the last series giving higher salt contents than the previous one in mid April. At this stage the diluting effect of percolating rain water is nullified and the ion concentrations move towards initial state before Masika season.

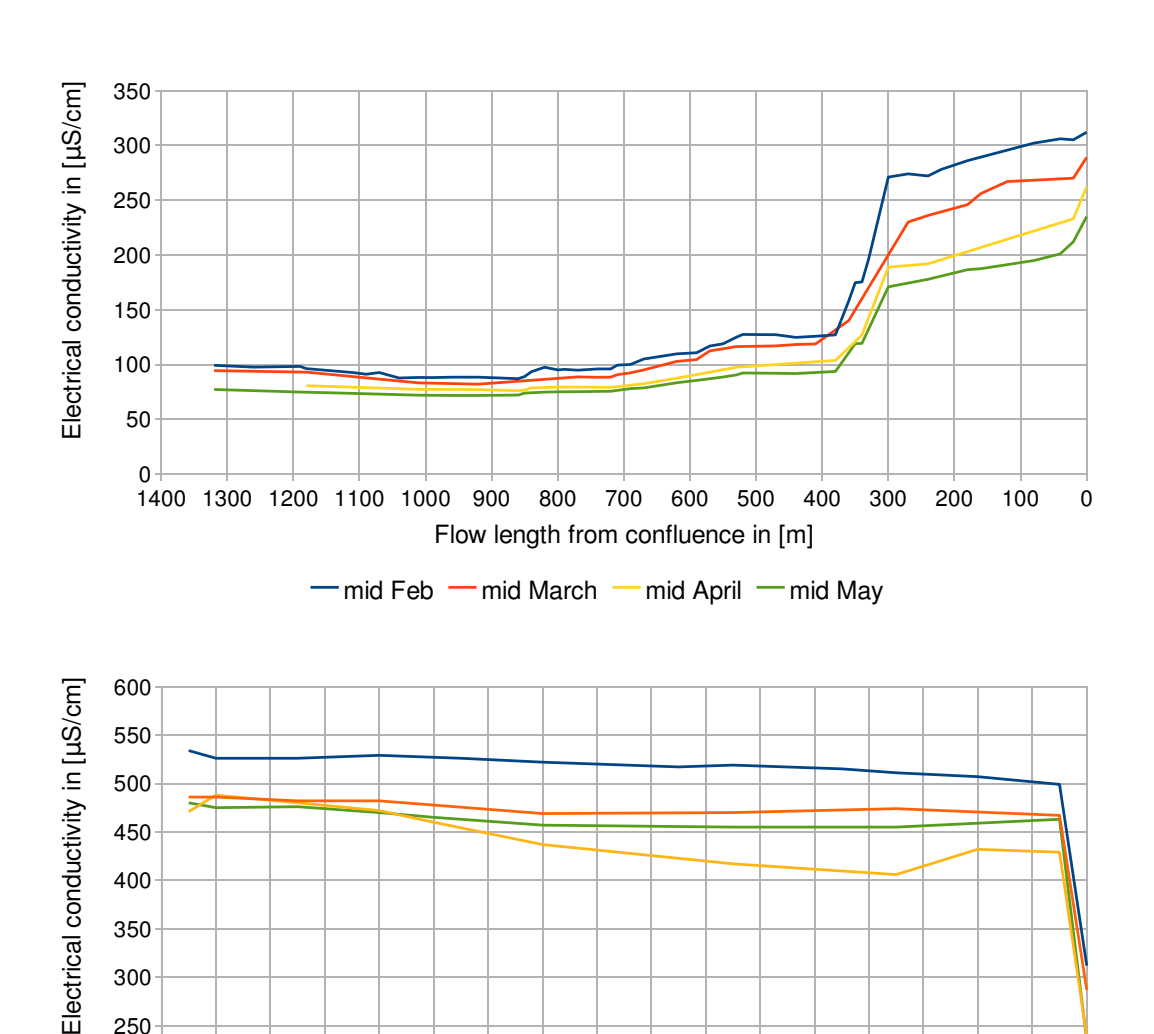


Figure 4.11: Longitudinal transects of electrical conductivity in Kiwene and Chamasae stream

Flow length from confluence in [m] - mid Feb - mid March - mid April - mid May

340 320 300 280 260 240 220 200 180 160 140 120 100 80 60

The transects do not only point a seasonal variation but also show a spatial trend. Interestingly, this trend is reversed in the two adjoined catchments. The spatial characteristics of the Kiwene stream shall be described first. The EC in the Kiwene stream increases steadily with flow length and leaps twice at 300 and 350 m upstream the confluence. At these leaping points two small springs of different hydro chemistry were identified. A detailed analysis of the hydro chemical characteristics of the two springs follows beneath.

The Kiwene stream is fed by groundwater contributions appearing at different stream points. A great deal of the Kiwene water originates from the near-surface groundwater reservoir in the spring area. The groundwater has low EC of approximately 70–80 μ S cm⁻¹ resulting from short percolation. Along the stream a continuous increment of discharge is observed. This contribution is formed by rain water that percolates slowly through the forested slopes diluting salts and minerals on its way down. When it reaches the stream the EC ranges between 120 and 200 μ S cm⁻¹ depending on the percolation length, the residence time and the small-scale geology of the hillslopes. Small exfiltration ponds along the stream mark the points were the underground water appears. The ponds are often associated with deposits of ferric and manganese precipitation (Fig. 4.12 a). These diffusive sources contribute insignificantly to the discharge, but can be responsible for the continuous increase of the EC along the stream. Besides the numerous diffusive sources, two neighbouring springs with EC of 240 μ S cm⁻¹ and 460 μ S cm⁻¹ respectively, lead to a remarkable increase of the stream water EC.





Figure 4.12: Images of Kiwene stream (a) metallic precipitation, (b) Mzawa tap source

In contrast, the spatial trend of the EC in the Chamasae stream declines downstream leaping only at the confluence. This inverse behaviour is due to the fact that the diffusive sources have lower EC compared to very high initial stream concentrations. Diffusive sources are difficult to identify, but saturated soils and debris flow observed in the top layer of the soil (Fig. 4.13 a, b) indicate the very existence of these contributions. The map of the catchment (Fig. 2.4) displays that only on the last 330 m of the Chamasae streambed runoff is perennial. Rainfall that reaches the surface near the catchment boundaries undergoes a long longitudinal subsurface passage before it appears in the stream. The spring itself is a dram of water with exceptionally high ion concentrations of 480–540 μ S cm⁻¹, trickling out at a small rock outcrop. It can be assumed that water coming from far uphill dissolves great amounts of salt percolating through unknown paths down the catchment slopes. The inflows downstream the spring dissolve less salts on the fairly short, lateral subsurface passage resulting in low EC and a derogating effect on the EC of the Chamasae stream.





Figure 4.13: Images of Chamasae stream (a) soil exposure, (b) debris flow

Two sources at Kiwene stream

Two significant springs along the Kiwene stream were found in the downstream section of the catchment 350 m upstream the confluence with Chamasae stream. The first source namely 'Mzawa tap' (Fig. 4.12 b) springs directly next to the stream from a steep hillslope. The second source is located little downstream the 'Mzawa tap' on the opposite side of the stream. Its origin is near the catchment boundary and the water has

fairly short subsurface passage before it springs at the head of a 50 meter landslide. It discharges on the landslide face joining the stream in scattered runlets. During the second half of Masika the sources have been sampled regularly including samples prior to, during and shortly after the rain event on 28^{th} April. Besides the in-situ measurements of the electrical conductivity and pH, the major ions and dissolved silica were analysed in the field laboratory (Section 3.3.2). The results of some selected parameters are presented in Tab. 4.2.

A comparison of the hydro chemical signatures of the two sources brought some outstanding criteria forward. The most obvious difference is the range and the magnitude of the ion concentrations. Both springs are located close to each other with similar slopes, flow lengths, geological attributes, micro-climates, and soil conditions. Despite these similarities the water from the landslide source has in some cases twice the concentrations of the Mzawa tap (Tab. 4.2). For instance, the EC of the 'Mzawa tap' was found at 241 μ S cm⁻¹ and the EC of the landslide source oscillates around 465 μ S cm⁻¹. The disparity may be due to the short surface runoff down the debris avalanche. The water running down the landslide dissolves salts that were conveyed to the surface when the slope started moving and slided downhill. This process has been proved with EC measurements uphill the landslide, where moderate EC of 270 μ S cm⁻¹ was found.

Except for the parameter dissolved silica and to smaller extent the hydro carbonate all ion concentrations show extreme variations between the two springs (*not all parameters shown in table*). The parameter dissolved silica shows similar values between 45 and 49 mgl⁻¹ because it does not respond as fast to the surface passage. In particular, the dissolution of the crystallised silica molecules embedded in clay minerals is slow and the surface passage too short to initiate the process. The delayed reaction is also true for the hydrogen carbonate. Here, a deviation of 143 to 187 mgl⁻¹ was found between the springs. The HCO₃⁻ molecules are in a chemical equilibrium (Equ. 4.1 and Equ. 4.2), that is shifted depending on the physical and chemical characteristics of the water.

$$CO_2 + 2 H_2 O \rightleftharpoons HCO_3^- + H_3 O^+$$
 (4.1)

$$HCO_3^- + H_2O \rightleftharpoons CO_3^{2-} + H_3O^+$$
 (4.2)

The carbonate equilibrium is primarily controlled by the pH-value or the concentration of hydronium ions H_3O^+ in the water. The pH of groundwater near the Kiwene spring ranges between 5.7 and 6.3 whereas stream-flow pH was found between 7.8 and 8.1. Measurements have shown that the physical characteristics such as temperature and pH change rapidly once the water appears at the surface. The link between the pH-value and the concentration of hydronium ions H_3O^+ implies a shifting of the carbonate equilibrium towards greater HCO_3^- contents. However, the adaptation of the equilibrium to altered physical conditions takes time. The delay could be one explanation for the moderate HCO_3^- contents downstream the landslide passage.

	Mzawa tap				Landslide source			
	EC	HCO_3^-	SiO ₂	σ^2 H.	EC	HCO ₃	SiO ₂	σ^2 H.
	μS/cm	mg/l	mg/l	%o.	μS/cm	mg/l	mg/l	% 0.
03 rd April	245.0	130.5	49.9	-20.3	478.0	185.8	47.2	-19.6
25 th April	242.0	143.9	48.2	-19.3	462.0	187.8	45.4	-18.9
28 th April	241.0	143.9	48.8	-19.1	367.0	136.6	32.6	-14.0
30 th April	241.0	141.5	47.6	-19.1	462.0	189.1	45.7	-17.9
05^{th} May	241.0	140.3	48.0	-17.7	465.0	191.5	45.5	-18.5
20 th May	235.0	140.3	47.9	-19.4	439.0	185.4	46.1	-18.8
Mean	240.8	140.1	48.4	-19.16	445.5	179.3	43.8	-17.95
StDev	3.3	5.0	0.8	0.84	40.5	21.0	5.5	2.03

Table 4.2: Hydro chemical analysis of two small springs along the Kiwene stream

Besides the difference in base-flow concentrations, the small springs also show interesting behaviour during rain events. The Chamasae rain gauge recorded 29.2 mm of rainfall for the 28^{th} April event with a steady temporal distribution and a low intensity. Interestingly, the chemical parameters of the 'Mzawa tap' source do not respond to the event, but show stable hydro chemical properties. The constancy of parameters is surprising as diluting effects were anticipated regarding high initial EC of 240 μ S cm⁻¹. Nonetheless, the source seems to originate from deeper regions that are either not or only poorly connected to soil zones that are promptly penetrated by rain water. On the

other hand, the chemistry of the landslide source is responding instantaneously to rainfall. The mean EC of 460 μ S cm⁻¹ dropped to 367 μ S cm⁻¹ during the event, but recovered pre-event concentrations only two days after the event. The fast reactions argue for the influence of direct event water diluting the surface flow.

Looking at the isotope data of the landslide source we can identify one outlier during the rain event on 28^{th} April. This value of 14 % falls below all other values ranging between 18 and 19 %. The observed decrease is likely caused by mixing processes of groundwater with isotopic light rain water. The isotope fraction of a rainfall sample taken during this event was determined on -9.81 %. Considering conservancy of the isotope tracer and a pre-event isotope fraction of -18.9 %, the mixing ratio is approximately 50.50. It is not yet clear whether the mixing occurred subsurface or on the short surface passage down the landslide.

Unlike the diffusive sources along the entire stream, the Masika tap and the landslide source add notably to the total discharge of the stream. According to field observations the delivery of the Mzawa tap is fairly constant over time, but the landslide source varies with rainfall. The exact contributions can be calculated with mass balance equations (Equ. 3.4 and Equ. 3.5),

$$Q_{dstr} * c_{dstr} = Q_{upstr} * c_{upstr} + Q_{source} * c_{source}$$

$$\tag{4.3}$$

$$Q_{dstr} = Q_{upstr} + Q_{source} \tag{4.4}$$

where Q is the discharge in 1 s^{-1} and c is the electrical conductivity in $\mu\text{S cm}^{-1}$.

For the determination of the inflows we assume an averaged discharge during baseflow of $1.4~l~s^{-1}$ measured at the forest stream gauge some 400 meters upstream. The resulting contributions amount to 18 % for the Mzawa tap and 21 % for the landslide source respectively. This means an augmentation of almost 40 % within a stream section of 50 meters indicating an important localised subsurface flow system in the adjacent hillslopes.

Chapter 5

Storm-flow investigation

In the following chapter the results of the event investigation are presented. It includes amongst other things a rainfall-runoff analysis, an evaluation of stream sampling during storm-flow, as well as a quantification of end-members. The investigation has been undertaken primarily at the forest stream gauge in the Kiwene catchment. The stream sampling facilitating water quality analysis is a useful method to approach a clear understanding of runoff generation in small-scale catchments. It aims in the first instance the identification of flow components and the determination of flow paths and source areas. In the second instance the application of hydrograph separation allows the quantification of associated contributions of diverse end-members during storm-flow. This is an important element to precisely describe hydrological responses and to draw conclusions about dominant runoff components over the duration and the recession of rain events.

5.1 Rainfall-runoff analysis

The discharge at the forest stream gauge was recorded in 15 minutes intervals over whole Masika season. In Fig. 5.1, the time variation curve from mid March to mid May is plotted on a logarithmic scale. The chart reveals a long rain period between the 22^{nd} and 28^{th} April in which several intense rain events occurred. The events all show short-term recessions, but the post-event base-flow one week after the rain period remains on a higher level compared to the pre-event base-flow. The subsequent rain events were mostly of short duration but indicate different recession curves.

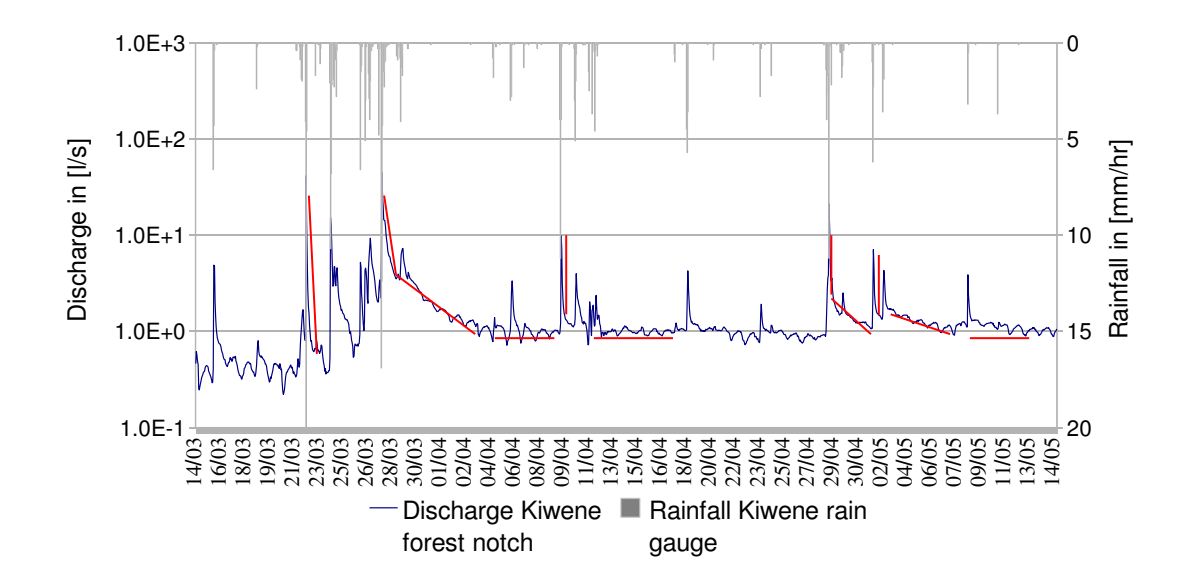


Figure 5.1: Time variation curve of discharge recorded at the Kiwene forest notch

The logarithmic scale of the graph allows the classification of the recession after rain events. Three classes with specific recession coefficients were identified. Depending on the amount and the intensity of rainfall the recession classes develop to different extent. In Fig. 5.1 the recession curves are approximated with red lines, the slope representing different classes. The first recession class α_1 is observed immediately after the peak discharge and is characterised by short duration and a steep decline. It appears in all rain events but is especially pronounced after rainfall with high intensity. The α_1 -recession is in some cases followed by a moderate recession α_2 that can last up to several days after the event. The slope is not as extreme as of the immediate recession and the logarithmic decline has a smoother shape. The α_2 -recession is dominant until the prevent discharge of smaller events is restored. A third recession class α_3 was discovered after the rain period end of March. The base-flow after the end of the moderate recession remained on a higher level at approximately 1.0 ls^{-1} compared to 0.6 ls^{-1} prior to the series of events. The α_3 -recession has a long-term or seasonal trend with a gentle slope.

The occurrence of the different recession classes α_1 - α_3 shall be clarified with some examples in Tab. 5.1. The selected rain events exceed an hourly amount of rainfall of 10 mm hr⁻¹ and are considered to be appropriate for a comparison. The events on 22^{nd}

March and 9^{th} April show a steep recession α_1 , but lack a distinct moderate recession α_2 (Fig. 5.1). A comparison with the events on 27^{th} March and 28^{th} April demonstrate that there is no obvious correlation between the amount of rainfall and the character of the recession. Yet the duration and the intensity of rainfall seem to better explain the different behaviour. More specifically, during short and intense rainfall, for instance on 22^{nd} March, the direct α_1 -recession dominates and fades directly back to base-flow discharge. This rain event lasted for only three hours with an extremely high intensity of 10.3 mm per hour (Tab. 5.1). On the other hand, enduring rainfall spread over a longer period of time is followed by a distinct α_2 -recession. The 27^{th} March event with 46.6 mm of rain falling within 17 hours is a good example for that case. The α_3 -recession can hardly be interpreted here, as it was observed only after one event (26^{th} March) and the data series is too short for a valid comparison.

Event	Rainfall	Duration	Intensity	Runoff coeff
	[mm]	[hrs]	$[\mathrm{mm}\ \mathrm{hr}^{-1}]$	[-]
22 nd March	30.9	3	10.3	0.087
27 th March	46.6	17	2.74	0.058
09 th April	19.4	3	6.47	0.063
28 th April	25.3	10	2.53	0.022

Table 5.1: Rain amount, duration and intensities of selected events during Masika 2008

The runoff coefficients, that are defined as the total volume of runoff divided by the total amount of rainfall, are remarkably low with values ranging between 2 and 9 %. This means that a great part of the rain water infiltrates or is lost before it reaches the stream. The most important process to mention here is evaporation including interception. Another fact to consider is that the Kiwene catchment is contributing unevenly to stream runoff. Particularly the large area uphill the Kiwene spring is likely not completely involved in the direct runoff generation. Rainfall reaching the steep slopes below the mountain ridge, however, primarily contributes to the stream flow during early recession. The runoff coefficients were smallest for low intense rainfall when soil infiltration is advantaged. Interestingly, the 27th March event has a low intensity of 2.74 mm hr⁻¹, but has a runoff coefficient of 5.8 %. Intensive rainfall produces an increased runoff coefficient as the infiltration threshold can be exceeded and rainfall forms overland flow.

In Section 4.1 it was demonstrated that during base-flow conditions most of the runoff is generated in the spring basin of the Kiwene stream. The storm-flow analysis feeds the assumption that the steep areas below the ridge become important to the runoff generation during rain events. The rainfall on 08^{th} and 10^{th} May amounts in both cases 4 mm at the Kiwene rain gauge (Fig. 5.1). The Chamasae rain gauge is more representative for the lower part of the catchment including the forested slopes, but recognised rainfall only on 08^{th} May. Accordingly, only during the first event the forest stream gauge detected a response to the rainfall in the stream. With respect to the steep slopes downstream and the fairly flat topography upstream the mountain ridge, it becomes evident that storm-flow runoff is generated on the forested slopes to a notable extent. It is important to remark that on the forested slopes runoff is facilitated by steep gradients and eroded top soils, that would otherwise hinder a fast and direct runoff.

The sampled rain events

Three distinct rain events were identified during Masika 2008 that have been sampled and analysed. They were defined by a peak runoff value exceeding 15 times the mean seasonal discharge, calculated from hourly discharge values. The focus of the analysis was laid on the greatest rain event on 27^{th} March, but also the smaller event on 9^{th} April was considered in order to compare the runoff responses.





Figure 5.2: Images of (a) forest stream gauge, (b) storm-flow on 27th March event

On 27th March 41.1 mm of rain were recorded at Kiwene rain gauge (Fig. 2.4) during a period of 8 hours. The Chamasae rain gauge downstream the forest notch recorded 31.2 mm of rain in the same period, a difference of 25 %. The rain fell with high intensity as 82 % and 77 %, Kiwene and Chamasae gauge respectively, occurred during the first two hours. The steep topography prevented flattening of the flood wave and led to a sharp peak discharge of 60 ls⁻¹ at the forest notch. Concurrent to the concentrated rainfall the peak discharge lasts only for a short moment and declined soon after.

The forest stream gauge measured a total event discharge of 1032 m³ for the 27th March event. In this calculation only the surplus of water compared to the pre-event discharge is accounted. In contrast, above the catchment area upstream the forest notch fell 33,060 m³ rain, resulting in a runoff coefficient of 3.1 % and 4.2 % respectively for the lower rainfall recorded at the Chamasae rain gauge. Overall, this is a small fraction of rainfall ending in the stream channel during early recession. The bulk of rain water infiltrates into the ground recharging the underlying aquifers of the spring basin or is lost through evaporation including interception.

5.2 Hydro chemical stream responses

The hydro chemistry was examined analysing water samples from the Kiwene forest notch and doing in-situ measurements of electrical conductivity. The sampling campaign for the 27th March event started about 12 hours prior to the event and was continued until the EC leveled off during recession. The samples have been analysed on both, hydro chemicals and isotopes to allow a thorough hydrograph analysis. In Fig. 5.3, the hydrographs including the different tracer concentrations are presented. The EC and the ions HCO_3^- , Ca^{2+} and Mg^{2+} show a similar trend in terms of the time variation curve of the concentrations. At peak discharge shortly after the beginning of the event the four parameters responded with an abrupt rise in concentration. The greatest rise was found for the HCO_3^- and Ca^{2+} parameter. The following stream samples demonstrate a rapid drop of EC and ion contents to a minimum of 50 % of the initial concentrations (Fig. 5.3). These samples were taken only one hour after the first storm-flow sample, but stream discharge dropped already to less than half of the peak discharge of 60 ls⁻¹. During recession on the falling limb of the hydrograph the EC and the ion concentra-

tions slowly recovered. Here we can state that especially the parameter EC, HCO_3^- and Ca^{2+} show a very smooth developing towards the pre-event concentrations.

The parameter dissolved silica and the isotopes show a different behaviour during the hydrograph. In particular, a peak concentration of dissolved silica was not observed and the parameter dropped instantaneously to minimum values at peak flow. Also, the recovery seems to be different, as initial concentrations were restored only three hours after the beginning of storm-flow. This special behaviour will be scrutinised later on in this section. The same applies for the response of the isotopic parameter that resembles the one of dissolved silica.

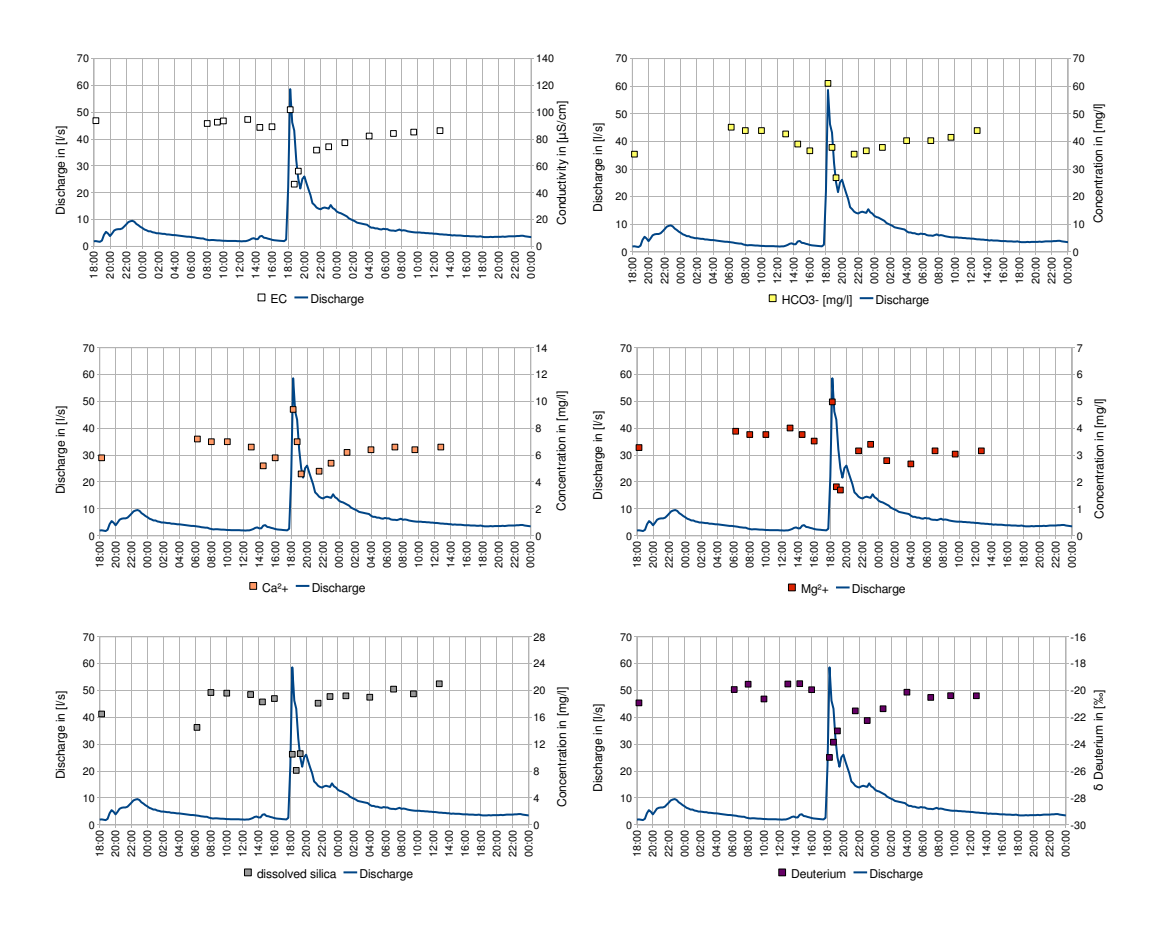


Figure 5.3: Hydrographs of rain event on 27th March with different tracers

Ions and EC

The peak concentrations of EC and ions with one single outlier can be attributed to different processes. One scenario is based on near-surface groundwater levels and fast lateral subsurface flows towards the stream. Infiltrating rain water could rapidly raise the phreatic level in the groundwater body close to the stream. As a result, the increased hydraulic pressure would lead to outflow of old, high concentrated water stored in the saturated zone. The following drop in concentration would then be caused by subsequent low-concentrated event water exfiltrating into the stream.

Another explanation is the occurrence of overland flow during the first stage of the event. In case of intensive rainfall the infiltration limit of the soil can be reached and excess rain water forms overland flow. Rain water has negligible ion contents evidenced by rainfall samples indicating EC of 4–5 μ S cm $^{-1}$. The reason for the peak concentration are salts originating from subsurface that were transported to the surface by evaporation during dry periods. If rainfall forms overland flow, runoff picks up salts and minerals from the surface on its way down the slopes. The salts are washed into the stream causing a short, yet significant leap in concentration. This process occurs as a short flush and in the process the concentrations drop to a minimum. The minimum concentrations last until overland flow reduces and high concentrated groundwater gradually contributes the bulk of discharge. This process is often overlapped of mixing processes between groundwater and infiltrating rain water. The mixing dilutes the aquifer leading to reduced groundwater concentrations and a dampened recovery. As a result, the ion concentrations remain on a slightly lower level compared to the pre-event concentrations.

Dissolved silica

The missing peak of the silica content supports the overland flow scenario. Silica molecules are embedded in crystallised form in rocks and solid material that are abundant only in deeper soil regions. Furthermore, for dissolved silica it requires unlike other natural tracers long contact times to dissociate the molecules from mineral structures. Pre-event water stored in the ground would have high silica contents, due to slow percolation and long residence times. Instead, there is no peak concentration visible as

it was observed for the ion concentrations on the rising limb of the hydrograph. During peak flow the dissolved silica content ranges around 50 % of the base-flow content. The constancy of the values and the abrupt upward leap argue for the occurrence of overland flow with minimal silica content. Short contact times between runoff water and minerals and fast infiltration prevent a significant alteration of the dissolved silica contents. The rapid recovery of pre-event contents marks the point of time when overland flow ends and the groundwater contributions again become dominant. This point coincides with the end of intense rainfall some two hours after the beginning of the event.

In spite of the slow reaction the dissolved silica is a non-conservative tracer. The alteration of silica contents becomes most obvious if stream water samples are analysed in different time steps after the collection. Several silica retests revealed an increase in concentration of up to 83 % within 24 hours. The effect is extreme in storm-flow samples containing higher loads of sand and solid material than base-flow samples. This fact is illustrated in Fig. 5.4. The suspended material comprises silica molecules that are dissociated during long holding times in the sample bottles. In order to prevent alteration of silica contents, the analysis of the dissolved silica tracer has been done immediately after the sampling with portable field equipment.



Figure 5.4: Samples of the storm-flow on 27th March

Hydrogen isotopes

The isotope analysis in this study includes ¹⁸O as a oxygen isotope and Deuterium as a hydrogen isotope. The reliability of the isotope analysis has been verified with one isotopically light and one isotopically heavy standard sample. Statistical tests uncovered some uncertainties in the Oxygen analysis, *i.e.* a greater fluctuation of repetitive measurements. The results of these tests are illustrated in App. C.1 with standardised error bars showing the aimed range of the two isotopes. Therefore, only the Deuterium results are presented in this chapter. Regardless, the results of ¹⁸O are provided in App. D.1.

The time variation curve of Deuterium isotopes as a conservative tracer resembles the results of the dissolved silica. High δ -values in the graph represent high fractions of heavy ²H isotopes in the samples. The isotopic composition of rainfall varies from event to event, but has a distinct signature compared to the base-flow. Rain water was collected and the Deuterium fraction was determined on -30.31 ‰, whereas the baseflow showed approximately -20.0 %₀. The sharp decrease of the ²H isotope ratio on the rising limb of the hydrograph suggests event water contributions during peak flow. As the isotope tracer is more or less conservative, simple mixing processes in the stream of isotopically light rain water and isotopically heavy subsurface water can explain the change in composition. During recession when the isotopic fractions recover, subsurface mixing processes of infiltrating event water and stored pre-event water come into play. These mixing processes are in most cases non-linear because diverse processes, such as evaporation impact the isotopic composition. Light hydrogen (¹H), for instance, is evaporated prior to the heavier ²H, leading to a shifting of the isotope ratio. Particularly soil water or near-surface water bodies often have higher Deuterium fractions as they are exposed to soil evaporation.

5.3 End-members of runoff

In order to identify potential end-members in the runoff generation of the forested catchment an end-member mixing analysis (EMMA) has been applied [Burns et al., 2001]. Dissolved silica and Deuterium isotope ratios of the stream samples logged against each other form a time line displayed in Fig. 5.5. The coloured triangles represent single samples taken prior to and during the event. The pre-event groundwater sample collected in

the piezometer at the Kiwene spring site has a similar signature as the pre-event base-flow sample at the forest stream gauge. The similarity legitimates the assumption that the isotopic composition and the silica content of base-flow conform with groundwater. The rain water sample of this event is isotopically light at -30.31 ‰ with a negligibly low silica content. In addition, an overland flow sample has been collected during the event and is also plotted in Fig. 5.5. The high value of -23.4 ‰ demonstrates the rapid alteration of the isotopic composition of rain water after reaching the ground. It has to be noted that overland flow samples are only punctual data and are not representative for the catchment. For the interpretation of the end-member analysis it is crucial to know about the processes affecting the silica contents and the isotopic composition of the water. From the chemical analysis we learned that dissolution of silica molecules is short-term not relevant, but mixing of different waters alters the silica concentration. For the isotope fraction it is essential to respect evaporation as a secondary process.

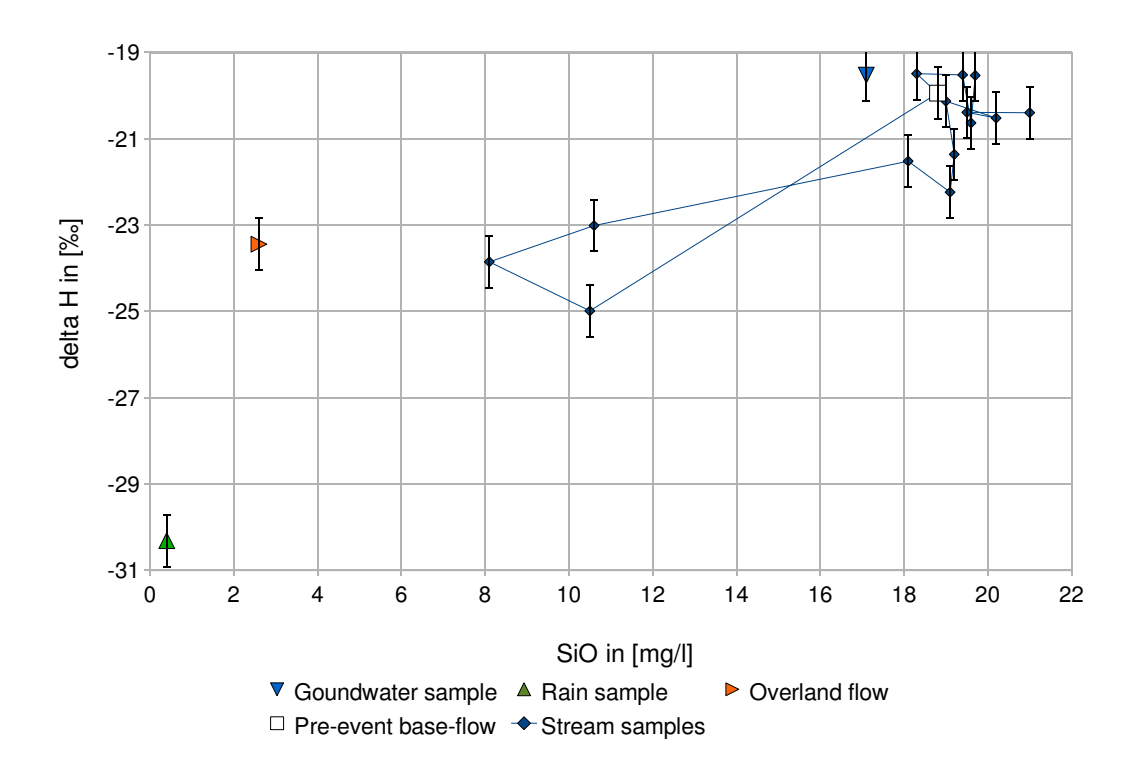


Figure 5.5: Mixing analysis of the runoff end-members at the forest stream gauge

The stream samples taken during storm-flow at the forest stream gauge lie in a fairly linear formation between the base-flow sample and the event water samples. The three points in the centre of the chart represent the samples taken during peak flow. The first point converges the rain sample evidencing direct rain water contribution. During the early stage of the event surface runoff reaches the stream that was formed on nearby hillslopes. Due to the short flow path in the riparian forest, evaporation can be neglected, and as a result the first stream sample is located on a straight line between the base-flow and the rain water sample. As the event continues subsequent samples were slightly heavier and lie closer to the surface runoff sample. Overland flow that was exposed to evaporation in open areas uphill can have a different isotope ratio, but reaches the stream delayed. The abrupt return to the starting point of the time line mark the end of the overland flow. From this point the discharge is again controlled by groundwater contributions. The dense cloud of data points is an indication that neither evaporation, nor mixing processes affect the pre-event water stored subsurface. A lot precise interpretation is complicated because the isotopic composition of rainfall can vary over the duration of an event. However, the sampled rain water is a bulk sample.

5.4 Quantification of contributions

The total discharge of the Kiwene stream consists of different water contributions that can be separated and quantified. The most obvious separation is to distinguish between event and pre-event water applying a time-source hydrograph separation. The Deuterium isotopes as a conservative tracer with distinct isotope ratios for rain water and groundwater are most applicable for this analysis. The results of the separation are illustrated in Fig. 5.6. Over the stream length the water has a constant isotopic composition because all samples taken in the run-up of the hydrograph indicate 100 % pre-event water contribution. The event water comes into play when the rainfall started around 17:30 *p.m.* and the discharge instantaneously rose. At peak discharge the contribution of event water amounts 29 ls⁻¹, which is approximately 50 % of the total discharge. At this point the rainfall reached its highest intensity. Concurrent to the following decline of rainfall the contribution of event water decreases and dropped to 25 % only 1.5 hours after peak discharge. Another 1.5 hours later the pre-event water is already responsible for 90 % of the total discharge and soon after the influence of event water has vanished.

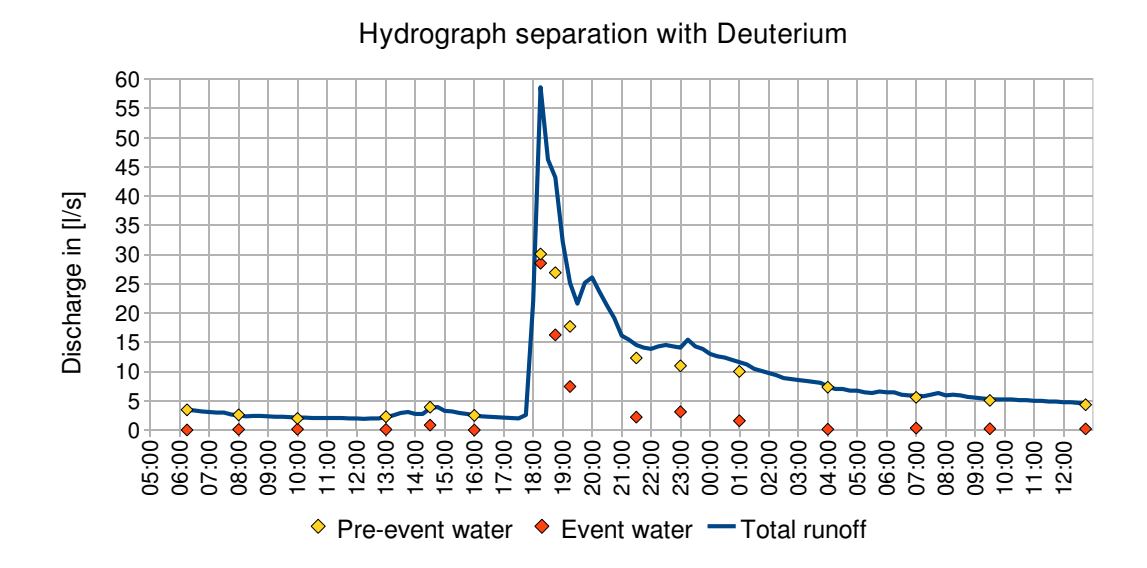


Figure 5.6: Time-source hydrograph separation using Deuterium isotopes

The early appearance of event water in the stream coincides temporally with the most intensive rainfall in the catchment. The missing delay argues for the mixing of groundwater contributions with fast surface runoff components. Field observations substantiate this scenario as overland flow was seen during the very first stage of the event. It is noteworthy that a small proportion of less than 10 % event water occurs up to 8 hours after the peak flow. This water did reach the stream delayed, possibly because of a subsurface passage in the riparian zone. In the later recession the event water contribution drops to zero. It seems that it has to be differentiated between rain water infiltrating in soil regions adjacent to the stream and water infiltrating further uphill. The latter is marked with a long delay that prohibits a visible effect in the 24 hours hydrograph.

The computation of absolute discharge contributions gives an idea of the influence of event water. A total event caused discharge of 1032 m³ was measured for the 27th March event at the forest stream gauge. The separation makes only 143 m³ event water contribution and 889 m³ pre-event water contribution. This is a ratio of 14 % of direct event water passing the stream gauge. This value is surprisingly low considering the heavy rainfall and the remarkable contribution during peak flow.

The geographical-source hydrograph separation divides the stream discharge into contributions from different sources. The end-member mixing analysis suggests to consider groundwater, rain water and overland flow from adjacent hillslopes. Both, the rain water and the overland flow has been separated from the groundwater in two discrete hydrograph separations. As the results resemble each other, only the chart of the overland flow separation is shown here. The chart with the rain water separation is provided in App. D.4.

The hydrograph separation applying the electrical conductivity (EC) indicates negative contributions of the overland flow during peak flow (App. D.5 and App. D.6). To understand this error value it is important to remember that the EC greatly varied at the beginning of the event. The flush of water diluting the salt deposits on the surface has likely higher EC as both of the reference samples. These exceeding values self-evidently lead to false contributions. The separation with EC can also be defective because this parameter is non-conservative and the concentrations are afflicted with a great spatial variability. The hydro chemical signature of the overland flow sample which was used as reference is spot data and can not represent the shifting inflows to the stream. In the present case the EC of the overland flow sample is likely too little during the flush.

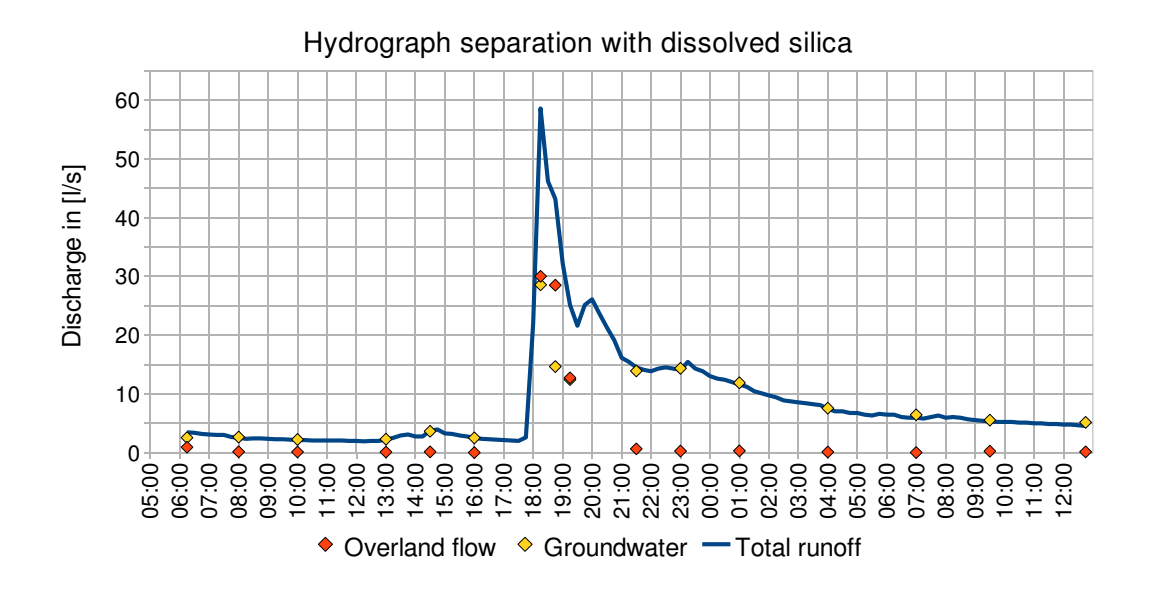


Figure 5.7: Geographic source hydrograph separation using dissolved silica

A more reliable separation is obtained using the parameter dissolved silica. This tracer does not show the peak concentrations during the flush and is short-term more stable than the EC. The results presented in Fig. 5.7 resemble those of the time-source separation. The first sample indicates an overland flow contribution of 30 ls⁻¹, about 50 % of the total discharge. The next sample, however, exhibits an even higher rate of 65 % exceeding the inflow from groundwater. After the high flow and the intense rainfall three hours after the beginning, the overland flow rapidly declines to zero. Unlike the event water separation the geographic source separation does not give evidence for an extended recession. This means that overland flow stops immediately as soon as the rain intensity falls below a certain threshold. The total contribution of the overland flow is 13.6 %, but this time occuring in a very short period of approximately 3 hours.

Overall, the inflow of overland flow from the geographic-source separation is similar to the event water contribution determined with Deuterium. However, the time variation curves are not entirely congruent. In particular, during peak flow and during the advanced recession the flows vary. The overland flow is restricted to the direct recession up to 3 hours after the peak flow whereas event water was recognised in a period of 8 hours. In spite of some uncertainties in the analysis, the total inflows of event water and overland flow range in the same magnitude of less than 15 %. The bulk of the stream discharge seems to be generated by groundwater or pre-event contributions originating from the hillslopes within the catchment.

Chapter 6

Synthesis

The overall objective of this study was the hydrological process understanding. In order to achieve this goal, it is necessary to identify water source areas, to determine flow paths, and to estimate residence times of infiltrating rain water in subsurface storages. In the following chapter the results of the investigations with respect to runoff generation responses in the two study catchments Kiwene and Chamasae are discussed and schematised. The dominant processes are quantified and assembled in a simplified conceptual model. Two scenarios for base-flow and storm-flow conditions are presented separately, because the boundary conditions differ and different processes are involved. The synthesis includes also a rough estimation of water balances to better understand the surface and subsurface fluxes and their relevance to the runoff generation.

6.1 Conceptualisation of runoff generation

6.1.1 Base-flow conditions

Base-flow conditions dominate runoff generation most of the year with fairly few processes involved. Flow paths and source areas are determined by a number of factors that depend on the hydrological regime. To better understand the different flows into the stream and their characteristics, it is advisable to divide the catchment into two parts, the spring basin above and the forested slopes below the mountain ridge.

The discharge analysis documents that during base-flow the bulk of the Kiwene discharge is generated in the spring basin uphill the forest. The surrounding has a flat topography and perennial swamplands are abundant. Rainfall infiltrates quickly and accumulates in the basin creating a high groundwater table at 1.2 m below surface. This aquifer seems to outlast the dry season and feeds a constant delivery of the Kiwene springs all year round. Outside the immediate recession of rain events the water originating from the swamplands account for 85–95 % of the total discharge, depending on the diurnal fluctuations. These fluctuations are scrutinised later on in Section 6.2. Both, the spring water and several groundwater samples from the piezometer in the basin show identical chemical signatures proving the supposed source area. Consequently, the groundwater in the local basin determines the hydro chemistry and the physical properties of the stream water. Low electrical conductivities of 70–80 μ S cm−1 speak for limited flow paths and short residence times. It can be assumed that the infiltration length of rain water is small and the water is transported primarily horizontally within the saturated zone. The flow scheme in the spring basin is conceptualised in Fig. 6.1.

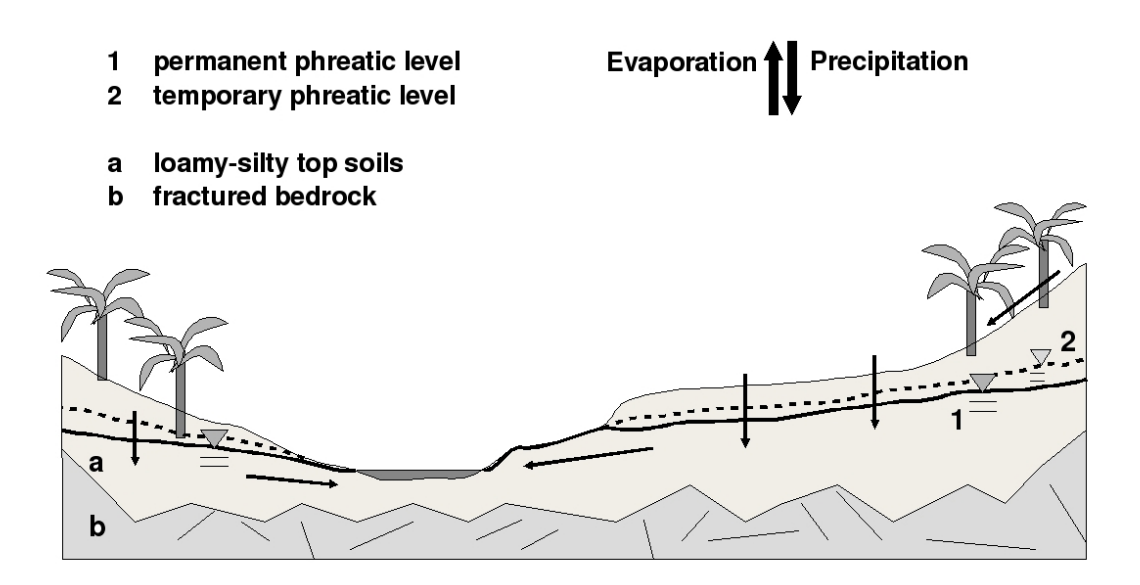


Figure 6.1: Conceptual model of flow mechanisms in the Kiwene spring basin

The lower part of the catchment contributes little to the total discharge as significant groundwater inflows are missing. Only diffusive sources altogether adding up to 15 % of the total discharge have been observed at certain locations along the stream. The origin of this water seems to be uphill as electrical conductivities are high indicating high salt contents. One explanation could be a long vertical percolation through the clayey matrix dissolving salts stored in the unsaturated zone. Finally, after reaching the groundwater table, the water flows towards the stream and trickles into the stream at the toe of the slopes. This seeping out has been observed at various spots along the stream showing saturated soils. The groundwater table is expected to have a slight slope that does not follow the ground slope equally. Whilst the phreatic level hits the ground surface in the proximity of the stream, it is in greater depth with increasing distance from the stream channel. The different hypothesised slopes of ground surface and groundwater table are illustrated in Fig. 6.2.

Infiltrating rain water that reaches the ground uphill undergoes a long vertical subsurface passage where the chemical constitution alters. Besides the flow path, also other factors impact the hydro chemistry, such as the residence time and the geology of the slopes. Despite the steep topography the residence time during base-flow conditions can be quite long, because the hydraulic permeabilities in the clay matrix are low and lateral fluxes were observed long after the preceding rain event. The combination of slow velocities and long vertical percolation likely causes the high salt contents measured in the exfiltration ponds along the Kiwene stream. These ponds show EC up to 220 μ S cm-1 and above and are possibly the reason for the continuous increase in EC that was found with the longitudinal transect of the Kiwene stream.

Chamasae stream

Interestingly, the Chamasae catchment shows a different trend concerning the EC and the associated salt contents. We can explain the reversed behaviour with the same approach we formulated for the diffusive sources at the Kiwene stream. For this subcatchment we must consider that the stream is not fed by a large aquifer, but rather by an accumulation of diffusive sources in the downstream section of the catchment. We can assume that percolation in longitudinal direction and long residence times in subsurface storages are the main cause for EC of 550 μ S cm⁻¹ for the Chamasae spring. Lateral in-

flows from adjacent hillslopes into the downstream channel, however, have short travel paths and accordingly a declining effect on the stream EC. The seeping out of water into the stream was nicely illustrated with the profile probe evidencing saturated soils in small distances to the stream. The exceptionally high soil moisture contents were maintained during the whole month May. This behaviour shows that rainfall has probably a much longer impact on the runoff generation as the visible recession of stream flow would let expect.

6.1.2 Storm-flow conditions

During rain events the runoff generation in the Kiwene headwater catchment alters remarkably. Rain water infiltration affects subsurface flow processes and also additional processes come into play. The total discharge of the Kiwene stream now consists of two temporally variable sources. The spring basin generates a minor, yet constant fraction of the storm discharge. The piezometer and the watermark data from the spring basin give evidence for delayed response, despite the short infiltration path and the high groundwater table (Fig. 6.1). A low permeability of the soil and slow horizontal velocities may be the reason for the delayed and dampened inflow. The major source of water during rain events are lateral inflows from adjacent hillslopes in the forested part of the catchment. This source of water was discovered in the discharge analysis showing that more than twice the spring notch discharge was recorded at the forest notch during peak flow. The lateral contributions can originate from either subsurface or occur as overland flow. Which flow path is dominating depends on the rainfall characteristics, the pre-event soil conditions and the point of time during the event. If we look at a hydrograph from the rising limb to the recession, we can state that overland flow occurs mainly during the very beginning, whereas subsurface flow contributes constantly over the whole period of an event. The latter can be induced by increased water heads or by the developing of perched aquifers on the hillslopes [Wenninger et al., 2008].

In the Kiwene catchment overland flow was observed regularly and is considered as the fastest response, as flow paths are generally short and steep slopes facilitate high flow velocities. In case of intensive rainfall the infiltration rate of the soil can be exceeded and excess water forms surface runoff. This process is well known in dry basins with high rainfall intensity [Sklash and Farvolden, 1979]. According to rainfall data and field

observations the overland flow often lasts only for a period of several minutes to half an hour. However, hydrograph separation of some storm-flow events suggests extended overland flow occurrence of up to three hours after peak flow. This calculation is almost in accordance with the event water separated with the isotopes. Except for the period of three to seven hours after peak flow, when a small portion of event water was detected in the stream. This occurrence of event water on the falling limb of the hydrograph was also found by Uhlenbrook and Hoeg [2003]. However, overland flow did not play a role in their research.

Overland flow contributed at no point of a hydrograph more than 50 % of the total discharge. Therefore, another fast-responding process must be involved, that amplifies the discharge in the first hours of the hydrograph. The question is of either event water infiltrating in the vicinity of the stream or pre-event water that was removed from nearstream subsurface storages. Percolating rain water can short-term lift the phreatic level and lead to increased hydraulic heads [Gribovszki et al., 2008]. This would naturally cause water seeping out at the foot of the slopes and eventually increase the stream discharge. In the Kiwene catchment the saturated zone was found close to the surface in a sector of 5 meters from the stream channel. Infiltrating rain water has short vertical travel paths and would soon reach the shallow groundwater that has been established already prior to the event. This process is demonstrated in Fig. 6.2, also showing the enhanced temporary phreatic level developing during rain events. The high soil moisture contents in the riparian zone were evidenced by numerous field observations and profile probe measurements, for instance in the Chamasae catchment. Sklash and Farvolden [1979] suggest to distinguish between near-stream groundwater that experiences a large and rapid increase in hydraulic head after onset of rain and uphill area groundwater that has only little influence on the early runoff. This hypothesis seems to particularly apply in the Kiwene catchment considering the topography of the hillslopes and the deep groundwater table in a distance to the stream channel (Fig. 6.2). The scenario of runoff generation from shallow groundwater in the riparian zone was emphasised by Brown et al. [1999] and McGlynn et al. [2004], who consider the shallow flow component as the major storm-flow contribution.

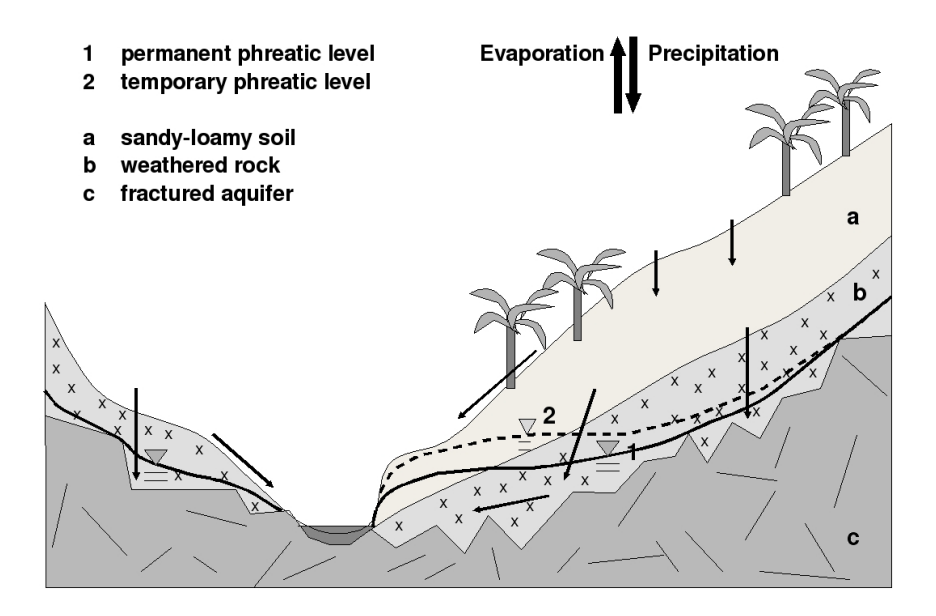


Figure 6.2: Conceptual model of flow mechanisms on the forested slopes

To comprehensively understand the subsurface inflows it is worthwhile to have a closer look at the infiltration processes occurring on the upper hillslopes. In general, rain water that infiltrates in a distance to the stream seems not to affect the runoff generation, as event water was found in the stream only during early recession [Sklash and Farvolden, 1979]. Fig. 6.2 illustrates that the travel paths in vertical direction grow longer with increasing distance from the stream channel. It becomes obvious that rain water can not reach the underlying aguifer in a short time. The most interesting question is the disposition of the rain water after it infiltrated into the soil. The watermark sensors indicated that the time delay of infiltration is rather negligible. An immediate response was recognised in all measured depths. On the other hand, the profile probe measurements showed clearly that there is no indication for a wetting front moving downwards into the soil. Besides approximately 10 % of moisture that was captured in the upper 30 cm, the soil horizon below did not experience significant wetting. One scenario sees infiltrating rain water hold back from further percolation, either because the saturation deficit in the top layer was never satisfied or by an increased suction pressure induced by surrounding vegetation. An alternative explanation is based on preferential flow via macro pores [Noguchi et al., 2001]. A fine network of macro pores, for example root holes, allow enhanced flow through connected pipes with high hydraulic conductivities [McDonnell, 1990]. In this case water could be transferred rapidly into greater depths without wetting the whole soil matrix. This process can be even accelerated by pressure propagation from macro pores [Laudon and Slaymaker, 1997]. The available soil moisture data as well as the dry piezometers on the hillslope argue that part of the water remains in the top soil layer, whereas another part is transferred towards the groundwater level or even further down into the fractured bedrock. This transport can be either slow vertical trickling through the matrix or preferential flow through a network of channels. A third possible pathway is return flow towards the surface induced by suction pressure of transpiration or evaporation.

Hydrograph of the 27th March event

In order to substantiate the theory presented in the conceptual model in Fig. 6.2, the specific runoff dynamics of the 27^{th} March hydrograph are scrutinised. This rain event was intensively sampled and provides a profound database. First of all, it is most important to consider the short time scale. The hydrograph is sharp with peak flow lasting less than one hour. Also the immediate recession α_1 is limited to less than 24 hours after the beginning of the event. It was shown in the discharge analysis that the delay of stream responses are negligible and signals are transmitted straight to the stream gauge.

The hydro chemical stream data shows that overland flow controls the short flush and the rapid drop of ion concentrations at the beginning of the event. These fast and abrupt responses are likely caused by mixing processes in the stream during the rising of the hydrograph. In contrast, during recession a rapid delivery of event water through the surface affects the runoff generation [Brown et al., 1999]. The ion concentrations smoothly recover indicating that the hydro chemistry of infiltrating rain water is altered. Rain water dissolves salts from the soil depending on the travel path and the contact time with minerals. However, the ion contents likely remain smaller compared to the pre-event water. As a result the near-stream aquifer would be diluted by infiltrating rain water. We can see this as stream water never reaches its initial concentrations again, not even during advanced recession.

The appearance and the type of flow components were identified with hydrograph separation. Most importantly, event water contribution is fairly small around 14 % of the total event caused discharge. Laudon and Slaymaker [1997] found a similar range between 10 and 30 % event water fraction. This demonstrates in the first instance that event water has a minor effect on the total storm-flow and over and above, is concentrated in a limited period of a few hours after peak flow. The bulk of discharge is produced by preevent water contributing constantly over the duration of storm-flow. Interestingly, the pre-event contribution also follows a time line similar to the event water with a maximum at peak discharge. As pre-event water basically corresponds groundwater, the peak inflows into the stream can only be caused by infiltrating rain water that increases the hydraulic pressure heads. In particular, old water stored near-stream can be mobilised and removed by increased pressure heads [Bazemore et al., 1994]. With the exception of peak flow, pre-event water, especially from shallow groundwater, can always be considered to be the dominant runoff component [Uhlenbrook and Hoeg, 2003].

In total the 27th March event had a discharge contribution from the forested part of the catchment of 25–30 %. The calculation of this rate is based on the occurrence of overland flow. In case of light rain without the appearance of excess water this rate can be found much lower. The same interpretation applies for the runoff coefficient that was calculated at 5.8 ‰. If the soil infiltration capacity is never exceeded, less water would reach the stream short-term and the runoff coefficient would be even lower.

6.2 Diurnal fluctuations in the saturated and unsaturated zone

Kiwene stream

Diurnal stream flow fluctuations have been clearly recorded at the forest stream gauge during entire Masika season 2008. The hypothesis that transpiration of riparian trees are responsible for the fluctuations [Mul et al., 2007a] was confirmed with additional stream gauges installed in stream sections without riparian vegetation. In the Kiwene spring basin for instance, trees stand in a distance to the stream and very little fluctuations were noticed. The underlying process is that tree transpiration induces suction pressure

in the soil and water from the saturated zone is lifted up and taken up by the tree. In respondence to the growing demand during the day the thickness of the saturated zone declines and the inflows into the stream are diminished. After sunset when transpiration is not active anymore, the process is reversed recovering the initial phreatic levels. The dependency between stream flow fluctuations and near-stream groundwater levels have been studied by Szilagyi et al. [2007] and Bond et al. [2002], who both found parallel fluctuating behaviour, but stated a phase shift between the groundwater and the stream flow. This phase-shift has also been recognised here, particularly in the afternoon when phreatic levels are recovered by lateral inflows from uphill.

In the flat topography of the spring basin the groundwater table is 1.4 m below surface and it can be assumed that trees take up water from roots reaching the saturated zone. On some days with exceptionally high potential evaporation a slight minimum of discharge was detected at the spring notch. These small signals feed the conclusion that the distant trees do initiate a remarkable decline of the groundwater table. However, only the very strong signals are transported to the stream. According to Wondzell et al. [2007], stream fluctuations have greatest amplitude if flow velocities are high and the fluctuations of the inflows are transported to the stream gauge more or less in phase. Both criteria do not necessarily apply in the spring basin.

The fluctuations recorded at the forest notch are greater and occur regularly with a clear diurnal cycle. They must be caused within a certain sector from the stream in the forested part of the Kiwene catchment. During May 2008 the mean potential transpiration was computed at 4.2 mmd⁻¹. In the same period the stream discharge is diminished by averaged $0.2 \, \mathrm{ls^{-1}}$ during day hours. Assuming infinite water accessibility of riparian trees and considering the saturated zone as the main water source, only a small portion of the riparian trees cause the stream fluctuations. In particular, the trees standing in a sector of 2–2.4 m next to the stream are involved in the process. This is in accordance to field observations that showed that large trees are abundant only in the vicinity of the stream. This scenario is supported by the clear detection and the small delay of the fluctuations transported to the forest notch. It can be hypothesised that large trees must reach the saturated zone in order to satisfy their water needs. The near-stream locations of trees also imply that groundwater tables are in greater depths with increasing distance from the stream. The small sector could mean that trees extract

water only from the alluvial aquifer. However, from the discharge analysis it is more likely that the trees diminish the lateral inflows by lowering the groundwater heads near the stream.

Kiwene forest site

During the day transpiration of trees has a double-effect. It lowers the groundwater table by extracting water from the saturated zone with deep root systems. At the same time the soil moisture content in the upper soil layer declines because lateral roots of trees and other vegetation consume moisture from the unsaturated zone. This phenomena was illustrated with the watermark sensors installed next to the large tree in the centre of the forest study site. The fluctuations in the unsaturated zone were observed only in the surrounding of the tree, feeding the assumption that the effect of trees on the soil moisture content is quite localised.

The central question is how the soil moisture contents recover during the night. In the literature it is mostly suggested that the soil moisture contents in the unsaturated zone is controlled by the phreatic level and the hydraulic properties of the soil. The soil moisture content is in a steady state that changes with the height of the phreatic level and is adapted by gravity and capillary forces. Other researchers, for instance Burt [1979] hypothesise that lateral inflows from uphill are responsible for water table recovery. In particular, during the wet season when soil moisture deficits disappeared the slope discharge becomes the dominant influence on riparian hydrology [Burt et al., 2002]. This scenario suggests a permanent equilibrium of in- and outflows in the surrounding of the tree. Groundwater inflows from uphill and capillary forces lifting water from the saturated zone provide a constant flux into the root zone of the tree. On the other hand the trees take up water by transpiration not only from deep roots but also with lateral roots from the unsaturated zone. The observed fluctuations are the result of a permanent shifting of this equilibrium. A high transpiration during the day exceeds the inflows causing a decline of soil moisture and the reversed process occurs during the night when inflows exceed the moisture extraction [Burt, 1979]. Both scenarios are based on the idea that there is a permanent moisture exchange between the saturated and the near-surface unsaturated zone and that an equilibrium between in- and outflows exists. This might be true for areas close to the stream. Further uphill the groundwater

level is presumed to be deep below the surface, as the dry piezometer in the forest evidenced. A third scenario hypothesises that trees take up water with deep roots reaching the saturated zone, but are able to release part of it with lateral roots in order to store it in the top layers of the soil. This idea could potentially give a more general explanation for moisture fluctuations in the unsaturated zone.

Chamasae stream

The lack of fluctuations in both, the saturated and the unsaturated zone can have different causes. First of all, the impact of riparian trees transpiring water and influencing the phreatic level is certainly missing in the cultivated catchment. The dominating crops such as beans, sugar cane and sprouting maize do likely not reach the saturated zone. Another possible explanation for the absence of fluctuations are the smaller discharge and the moderate slope of the stream, resulting in slow velocities. If signals are transported to the stream gauge with delay the fluctuations are often not visible anymore. The reason is that in case of slow velocities geomorphic dispersion can occur, leading to a dampening of the stream flow fluctuations [Wondzell et al., 2007].

The missing fluctuations in the unsaturated zone illustrate nicely the difference between transpiration and direct evaporation. Without a protecting canopy the soil in the Chamasae catchment is exposed to solar radiation. One would expect that during daytime soil water is evaporated and soil moisture contents are declining. The lack of fluctuations leads to the conclusion that the effect of direct soil evaporation on the soil moisture content is limited to a certain depth. In contrast, transpiration can affect the moisture content in much deeper soil regions because trees develop large vertical roots. Taking the previous assumption into account that only roots reaching the saturated zone impact the phreatic level, we can state that it is most likely a variable phreatic level and its interactions with the unsaturated zone that causes fluctuations.

6.3 Estimation of water balance

Besides the investigation of flow paths and source areas a rough estimate of the water balances can contribute an improved understanding of flows within the catchment. In particular, the water balance helps to evaluate the processes being important for the runoff generation and to quantify the processes that were considered in the conceptual model.

6.3.1 Simplification of flows in a box model

In general, a water balance can be explained with a box model. The whole catchment displays a box with specific in- and outflows. A simplified conceptual model of in- and outflows on a hillslope is presented in Fig. 6.3 with the most important terms highlighted.

The inflows in the Kiwene headwater catchment are reduced to precipitation because snow melt is not an issue in this catchment. The outflows are a bit more complex as they are diverse and not as easy to quantify. First of all there is evaporation that captures a great part of the precipitation before the rain water could possibly generate surface or subsurface runoff. The different evaporation terms in Fig. 6.3 can be summarised to the total evaporation losses showed in Equ. 6.1.

$$E_{tot} = E_I + E_T + E_S + E_{OW} \tag{6.1}$$

The terms soil evaporation (E_S) and open water evaporation (E_{OW}) can be neglected due to a dense forest canopy preventing soil penetration of solar radiation. The surface area of the narrow Kiwene stream is limited and largely shaded by overhanging trees. The remaining terms interception and transpiration are more complicated to estimate. Especially in semi-arid climates in Southern Africa the interception term can be significant and is considered to range between 2–5 mmd⁻¹ De Groen [2002]. The daily potential evaporation in the Pare mountains averages 5–10 mmd⁻¹ giving a rate of up to 50 % evaporation from interception. This estimation sounds reasonable as [Savenije, 2004] considers interception especially during wet months to be dominant. In practice the interception is lower because during wet months and particularly after rain events cloud

cover reduces solar radiation and moisture from the previous day remains on the vegetation cover, consuming precedent interception. The transpiration could not be measured within the Kiwene catchment, but was approximated with the potential transpiration (Equ. 2.2), determined with empirical parameters at the weather station in the floodplains of the catchment. Similarly, this term is over-estimated as solar energy is often consumed by interception from moisture on the leave surface before transpiration can be initiated. For the water balance it is important to estimate both evaporation terms best accurately as they have different impacts on soil moisture contents. Interception captures rainfall that is ineffective to soil moisture whereas transpiration evaporates water that contributed and replenished soil moisture stocks before being evaporated Savenije [2004].

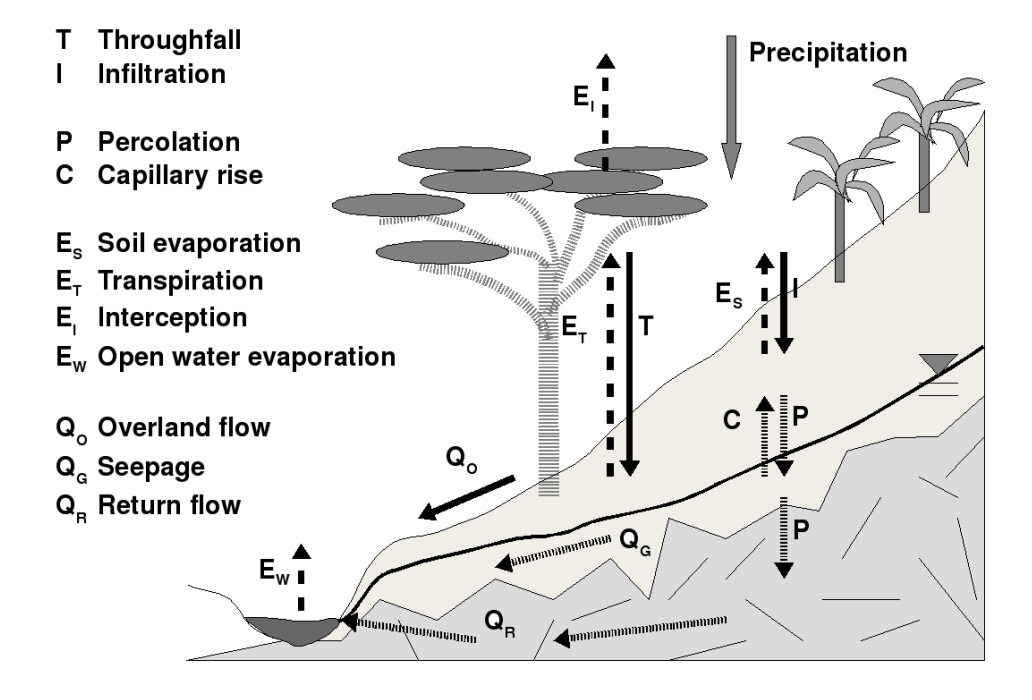


Figure 6.3: Simplified model of water flows

The second term to consider in the total balance is surface runoff that is quantified at the stream gauges at the outlet of the catchment. Even though not all surface runoff is captured at the stream gauge, the runoff term can be determined most accurately. The

total discharge of the Kiwene stream consists of three main components summarised in Equ. 6.2. The term return flow Q_R can be neglected because the only significant underground sources were observed downstream the forest notch and are not considered in the water balance upstream. The relevant components are therefore the overland flow Q_O occurring during peak flow of rain events and groundwater inflows Q_S during stormflow and base-flow. The latter consist to a small extend of groundwater from the adjacent groundwater storages in the hillslopes and to a greater extend from the Kiwene spring basin.

$$Q_{tot} = Q_O + Q_S + Q_R \tag{6.2}$$

The last flow component to consider is the part of the precipitation that infiltrates and is transferred into the ground. This flow is most tricky as flow velocities and residence times are in most cases highly unknown. It is also complicated to predict the subsurface pathways. For instance, infiltrating rain water can be evaporated through water uplift and transpiration, it can add to a shallow aquifer and is then displaced, or it even disappears from the box percolating into greater depths via fractures in the underlying bedrock.

The combination of the inflows and the water losses leads to the final equation for a simplified water balance for the hereby investigated Kiwene catchment (Equ. 6.3).

$$Prec - E_{tot} = Q_O + Q_S + P \tag{6.3}$$

The remaining question is the time scale the water balance shall be made for. It seems to be reasonable to consider a whole rain period from the rising limb of the hydrograph until the end of the direct recession. The major rain event on 27^{th} March was chosen for this purpose. It was also decided to only consider the lower part of the catchment between the mountain ridge and the forest notch because subsurface flows in the spring basin are expected to be slow.

6.3.2 Quantification of flow ratios

The extended rain event on 27^{th} March lasted for approximately three days interrupted by several dry periods. The total amount of rainfall detected at the Kiwene rain gauge adds to 46 mm. The water losses (*e.g.* evaporation) is the most uncertain estimation. An orientation could be the potential evaporation that was computed to 17.9 mm for this period. Certainly this number over-estimates the true value as cloud cover is denser in the uplands of the mountains, and real evaporation differs from potential evaporation. Interception is expected to account for less than 50 % of evaporation, due to iterant rain events and dense cloud cover.

The runoff includes surface runoff and groundwater inflows. The runoff coefficient was determined on 4–9 % depending on the catchment area. Due to the short period of time it seems to be wise not to consider the whole basin above the mountain ridge because surface runoff was not observed here and groundwater velocities are expected to be slow. A number of 5 % corresponds a total runoff of 2.3 mm. The hydrograph separation indicated that only 14 % of the total runoff is event water, leading to the conclusion that 2 mm out of the 2.3 mm is pre-event water. It was also shown that event water is more or less equal to surface runoff, meaning that this contribution (Q_O) is 0.3 mm.

According to Equ. 6.3 the remaining water infiltrates into the ground. We can distinguish between short percolation in the upper 50 cm of the ground and deep percolation in greater depths. The profile probes showed that in the uppermost layer of the soil approximately 10% ($\tilde{5}$ mm for this event) of rainfall can be stored short-term. The major part of the water ($\tilde{2}0$ mm) is likely transferred into deeper soil regions, where it can go diverse pathways. Besides the return into upper soil regions through suction pressure of trees, the water can be displaced into perched aquifers or into the fractured bedrock via preferential flow paths or macro pores ([Noguchi et al., 2001] and [McDonnell, 1990]).

We can state that for the total water balance stream discharge is a negligible small portion. It is the evaporation term and the percolation of water into the soil that captures the bulk of rainfall during events. As these terms are most difficult to estimate and to predict, further research should be done on how to measure interception and transpiration in forested catchments. In particular, sap flow measurements can contribute an

insight into the transpiration processes of riparian vegetation. Furthermore, the subsurface flow paths deeper than 1.5 m could not be sufficiently investigated. The large amount of water that is expected to percolate asks for further research of subsurface flow processes with focus on preferential flow.

Chapter 7

Conclusions

The measuring campaign in the small-scale Kiwene and Chamasae catchments provided detailed information on the relevant hydrological processes. The specific knowledge about source areas, flow pathways and residence times is of great value to characterise the complicated runoff dynamics. In addition, the applied multi-method approach contributed an improved process understanding and enabled a conceptualisation of the catchment hydrology. It was particularly useful to combine different methods when processes are only little known and not completely understood. Also, each method has shortcomings and limitations, but in combination they can form a consistent picture. In a small but densely monitored study catchment a multiple approach is especially advisable when knowledge and field experiences are limited.

The main objective of the study was the investigation of runoff generation responses in headwater catchments. The analysis of the data suggested to look at the processes during base-flow and storm-flow separately. In each regime different processes dominate the runoff generation and a distinction seemed reasonable.

During base-flow the bulk of discharge is generated in the spring basin of the Kiwene stream. The rich aquifer underneath the swamplands feed the Kiwene stream all year round. At the same time lateral fluxes from the forested slopes below the mountain ridge create diffusive sources along the stream. These sources impact the stream hydro chemistry but contribute insignificantly to the total discharge. During base-flow conditions the total discharge is limited to approximately $1 \, \mathrm{ls}^{-1}$ and diurnal stream flow fluctuations of up to 20 % were observed. It was shown that the fluctuations are caused

by riparian trees and the fluctuations correlate to some extent with the potential transpiration. The variations were recorded in both, the saturated and the unsaturated zone, meaning that trees take up water not exclusively from the saturated zone, but that trees control the moisture exchange between the different soil zones.

Rainfall alters the runoff generation and contributions from the forested slopes become important. In particular, overland flow occurring during peak flow amplifies the stream discharge after entering the forested part of the catchment. The overland flow is limited to short duration when the rain intensity is highest and the infiltration rate of the soil is exceeded. The hydrograph separation showed that the storm-flow runoff is still dominated by pre-event water. Despite the overland contributions, most of the storm-flow is old water that was stored subsurface and was then removed by infiltrating rain water. The recharged water heads near the stream are also responsible for the enhanced discharge during recession. The recession has been classified into different periods to better describe the event caused stream discharge.

In terms of the runoff generation responses the conclusions from the Kiwene stream generally apply for the Chamasae stream for the exception that no spring basin was identified in this catchment and the water undergoes much longer subsurface passages before appearing at the surface. In addition, no diurnal fluctuations were recognised here as riparian vegetation is missing.

The study focused on the description and the explanation of the hydrological processes in the catchment. A number of satisfying and good results were gained and a rough conceptualisation of the runoff generation responses could be achieved. Apart from the characterisation, the existing data was not used to fit a conceptual model to verify the proposed processes at the hillslope scale. The missing model application is mainly due to limited time during the thesis work. A great part of the time has been spent in the field because most of the gauging stations and measurement equipment had to be installed first. Furthermore, the measurement campaign was designed for whole Masika season in order not to miss any rain events and to cover part of the recession.

As the data and the results are very promising for the two study catchments, it is advisable to follow up the research in the future. The data collection should be continued and extended to get long-term data series that could make predictions more secure. Intensive data collection can of course not be done for the whole South Pare catchment as resources are limited. It should therefore be considered to carry out simultaneous modeling studies in order to test future hypotheses and to upscale processes from the hillslope to the catchment scale. A high resoluted hydrological model could be useful to produce accurate predictions of runoff responses for other poorly gauged catchments within the region. These results can contribute to improved water resources management, and in a long term can enable sustainable development in the South Pare Mountains.

Bibliography

- R.G. Allen, L.S. Perreira, D. Raes, and M. Smith. Crop evapotranspiration guidelines for computing crop water requirements. FAO technical paper 56, United Nations Food and Agricultural Organisation, Rome, Italy, 1998.
- M.G. Anderson and T.P. Burt. A laboratory model to investigate the soil moisture conditions on a draining slope. *Journal of Hydrology*, 33:383–390, 1977.
- P.S. Bagnall. The geology of the north pare mountains. *Bulletin of the Geological Survey of Tanganyika*, 10:7–16, 1963.
- D.E. Bazemore, K.N. Eshleman, and K.J. Hollenbeck. The role of soil water in storm-flow generation in a forested headwater catchment: synthesis of natural tracer and hydrometric evidence. *Journal of Hydrology*, 162:47–75, 1994.
- Y. Bhatt, D. Bossio, E. Enfors, L. Gordon, V. Kongo, J.R. Kosgei, H. Makurira, K. Masuki, M. Mul, and S.D. Tumbo. Working paper 109 (ssi working paper 1) strategies of water for food and environmental security in drought-prone tropical and subtropical agro-ecosystems. Technical report, International Water Management Institute, 2006.
- T. Blume, E. Zehe, D.E. Reusser, A.. Iroume, and A.. Brondster. Investigation of runoff generation in a pristine, poorly gauged catchment in the chilean andes i: A multiÂ-method experimental study. *Hydrological Processes*, in press, 2008.
- B.J. Bond, J.A. Jones, G. Moore, N. Phillips, D. Post, and J.J. McDonnell. The zone of vegetation influence on base-flow revealed by diel patterns of stream flow and vegetation water use in a headwater basin. *Hydrological Processes*, 16:1671–1677, 2002.

- M.G. Bos, editor. *Discharge measurement structures*. ILRI International Institute for Land Reclamation and Improvement, Wageningen, The Netherlands, third revised edition, 1989.
- V.A. Brown, J.J. McDonnell, D.A. Burns, and C. Kendall. The role of event water, a rapid shallow flow component, and catchment size in summer stormflow. *Journal of Hydrology*, 217:171–190, 1999.
- D.A. Burns, J.J. McDonnell, R.P. Hooper, N.E. Peters, J.E. Freer, C. Kendall, and K. Beven. Quantifying contributions to storm runoff through end-member mixing analysis and hydrologic measurements at the panola mountain research watershed. *Hydrological Processes*, 15:10:1903–1924, 2001.
- T.P. Burt. Diurnal variations in stream discharge and throughflow during a period of low flow. *Journal of Hydrology*, 41:291–301, 1979.
- T.P. Burt, G. Pinay, F.E. Matheson, N.E. Haycock, A. Butturini, J.C. Clement, S. Danielescu, D.J. Dowrick, M.M. Hefting, A. Hillbricht-Ilkowska, and V. Maitre. Water table fluctuations in the riparian zone: comparative results from a pan-european experiment. *Journal of Hydrology*, 265:129–148, 2002.
- J. Chard. Watermark soil moisture sensors: Characteristics and operating instructions. Technical report, Utah State University, 2005.
- M.M. De Groen. *Modelling interception and transpiration at monthly time steps; introducing daily variability through Markov chains*. PhD thesis, UNESCO-IHE, Delft, The Netherlands, Lisse, The Netherlands, 2002.
- DeltaT-Devices. User manual for profile probe. User manual, Macaulay Land Use Research Institute, Cambridge, UK, 2001.
- E. Enfors and L. Gordon. Analyzing resilience in dryland agro-ecosystems: a case study of the makanya catchment in tanzania over the past 50 years. *Land degradation and development*, 18:680–696, 2007.
- Z. Gribovszki, P. Kalicz, J. Szilagyi, and M. Kucsara. Riparian zone evapotranspiration estimation from diurnal groundwater level fluctuations. *Journal of Hydrology*, 349: 6–17, 2008.

- Kendall and McDonnell, editors. *Isotope Tracers in Catchment Hydrology*. Elsevier, 1998.
- D. Kobayashi, K. Suzuki, and M. Nomura. Diurnal fluctuations in stream flow and in specific electric conductance during drought periods. *Journal of Hydrology*, 115: 105–114, 1990.
- H. Laudon and O. Slaymaker. Hydrograph separation using stable isotopes, silica and electrical conductivity: an alpine example. *Journal of Hydrology*, 201:82–101, 1997.
- D. Mazvimavi. *Estimation of flow characteristics of ungauged catchments: case study in Zimbabwe*. PhD thesis, Wageningen University, 2003. Collation VIII.
- J.J. McDonnell. A rationale for old water discharge through matropores in a steep, humid catchment. *Water Resources Research*, 26:2821–2832, 1990.
- B.L. McGlynn, J.J. McDonnell, J. Seibert, , and C. Kendall. Scale effects on headwater catchment runoff timing, flow sources, and groundwater-streamflow relations. *Water Resources Research*, 40, 2004.
- M. Mul, H.H.G. Savenije, S. Uhlenbrook, and M.P. Voogt. Hydrological assessment of makanya catchment in south pare mountains, semi-arid northern tanzania. *Conference proceedings*, 308:37–43, 2006.
- M.L. Mul. *Understanding hydrological processes in an ungauged catchment in sub-Saharan Africa*. Draft, UNESCO-IHE, The Netherlands, 2008.
- M.L. Mul, R.K. Mutiibwa, J.W.A. Foppen, S. Uhlenbrook, and H.H.G. Savenije. Identification of groundwater flow systems using geological mapping and chemical spring analysis in south pare mountains, tanzania. *Physics and Chemistry of the Earth*, 32: 1015–1022, 2007a.
- M.L. Mul, H.H.G. Savenije, and S. Uhlenbrook. Base flow fluctuations from a forested and a cultivated hill slope in northern tanzania. *Physics and Chemistry of the Earth*, 2007b. Conference proceedings.

- M.L. Mul, R.K. Mutiibwa, S. Uhlenbrook, and H.H.G. Savenije. Hydrograph separation using hydro-chemical tracers in the makanya catchment, tanzania. *Physics and Chemistry of the Earth*, 2007c.
- M.L. Mul, H.H.G. Savenije, and S. Uhlenbrook. Spatial rainfall variability and runoff response during an extreme event in a semi-arid, meso-scale catchment in the south pare mountains, tanzania. *Physics and Chemistry of the Earth*, Conference Proceedings Waternet Symposium 2006, 2007d.
- D. Mwamfupe. Shortages of water for irrigation and farmers responses. Workshop proceedings water management in pangani river basin, Institute of Resource Assessment, Dar Es Salaam, 1999.
- S. Noguchi, Y. Tsuboyama, R.C. Sidle, and I. Hosoda. Subsurface runoff characteristics from a forest hillslope soil profile including macropores, hitachi ohta, japan. *Hydrological Processes*, 15:2131–2149, 2001.
- PBWO. Pangani basin flow assessment initiative. *Hydrology and System Analysis*, 1 of 2: Hydrology of the Pangani River Basin, 2006.
- H.H.G. Savenije. The importance of interception and why we should delete the term evapotranspiration from our vocabulary. *Hydrological Processes*, 18:1507–1511, 2004.
- M. Sivapalan. Prediction in ungauged basins: a grand challenge for theoretical hydrology. *Hydrological Processes*, 17:3163–3170, 2003.
- M.G. Sklash and R.N. Farvolden. The role of groundwater in storm runoff. *Journal of Hydrology*, 43:45–65, 1979.
- J. Szilagyi, Z. Gribovszki, P. Kalicz, and M. Kucsara. On diurnal riparian zone groundwater-level and streamflow fluctuations. *Journal of Hydrology*, 349:1–5, 2007.
- S. Uhlenbrook and S. Hoeg. Quantifying uncertainties in tracer-based hydrograph separations: a case study for two-, three- and five-component hydrograph separations in a mountainous catchment. *Hydrological Processes*, 17:431–453, 2003.

- S. Uhlenbrook, M. Frey, C. Leibundgut, and P. Maloszewski. Hydrograph separations in a mesoscale mountainous basin at event and seasonal timescales. *Water Resources Research*, 38(6), 2002.
- S. Uhlenbrook, J. Didszun, and C. Leibundgut. *Runoff generation processes on hill-slopes and their susceptibility to global change*, pages 297–307. Springer, 2005.
- H. Walter and H. Leith. *Klimadiagramm-Weltatlas*. Gustav Fischer Verlag, Jena, Germany, 1960–1967.
- C. Wels, R.J. Cornett, and B.D. Lazarte. Hydrograph separation: a comparison of geochemical and isotopic tracers. *Journal of Hydrology*, 122:253–274, 1991.
- J. Wenninger, S. Uhlenbrook, S. Lorentz, and C. Leibundgut. Identification of runoff generation processes using combined hydrometric, tracer and geophysical methods in a headwater catchment in south africa. *Hydrological Sciences*, 53(1), 2008.
- S.M. Wondzell, M.N. Gooseff, and B.L. McGlynn. Flow velocity and the hydrologic behaviour of streams during base-flow. *Geophysical research letters*, 34, 2007.

Appendix A

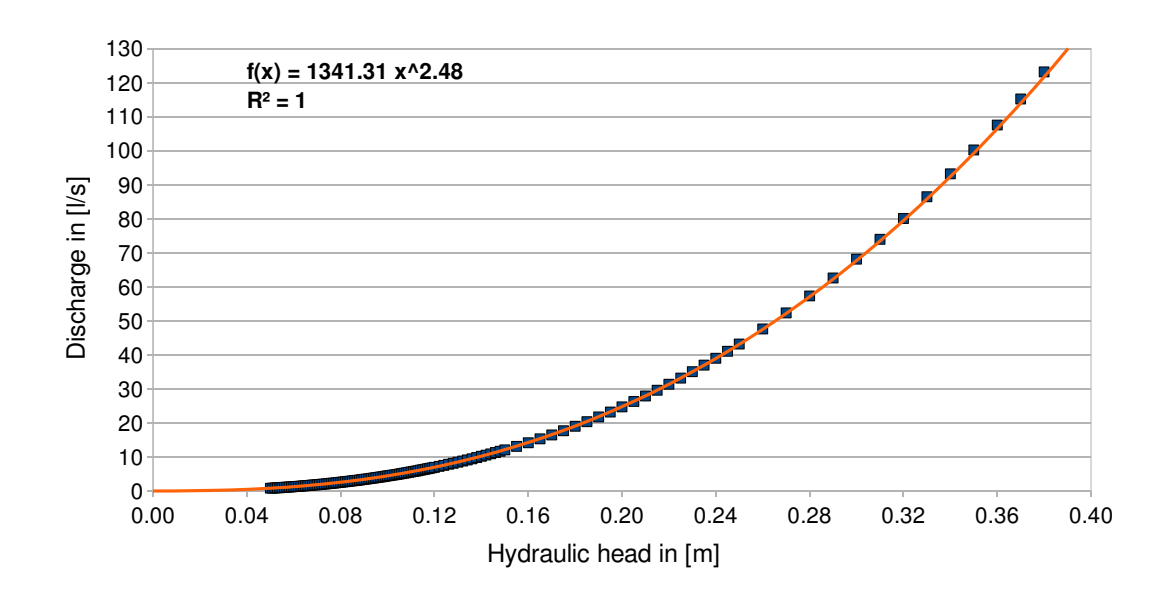
A.1 Data for notch rating curve

h [m]	Q [l/s]								
0.050	0.803	0.110	5.592	0.170	16.477	0.230	35.039	0.290	62.560
0.051	0.843	0.111	5.719	0.171	16.719	0.231	35.421	0.291	63.101
0.052	0.884	0.112	5.847	0.172	16.964	0.232	35.806	0.292	63.645
0.053	0.926	0.113	5.977	0.173	17.210	0.233	36.139	0.293	64.195
0.054	0.970	0.114	6.108	0.174	17.459	0.234	36.582	0.294	64.748
0.055	1.015	0.115	6.242	0.175	17.709	0.235	36.974	0.295	65.303
0.056	1.061	0.116	6.377	0.176	17.963	0.236	31.369	0.296	65.858
0.057	1.108	0.117	6.514	0.177	18.219	0.237	37.766	0.297	66.416
0.058	1.156	0.118	6.653	0.178	18.478	0.238	38.166	0.298	66.976
0.059	1.206	0.119	6.793	0.179	18.378	0.239	38.568	0.299	67.539
0.060	1.257	0.120	6.935	0.180	19.001	0.240	38.973	0.300	68.106
0.061	1.309	0.121	7.079	0.181	19.265	0.241	39.380	0.301	68.675
0.062	1.362	0.122	7.224	0.182	19.531	0.242	39.790	0.302	69.246
0.063	1.417	0.123	7.372	0.183	19.800	0.243	40.202	0.303	69.821
0.064	1.473	0.124	7.522	0.184	20.071	0.244	40.617	0.304	70.398
0.065	1.530	0.125	7.673	0.185	20.345	0.245	41.034	0.305	70.980

h [m]	Q [l/s]								
0.066	1.588	0.126	7.827	0.186	20.621	0.246	41.454	0.306	71.568
0.067	1.648	0.127	7.982	0.187	20.899	0.247	41.877	0.307	72.159
0.068	1.710	0.128	8.139	0.188	21.180	0.248	42.302	0.308	72.750
0.069	1.772	0.129	8.298	0.189	21.463	0.249	42.730	0.309	73.341
0.070	1.836	0.130	8.458	0.190	21.748	0.250	43.160	0.310	73.936
0.071	1.901	0.131	8.621	0.191	22.034	0.251	43.593	0.311	74.534
0.072	1.967	0.132	8.785	0.192	22.322	0.252	44.028	0.312	75.135
0.073	2.035	0.133	8.951	0.193	22.612	0.253	44.466	0.313	75.738
0.074	2.105	0.134	9.119	0.194	22.906	0.254	44.907	0.314	76.344
0.075	2.176	0.135	9.289	0.195	23.203	0.255	45.350	0.315	76.954
0.076	2.248	0.136	9.461	0.196	23.501	0.256	45.796	0.316	77.566
0.077	2.322	0.137	9.634	0.197	23.802	0.257	46.245	0.317	78.181
0.078	2.397	0.138	9.810	0.198	24.106	0.258	46.696	0.318	78.802
0.079	2.473	0.139	9.987	0.199	24.411	0.259	47.150	0.319	79.428
0.080	2.551	0.140	10.167	0.200	24.719	0.260	47.606	0.320	80.057
0.081	2.630	0.141	10.348	0.201	25.208	0.261	48.065	0.321	80.685
0.082	2.710	0.142	10.532	0.202	25.339	0.262	48.527	0.322	81.314
0.083	2.792	0.143	10.717	0.203	25.652	0.263	48.991	0.323	81.947
0.084	2.876	0.144	10.904	0.204	25.969	0.264	49.458	0.324	82.583
0.085	2.961	0.145	11.093	0.205	26.288	0.265	49.928	0.325	83.222
0.086	3.048	0.146	11.284	0.206	26.610	0.266	50.400	0.326	83.863
0.087	3.136	0.147	11.476	0.207	26.934	0.267	50.876	0.327	84.508
0.088	3.225	0.148	11.671	0.208	27.261	0.268	51.353	0.328	85.155
0.089	3.316	0.149	11.867	0.209	27.590	0.269	51.834	0.329	85.806
0.090	3.409	0.150	12.066	0.210	27.921	0.270	52.317	0.330	86.459
0.091	3.503	0.151	12.267	0.211	28.254	0.271	52.802	0.331	87.116

h [m]	Q [l/s]								
0.092	3.598	0.152	12.471	0.212	28.588	0.272	53.291	0.332	87.775
0.093	3.696	0.153	12.676	0.213	28.924	0.273	53.782	0.333	88.438
0.094	3.795	0.154	12.883	0.214	29.264	0.274	54.276	0.334	89.103
0.095	3.895	0.155	13.093	0.215	29.607	0.275	54.772	0.335	89.772
0.096	3.997	0.156	13.304	0.216	29.953	0.276	55.272	0.336	90.448
0.097	4.101	0.157	13.517	0.217	30.301	0.277	55.774	0.337	91.128
0.098	4.206	0.158	13.732	0.218	30.651	0.278	56.282	0.338	91.811
0.099	4.312	0.159	13.950	0.219	31.004	0.279	56.794	0.339	92.491
0.100	4.420	0.160	14.169	0.220	31.359	0.280	57.306	0.340	93.175
0.101	4.530	0.161	14.391	0.221	21.717	0.281	57.819	0.341	93.862
0.102	4.641	0.162	14.614	0.222	32.077	0.282	58.335	0.342	94.551
0.103	4.754	0.163	14.840	0.223	32.439	0.283	58.853	0.343	95.244
0.104	4.869	0.164	15.067	0.224	32.803	0.284	59.375	0.344	95.940
0.105	4.985	0.165	15.297	0.225	33.168	0.285	59.899	0.345	96.638
0.106	5.103	0.166	15.529	0.226	33.535	0.286	60.425	0.346	97.340
0.107	5.222	0.167	15.763	0.227	33.907	0.287	60.955	0.347	98.045
0.108	5.344	0.168	15.999	0.228	34.282	0.288	61.487	0.348	98.753
0.109	5.467	0.169	16.237	0.229	34.659	0.289	62.023	0.349	99.471

A.2 Rating curve notch formula

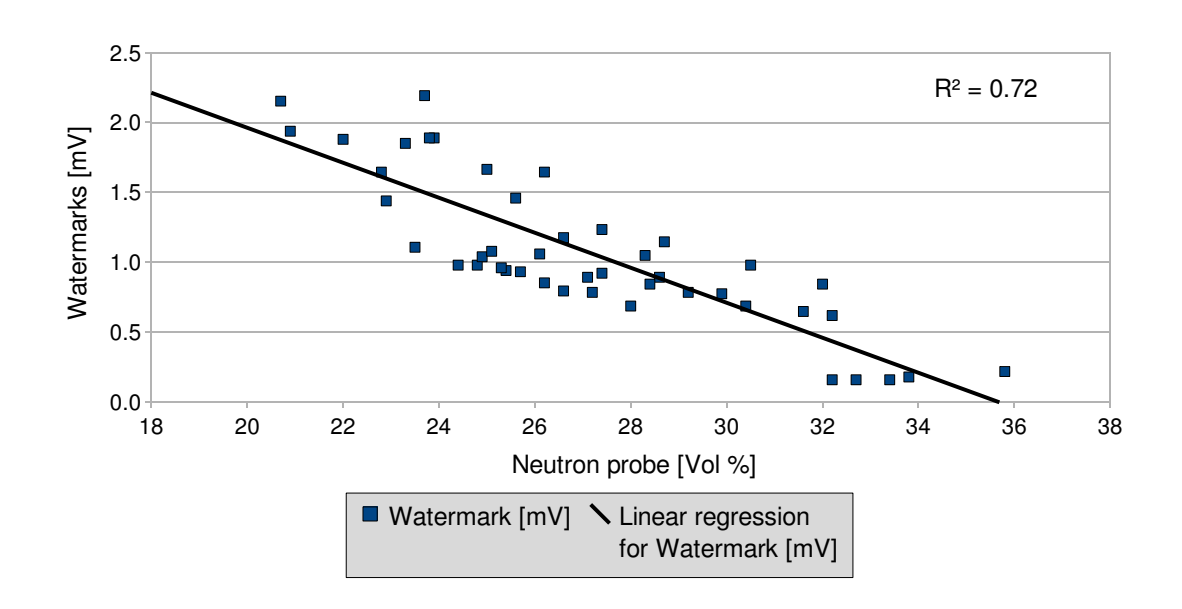


A.3 Notch field calibration

	Unit	18/03	19/04-1	19/04-2	25/04-1	25/04-2
Height notch	m	0.036	0.054	0.054	0.054	0.053
Notch formula	ls^{-1}	0.36	0.96	0.97	0.96	0.92
Salt dilution	ls ⁻¹	0.64	1.34	1.33	1.40	1.31
Bucket method	ls^{-1}				1.34	

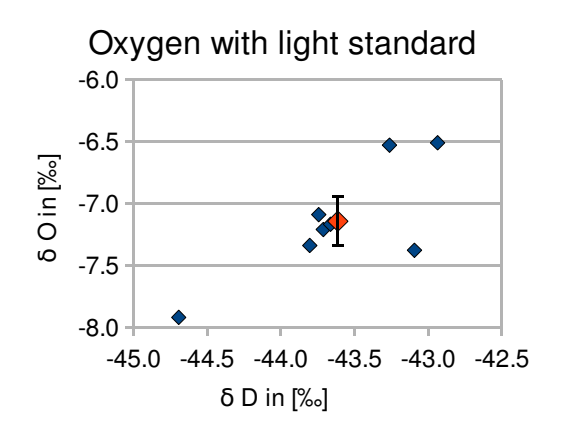
Appendix B

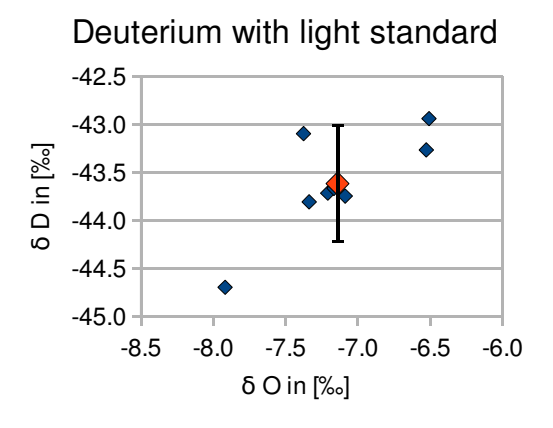
B.1 Watermark calibration

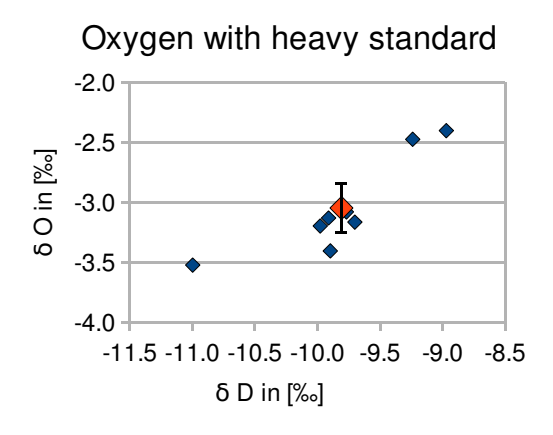


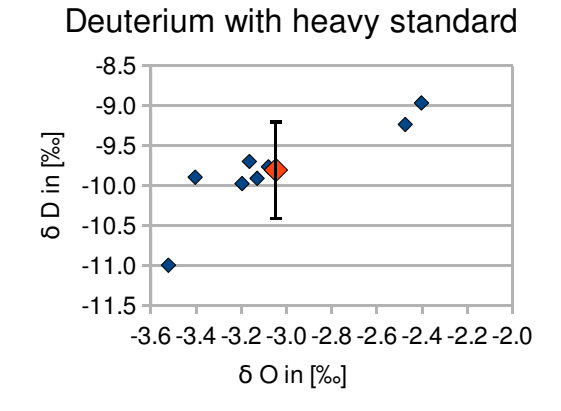
Appendix C

C.1 Results of the calibration of the isotope analyser



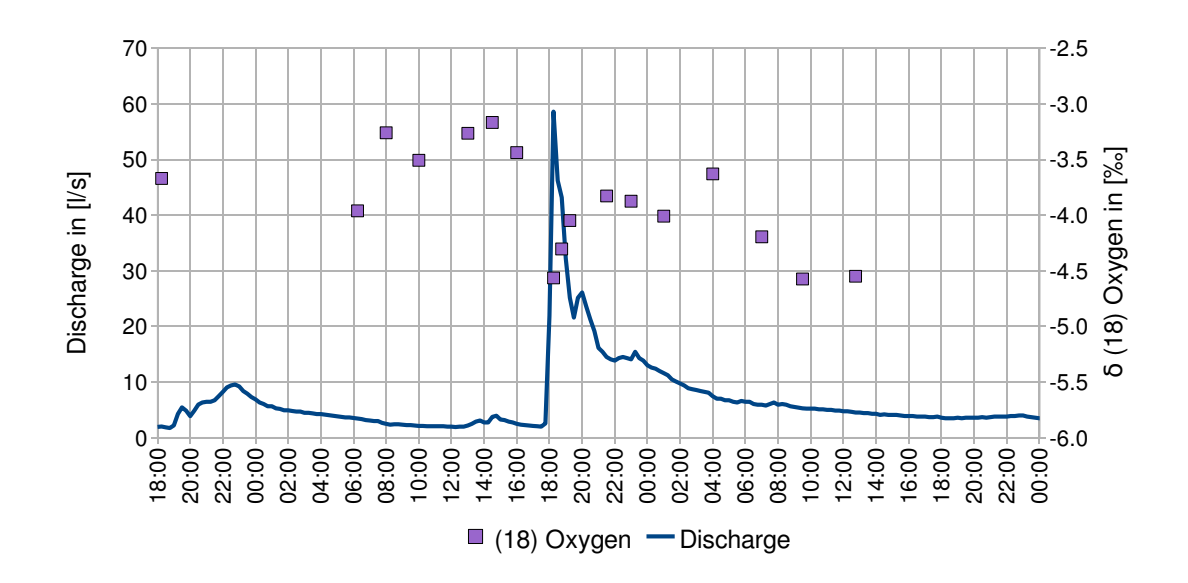




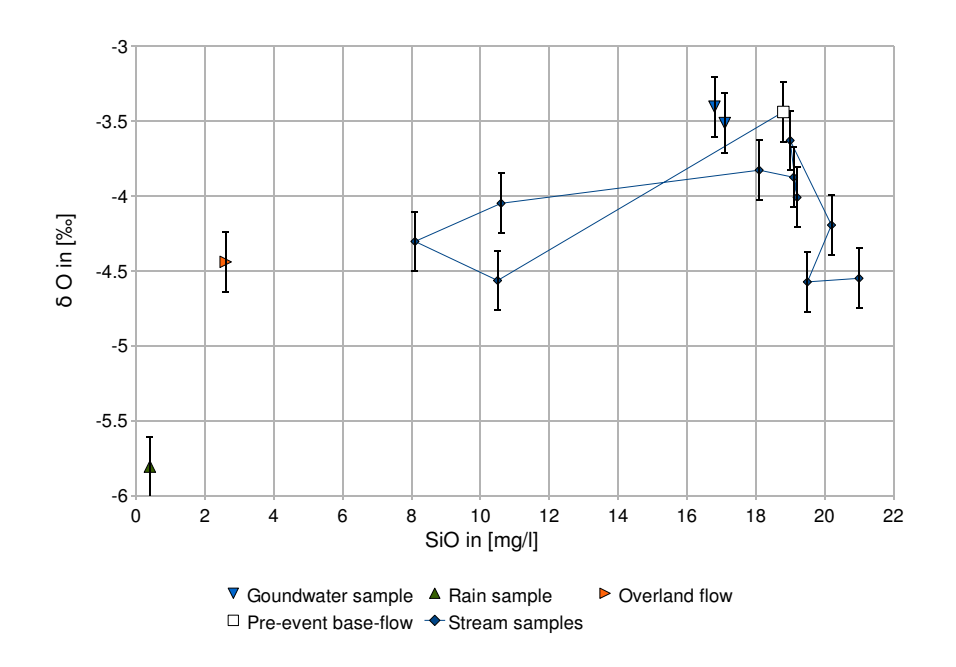


Appendix D

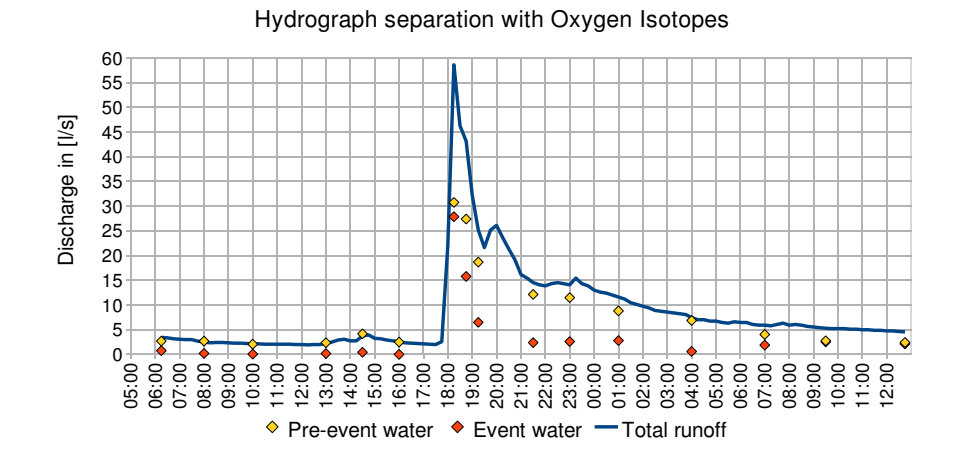
D.1 Hydrograph with Oxygen isotopes



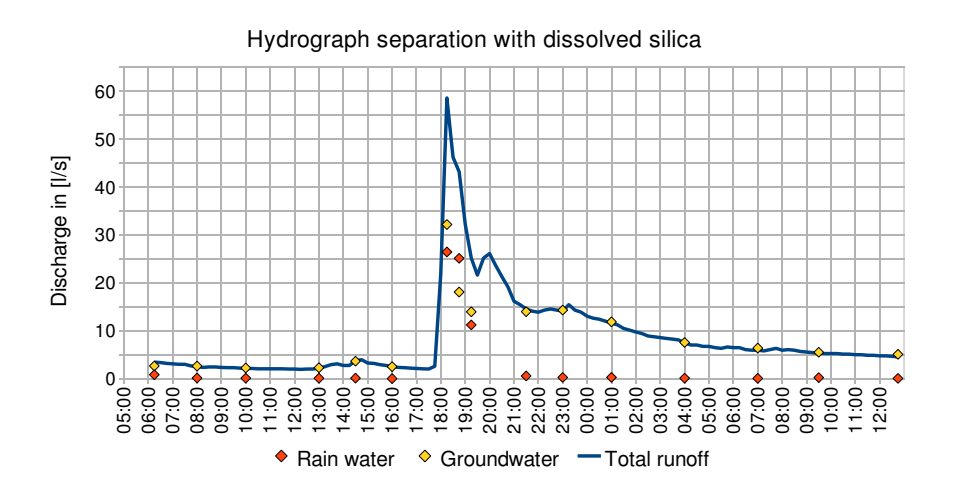
D.2 End-member mixing analysis with Oxygen isotopes



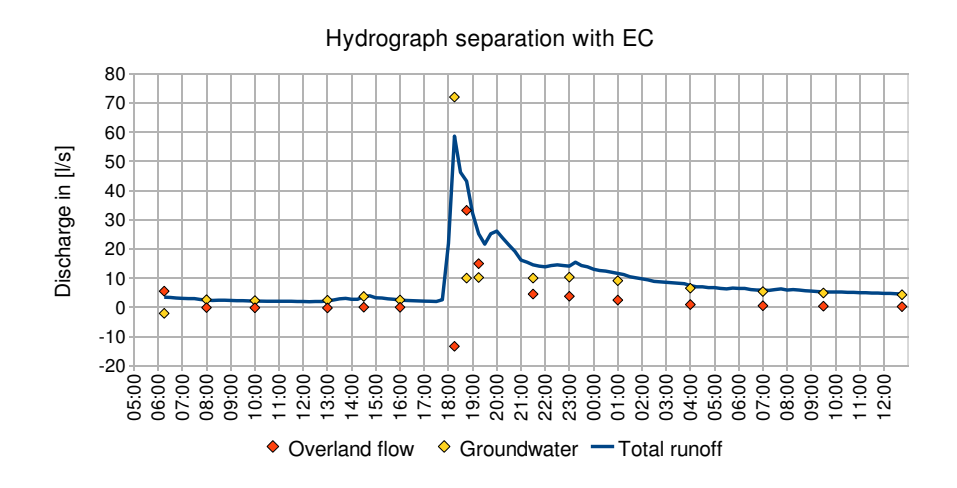
D.3 Hydrograph separation with Oxygen isotopes



D.4 Hydrograph separation with rain water and dissolved silica



D.5 Hydrograph separation with overland flow and EC



D.6 Hydrograph separation with rain water and EC

